Università degli Studi di Padova

Dipartimento di Fisica ed Astronomia "Galileo Galilei"

Corso di Laurea Magistrale in
Fisica

Tesi di Laurea Magistrale

The flavor problem in composite Higgs models

Laureando:
Andrea Pattori

Relatore:
Prof. Ferruccio Feruglio
Correlatore:
Dott. Paride Paradisi

Anno Accademico 2013/2014

Contents

Introduction

Nowadays, the most experimentally successful theory describing physics at its fundamental level is the Standard Model (SM) of Particle Physics. Despite its astonishing agreement with experimental data, it is widely believed that the SM needs an ultraviolet (UV) completion, that is a theoretical improvement to describe more properly the behaviour of nature at higher energies. The most compelling reason suggesting an UV completion of the SM is the hierarchy problem: the Higgs boson is a light particle, but within the SM no argument is given to justify the huge gap between the Higgs mass ($m_h \simeq 126$ GeV [1, 2]) and the fundamental mass scale, that is the Planck scale $M_P \simeq 10^{19}$ GeV.

Trusting the hierarchy problem, one would expect the existence of new physics (NP) at or below the TeV scale, a scale which we are probing now at the LHC experiments. This MSc thesis is inserted within this framework: its final aim will be to develop phenomenological consequences of a TeV scale NP candidate in order to verify if they are compatible with the current experimental results, finding out if that model is still a valid solution to the hierarchy problem.

To describe NP contributions to physical observables, a powerful tool is provided by the Effective Field Theory (EFT) approach [3, 4]. It allows to add to the SM Lagrangian non-renormalizable operators (i.e. with dimension $d > 4$): even though the new Lagrangian obtained is not renormalizable, it nevertheless provides definite predictions in a suitable energy range, where a perturbative expansion is applicable. Within an EFT approach, the NP effects are enclosed in the coefficients associated with the higher dimensional operators, called Wilson coefficients. This enables to set up a model-independent discussion where NP contributions are parametrized by the Wilson coefficients; then a model-dependent analysis can be used to derive the exact expression of such coefficients in specific NP models.

Among the most sensitive probes of NP signals there are flavor physics observables. In the SM all the fermions have three different replicas, called flavors, with the same quantum numbers and different masses. The term flavor physics refers to interactions that distinguish between families and the observables related to these interactions are highly suppressed within the SM for several reasons. Consequently, NP effects are expected to be source of significant deviations from SM predictions for this class of

observables [5].

Until now the search for NP signals has given negative results also in flavor physics. As a consequence, a tension arises between the assumption of TeV scale NP and the stringent bounds derived from flavor physics. Such tension is referred to at the new physics flavor puzzle. To solve it, one can imagine possible mechanisms that suppress NP contributions to flavor observables. Among the most popular ones, there are the Minimal Flavor Violation (MFV) hypothesis [6] and the Partial Compositeness (PC) paradigm [7]. The MFV hypothesis provides a rational for the suppression of flavor violating effects, postulating that the SM Yukawas are the only sources of flavor breaking also beyond the SM. The PC paradigm, on the other hand, could in principle explain not only the NP flavor puzzle, but also the hierarchies in the Yukawa matrices.

Among the most interesting proposals of TeV scale NP models, there are the Composite Higgs (CH) models [8]. They assume the existence of an additional (unbroken) $SU(N_{TC})$ technicolor gauge group and of a spectrum of technifermions charged under this group. Supposing the confining behaviour of this new strong sector to show up at the TeV scale, this theory predicts a full spectrum of new resonances with masses around the confining energy. The Higgs boson can then be thought of as one of these composite particles. Further, the Higgs lightness with respect to the other (so far unseen) resonances can be explained if we assume it to be a pseudo Nambu–Goldstone (pNG) boson arising from some unknown global symmetry breaking mechanism [9].

In these scenarios, one generates the fermion masses through the following mechanism: only the technifermions are assumed to interact with the Higgs boson, while the SM fermions cannot. However, since the SM fermions can nevertheless interact with the strong sector, they can still feel the EWSB, but only through the mediation of the technifermions. The weakness of such technifermion mediation could explain both the small fermion masses and suppressed flavor observables. This is the central idea of the PC paradigm.

This kind of CH models admits a different interpretation, that can shed light to the PC scenario. As already outlined, the strong sector generates a full spectrum of composite massive particles ("technibarions" and "technimesons"). Within this picture the existence of interactions between SM fermions and technifermons implies the existence of linear interactions between SM fermions and technibarions. These are nothing but off-diagonal mass terms, thus we conclude that the mass eigenstates (i.e. the states we observe through experiments) are actually an admixture of SM fermions and technibarions.

In this sense one talks about partial compositeness of the SM particles, referring now with SM particles to the experimentally observed mass eigenstates. Since such eigenstates also include a definite amount of technibarions in their admixture, they can feel the EWSB, with a strength proportional to their degree of compositeness. As already outlined, such degree of compositeness mitigates not only the fermion masses but also the flavor physics contributions from the NP sector.

The CH models are very attractive models for their phenomenological implications, but since they are defined through a strong dynamics, even approximate computations are often too difficult to be handled. To overcome this difficulty, one can describe the theory using directly the bound states of the strong sector to write the

Lagrangian, assuming that the interactions between strong resonances and the SM sector are weak enough to justify a perturbative approach.

In this framework, one can exploit the PC picture outlined above. For example, one can retain in its description only the lower-lying set of composite states relevant for the PC phenomenology, obtaining a simpler Lagrangian that allows perturbative computations [10]. Such models are called two-site models and have become popular in recent literature, since they permit to find reliable quantitative results. The importance of such simplified models is thus to furnish a method to work out predictions to be compared with the experimental results, in order to establish if the CH models are still a valid solution to the hierarchy problem.

In this thesis, we consider a very general two-site model that reproduces a realistic PC scenario for the SM particle content, considering for simplicity only the leptonic sector. After analysing the general features of the model, we focus on the contribution such NP model gives to a specific higher dimensional operator, the dipole operator. We have chosen the dipole operator for two reasons: on the one hand it turns out to be one of the most sensitive operators to NP effects in PC, on the other hand, the experimental resolution on the related phenomenological observables, that are the $\ell \to \ell'\gamma$ decays, the anomalous magnetic moments Δa_ℓ and the electric dipole moments (EDMs) d_ℓ, are extraordinary.

For these reasons, the last part of this work is devoted to the explicit loop calculations of the NP contribution to the Wilson coefficient associated with the dipole operator within the two-site model. The goal will be to find out whether the experimental bounds on $\mathrm{BR}(\mu \to e\gamma)$, Δa_ℓ and d_e are still compatible with a TeV scale strong sector.

This thesis is organized as follows. In chapter 1 we briefly review the reasons that motivate why and at what energies we are looking for an UV completion of the SM. In chapter 2, after having shortly recalled the SM and its flavor structure, we describe the EFT methods also in conjunction with the flavor physics and the search for NP signals, then we discuss in detail the MFV hypothesis. In chapter 3, after a concise summary of the proposed solutions to the hierarchy problem, we describe thoroughly the CH models, starting from the earlier Technicolor models and focusing also on the PC paradigm as an efficient method to suppress NP contributions in flavor physics. In chapter 4, we consider a specific two-site model and we work out some phenomenological consequences for it. For this purpose, we first describe the important features of the dipole operator, and then we elaborate in detail the dipole-mediated NP effects in our two-site model through loop calculations, focusing in particular on $\mu \to e\gamma$, Δa_ℓ and d_e.

Why going beyond the Standard Model

The *Standard Model* (SM) *of Particle Physics* is a very successful theory. Its predictions, tested in the last three decades with increasingly high precision, are in excellent agreement with experimental data for a wide range of phenomena. The coronation of this success has been the recent discovery of the Higgs boson [1, 2], the missing piece of this theory that was still seeking for an experimental confirmation. Thus, if we do not take into account a few number of discrepancies between the SM and cosmological observations, and with the notable exception of evidence for neutrino masses (all to be briefly discussed in section 1.1), we are facing a rather astonishing absence of *New Physics* (NP) signals.

Despite this lacking of experimental proofs, nowadays it is widely believed that the SM is just an *effective field theory* (EFT), i.e. it is a low energy approximation of a more fundamental theory. Then, if one consider as true that the SM needs an *ultraviolet* (UV) *completion*, the most urgent question becomes which is the energy scale of this new physics. A great number of scenarios have been proposed so far to answer this compelling question, and a complete list of them is far beyond the scope of this MSc thesis. Nevertheless, section 1.2 will describe some general theoretical arguments that suggest at which energy scale NP might show up.

The need for a *beyond standard model* (BSM) theory becomes more pressing when the concept of *naturalness* is introduced. This theoretical tool, if adopted as a research instrument, provides striking evidence that the SM is missing something and gives strict bounds on the energy scale where NP should first occur. This will be the topic of sections 1.3 and 1.4.

1.1 Experimental evidence for new physics

As already mentioned, there are just a few experimental clues for BSM physics and most of them come from the comparison of the SM predictions with cosmological observations. Referring to the literature for a more complete discussion, in the following the most important discrepancies are sketched:

- *Dark matter*: nowadays there is strong evidence that the 84.5% of the total

matter in the universe is constituted of dark matter [11], i.e. matter made of particles not included in the SM and with different properties. Then the SM obviously needs a completion that introduces one (or more) kind of particle(s) able to explain the presence of dark matter. So far among the most interesting proposals to solve this problem there are the *lightest supersymmetric particle* in the context of supersymmetric models [12] and the *axion* in models trying to solve the strong CP problem [13].

- *Baryon asymmetry*: another well established cosmological observation is that in the universe there is exceedingly more matter than antimatter, an anomaly known as baryon asymmetry. As a consequence of one of his accidental symmetries, in the SM the baryon number is conserved[1], then leading to a friction between the SM and our present cosmological models. Maybe new interactions and mechanisms in the NP sector could solve this problem.

- *Inflation*: the inflation mechanism was first proposed in the '80s to solve some serious cosmological problems (such as the horizon problem and the flatness problem). In the last decades this theory has become more and more accepted and recently the BICEP2 experiment has given striking experimental evidence for it [15]. But the SM is unable to explain in a satisfactory way the inflation era, resulting in a conflict between the two theories.

- *neutrino masses and mixing*: apart from the above cosmological arguments, the only known evidence for BSM physics are neutrino masses and oscillation. In the SM, neutrinos are massless particles. Instead, neutrinos are definitely massive particles, as shown by different experiments by now. In more recent years also the phenomenon of neutrino flavor oscillation has been studied and confirmed by experiments[2]. Both these observations impose a modification of the SM in order to accommodate neutrino masses and mixing. There is not a unique way to do that and the possible mechanisms can shed light to the NP sector, as it will be briefly sketched in the next section.

In summary, except for the neutrino masses and mixing, an unambiguous signal of NP (such as an experimental deviation from the SM predictions or an unexpected resonance at colliders) is still missing. Why is it so, despite the fact that an UV completion of the SM should exist, is an urgent question. The next sections will try to give an answer to this question.

1.2   The energy scale of new physics

Independently from experimental observations, it can be theoretically argued that the SM cannot be a theory valid up to arbitrarily high energies. The reason is a long-

---

[1]Actually, in the SM the symmetry associated with the baryon number conservation is anomalous. Thus, adding the C and CP violations (also present), the SM technically satisfy the first two Sakharov conditions for baryogenesis [14]. However, coming to the third condition, the SM in not able to quantitatively explain the departure from thermal equilibrium in the early universe.

[2]An overview of present experimental evidence regarding neutrino masses and oscillation can be found e.g. in [16].

standing problem: the SM does not include gravity interactions and furthermore
a consistent quantum theory of gravitation is still missing. Maybe this unification
cannot be reached within the context of quantum field theories and a dramatic change
of perspective might be needed, such as a string theory approach [17]. Nevertheless,
the energy scale at which the quantum gravity effects eventually show up represents
an ultimate UV cutoff for the SM. In other words, even in the absence of any other
kind of NP, the SM needs at least the UV completion necessary to include gravity.
Nowadays there is a broad agreement on putting this cutoff scale directly at the
Planck scale, $\Lambda \sim M_P \simeq 10^{19}$ GeV, since no theoretical reasons can be found to lower
this bound[3]. As mentioned, it is also believed that at those energies the quantum
field theory approach eventually stop to be applicable and new techniques have to be
developed.

The above argument put an ultimate cutoff scale for the SM at the Planck scale.
However, there are some theoretical and experimental clues that NP might exists at
slightly lower energies, the so-called GUT scale, $M_{GUT} \sim 10^{14} \div 10^{16}$ GeV.

The first indication of NP at this scale comes from the evolution of the three
SM gauge coupling under the RGEs. In the SM they all merge at nearly the same
value at energies $\sim 10^{14}$ GeV [18] and an even better situation occurs in the *Minimal
Supersymmetric Standard Model* (MSSM), where they exactly merge at energies $\sim$
10^{16} GeV [18]. This gauge coupling unification is a genuine prediction of *Grand
Unified Theories* (GUT), where the SM gauge group is embedded in a simple group
such as $SU(5)$ or $SO(10)$ [19].

A second theoretical clue comes from the see-saw mechanism, that tries to explain
the small non-vanishing neutrino masses. It is well-known that there exist only one
independent five-dimensional effective operator compatible with SM symmetries [20],
the Weinberg operator:

$$\mathcal{L}_5 = \frac{y}{\Lambda} (\tilde{\phi}^\dagger L)^T C (\tilde{\phi}^\dagger L) \, ,$$

where $\tilde{\phi}$ is the charge conjugate of the Higgs doublet, L is the leptonic left-handed
doublet and C is the charge conjugation matrix. Here Λ represents the energy scale of
the physics which originates this effective term and y is a dimensionless $\mathcal{O}(1)$ coupling
constant[4]. After the *Electroweak Symmetry Breakdown* (EWSB), this term generates
a mass for the left-handed neutrinos[5]:

$$m_{\nu_L} = \frac{y^2 v^2}{2\Lambda} \, ,$$

with $v = 246$ GeV the Higgs vacuum expectation value (VEV). Now, if one tries to
deduce the energy scale Λ by inverting this relation, one gets

$$\Lambda \simeq 3 \cdot 10^{14} \left(\frac{0.1 \ eV}{m_{\nu_L}} \right) y^2 \text{ GeV} \, ,$$

---

[3]It can be said that the choice of this scale is a "natural" one, since the Planck mass is directly
related to the Newton constant G_N: $M_P \equiv \sqrt{1/G_N}$. This concept of naturalness will be thoroughly
discussed later on.

[4]Again, this could be seen as a "natural" choice for the value of this parameter, see note 3.

[5]The current upper cosmological bound for neutrino masses is $\sum_i m_{\nu_i} \lesssim 0.3$ eV [21]. Weaker
bounds derive from laboratory experiments, for example $m_{\nu_e} \lesssim 2$ eV [22].

suggesting that, if the see-saw mechanism is the right answer to neutrino masses, then the NP behind it could be possibly found at the GUT scale.

A third, very recent suggestion comes from the results of the BICEP2 experiment [15]. According to its results, the inflation epoch begun when the primordial universe reached the temperature of $T \simeq 10^{16}$ GeV. If confirmed by other ongoing experiments (such as the Plank collaboration), this results would become strong experimental evidence of NP at the GUT scale.

The energy scales of NP discussed so far (M_P and M_{GUT}) are very far from nowadays experimentally achievable energies (such as the TeV scale at LHC). This enormous energy gap generates an high decoupling between the SM and the NP sector, which in turns could explain why experiments have not seen NP signals yet. But then the new question becomes if this is the end of the story, i.e. if NP appears only at very high energies, unreachable to nowadays collider experiments. Perhaps the answer is positive, but only if one completely ignores the naturalness problem. How this principle works and how it can be used to explore NP scenarios is the topic of the next sections.

1.3   The naturalness problem

If accepted as a physical principle, the concept of *naturalness* can be used as a powerful theoretical tool that can put in crisis the SM at very low energies, suggesting the existence of NP already at the TeV scale, as discussed in section 1.4.

Following the formulation of naturalness by 't Hooft [23], a theory is natural if, for all its parameters p which are small with respect to their fundamental scale Λ, the limit $p \to 0$ corresponds to an enhancement of the symmetry of the system.

To understand the meaning of this definition, we take as an example the fermion masses m_f. Regularizing the theory through an ultraviolet cutoff Λ and computing the loop corrections δm_f to m_f, naïvely one could have expected these corrections to be proportional to Λ. However, the limit $m_f \to 0$ restore the fermion chiral symmetry; thus, every contribution to δm_f should be proportional to m_f itself (i.e. every contribution to the chiral symmetry breaking should be proportional to coefficients associated with this breaking). Then the dependence of δm_f through Λ can only be logarithmic, $\sim \log \Lambda$. This mechanism, that is a direct consequence of the fulfilment of the 't Hooft condition, protect the fermion masses from planckian corrections and makes a small value for the m_f/M_P ratio natural.

A complementary request to a natural theory is that all its parameters that do not satisfy the 't Hooft condition should have an $\mathcal{O}(1)$ value with respect to their fundamental scale. Then, it can be said that a *naturalness problem* arise every time a theory exhibit a small parameter without furnishing any symmetry that protect its value.

We can turn this problem to a more quantitative form by introducing the notion of *fine tuning*. Once identified the unnatural small parameter p and its fundamental

scale[6] Λ, one may define the amount f of fine tuning by:

$$f \equiv \frac{p}{\Lambda} \; . \tag{1.1}$$

The smaller f, the bigger the required fine tuning. Then, for example, if we have a dimensionless constant $p \simeq 10^{-2}$, since in this case $\Lambda = 1$, without any symmetry protection we would say that our theory needs a fine tuning to the per cent level, $f \simeq 10^{-2}$.

Generally, an high fine tuning would go against the belief that the observable properties of a physical theory are stable under small variations of its fundamental parameters. One talks about the naturalness of a theory to describe such behaviour.

Once formalized these concepts, it can be easily argued that the SM is not a natural theory and a (sometimes huge) fine tuning is needed to explain the experimental values of several quantities. The most urgent questions arising from this principle and some attempts to solve them are:

- *Cosmological constant*: cosmological observation are consistent with the existence of a cosmological constant. However, experimentally it take the value $\Lambda_{cosmo} \sim 10^{-47}$ GeV^4 [11], while theoretically it would be expected the value $\Lambda_{cosmo} \sim M_P^4 \sim 10^{76}$ GeV^4. Then in this case $f \simeq 10^{-123}$. Until now this discrepancy has remained a true mystery to us.

- *Hierarchy problem*: the SM Higgs sector include one independent dimensionful parameter, equivalently the Higgs VEV or the Higgs mass, both of order $\sim 10^2$ GeV [22]. Theoretically one would have expected a value of order $\sim M_P \sim 10^{19}$ GeV for these parameters. The next section will return on this problem, called the hierarchy problem, while section 3.1 will discuss some attempts to solve it.

- *Charge quantization*: the experiments suggest that the proton and electron charges are equal and opposite in sign: $|Q_e + Q_p| < 10^{-21}$ [22]. In the SM this should be seen as a fine tuning ($f \simeq 10^{-21}$) since it does not provide any natural explanation. Theories of grand unification could be a possible solution, since they predict a quantization of hypercharge [19].

- *Strong CP problem*: the four-dimensional term $\int \mathrm{d}^4 x \, \theta_{QCD} \, \epsilon^{\mu\nu\rho\sigma} G^a_{\mu\nu} G^a_{\rho\sigma}$, that could in principle appear in the SM Lagrangian and would lead to a CP violation in the strong sector, has an extremely small coefficient, $\theta_{QCD} \lesssim 10^{-10}$ [22]. The Peccei-Quinn mechanism could explain this value, and in turn it also imply the existence of a new particle, the axion [13].

- *Flavor puzzle*: the fermion mass spectrum ranges from ~ 170 GeV, for the case of the top-quark, to $\sim 10^{-3}$ GeV, for the case of the electron. Even though the smallness of the fermion masses, as argued before, cannot be interpreted as a naturalness problem, this huge hierarchy in the mass spectrum (more that five

---

[6]We have already argued in note 3 that, for a parameter of mass dimension 1, its natural scale is $\Lambda = M_P$. Thus, for $[p] = d$ in mass unit, we will have $\Lambda = (M_P)^d$ and $f \equiv p/(M_P)^d$. Note that the alternative choice $f \equiv (p^{1/d})/M_P$ would led to significantly different values for f.

orders of magnitude) is unnatural. Furthermore, also the Cabibbo-Kobayashi-Maskawa matrix (V_{CKM}) presents hierarchies between families. These structures are still unexplained, although progresses were made in the last years in this direction.

According to the naturalness concept, all these problems require a SM completion that can accommodate them in a natural way. In particular, the hierarchy problem strongly suggests the existence of BSM physics already at the TeV scale, as it will be discussed in detail in section 1.4.

What itemized above are difficulties of the SM, arising from the naturalness concept, that can be put in a numerical form (i.e. the fine tuning f can be quantitatively evaluated). However, other questions can be related to naturalness, once this principle is somehow extended to include more qualitative aspects. These new problems can be summarized with the following question: why the SM is the way it is? In other words, is there any natural explanation for all the peculiar features of the SM (such as particle content, particle quantum numbers, number of families, gauge groups)? After all, one verify an amazing cancellation of all gauge anomalies due to the particular choices of these SM features. Can it be just a coincidence?

Of course, according to personal taste, these last issues can appear of philosophical nature and then with not much or no importance. But it is also completely licit to believe, as the author does, that a satisfactory physical theory should explain, or at least motivate, also these aspects.

1.4   The hierarchy problem

As already outlined, among the issues discussed in the previous section the hierarchy problem is of critical importance for present physics since it predicts NP at the TeV scale, i.e. energies that are becoming reachable to nowadays experiments. Thus, we are about to find out whether the notion of naturalness and its predictions are correct or whether there is something missing in its formulation.

The core of the hierarchy problem is that the Higgs boson is unnaturally light. When discussing the naturalness concept, it has been argued that the fermions can have masses far below the Planck scale in a natural way, since in the limit of massless fermions the chiral symmetry is restored. In the case of the Higgs boson mass m_h, no such enhancement of the symmetry is found in the limit $m_h \to 0$. This, in turn, implies that loop corrections δm_h^2 to m_h^2 are quadratically divergent, rather than logarithmically divergent as in the case of fermion masses, making unnatural a physical mass m_h far away from the fundamental scale M_P.

To make this last point clearer we can use a simple $\lambda\phi^4$ theory, that describe a single scalar boson ϕ. Indeed, introducing a finite cutoff scale Λ, the diagram given in Fig. 1.1 gives a contribution

$$\delta m^2 = \lambda \int^{\Lambda} \frac{\mathrm{d}k^4}{(2\pi)^4} \frac{1}{k^2} \sim \frac{\lambda}{(16\pi^2} \int^{\Lambda} \mathrm{d}k^2 \sim \lambda \frac{\Lambda^2}{16\pi^2} \ ,$$

that can be interpreted as the one-loop correction to the boson mass m^2; as anticipated, it presents a quadratic dependence on Λ.
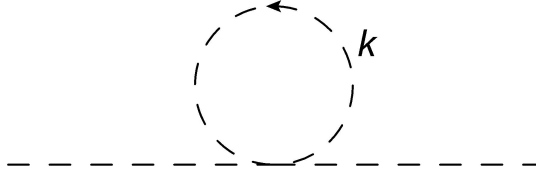
Figure 1.1: The scalar one-loop diagram leading to a quadratic divergence.

Thus, in this theory, at one-loop level the physical mass of the boson is

$$m^2 = m_0^2 + \frac{\alpha\lambda}{16\pi^2}\Lambda^2 \,, \qquad (1.2)$$

where m_0^2 is the bare mass, i.e. the parameter entering in the Lagrangian of the theory and α is an $\mathcal{O}(1)$ coefficient. We can now appreciate the problem arising from assuming the physical mass m far away from its fundamental scale Λ: even if we put a small value of the bare mass m_0 (that is a small value of the tree level boson mass), this hierarchy would be spoiled by one-loop corrections; if we insist to impose a small value of m at the one-loop order, we need an awkward fine tuning in order to gain a cancellation between the two contributions on the r.h.s. of Eq. (1.2).

In the case of the SM, the Higgs mass receives the following one-loop corrections [24]:

$$\delta m_h^2 = \frac{3\Lambda^2}{8\pi^2 v^2}\left[(4m_t^2 - 2M_W^2 - M_Z^2 - m_h^2) + \mathcal{O}\left(\log\frac{\Lambda}{\mu}\right)\right] \,. \qquad (1.3)$$

We can repeat the same argument outlined above to conclude that, if we put the fundamental physical scale directly at the Planck scale, in the SM is required a fine tuning

$$f \equiv \frac{m_h^2}{\delta m_h^2} \simeq \frac{m_h^2}{\Lambda^2} \sim 10^{-34} \qquad (1.4)$$

in order to give the correct value to the Higgs mass.

A possible solution to eliminate (or at least reduce) this huge fine tuning is to drastically lower the cutoff scale Λ. In other words, if we assume that NP first shows up at energies not far above the EWSB scale, that is around the TeV scale, and if we further supplement this NP with a mechanism that stabilize the Higgs mass, protecting it from planckian corrections, then we would have solved the hierarchy problem.

It is important to stress that, in order to have this solution to be truly natural, the NP scale should be near the EWSB scale, otherwise a *little hierarchy problem*, as sometimes is called, still remains. In the last decades various models satisfying this request were proposed, the most important and still plausible ones will be briefly described in section 3.1.

As already said, we are nowadays starting to be able to investigate experimentally the TeV scale, thus reaching a turning point in our understanding of fundamental physics: either NP will be found, solving the hierarchy problem and opening a new era of discoveries, or no deviation from the SM will occur, imposing a deep changing of perspective in order to understand why the apparently robust concept of naturalness does not work.

Until now no signal of BSM physics at TeV scale was found, also considering the runs at 7 and 8 TeV of the LHC experiments. Then it is evident that whether the present experimental data are compatible or not with models proposed to solve the hierarchy problem, and which experiments can definitely reveal the presence/absence of NP, are more than ever compelling questions, that deserve all the efforts needed to answer them.

Flavor physics

2.1 The Standard Model of particle physics

At present days, the most used and successful tools to describe nature at the quantum level are *Quantum field theories* (QFT). A QFT is described by its Lagrangian $\mathcal{L}$, that should obey some very general rules:

- Since, for any process, the probabilities of the possible outcomes should sum up to 1 at any time, the time evolution operator should be unitary. This imply that the Hamiltonian operator (and then the Lagrangian) should be *hermitian.*

- The Lagrangian should be *invariant under Poincaré transformations.* As a consequence, all field operators appearing in $\mathcal{L}$ should belong to a definite representation of the Poincaré group.

- If we want a renormalizable theory[1], the Lagrangian cannot contain operators with dimension $d > 4$.

These are properties that every Lagrangian should have in order to furnish a consistent theory. In addiction, to characterize a specific QFT we also need to define its three following features:

 (i) The gauge symmetry;

 (ii) The particle content, that is which particles are present and to which representation of the gauge group they belong;

(iii) The pattern of spontaneous symmetry breaking.

Once defined these three points, we are able to write down the most general Lagrangian satisfying them, i.e. we have completely defined our QFT. Of course, it will have a finite number of parameters. In the context of QFT no arguments can be

---

[1]This last requirement can be relaxed if one deals with effective field theories: in that case $d > 4$ operators can occur. In section 2.2 we will return on this point.

adduced in order to fix the value of any of them[2]; thus they represents free parameters to be measured via experiments. Only after these set of measurements are performed, the theory becomes predictive.

2.1.1 The Standard Model Lagrangian

Keeping in mind what outlined above, we can now define in a formal manner the Standard Model of particle physics:

(i) The gauge symmetry is

$$G_{SM} = SU(3)_C \times SU(2)_L \times U(1)_Y \ ; \tag{2.1}$$

(ii) There are three fermion *families* (or *flavors*, or *generations*), each consisting of five representations of G_{SM}:

$$Q_{Li}(3,2)_{+1/6} \ , \quad U_{Ri}(3,1)_{+2/3} \ , \quad D_{Ri}(3,1)_{-1/3} \ ,$$
$$L_{Li}(1,2)_{-1/2} \ , \quad E_{Ri}(1,1)_{-1} \ . \tag{2.2}$$

This means, in our notation, that for example Q_{Li} are left-handed quarks (the $i = \{1, 2, 3\}$ index runs over families), triplets of $SU(3)_C$, doublets of $SU(2)_L$ and carrying hypercharge $Y = +1/6$. Decomposing the two $SU(2)_L$ doublets into their components in order to fix the notation:

$$Q_{Li} = \begin{pmatrix} U_{Li} \\ D_{Li} \end{pmatrix}; \quad L_{Li} = \begin{pmatrix} E_{Li} \\ \nu_{Li} \end{pmatrix} \ . \tag{2.3}$$

In addiction, there is one scalar representation:

$$\phi(1,2)_{+1/2} \ ; \tag{2.4}$$

(iii) The scalar ϕ assumes a VEV:

$$\langle \phi \rangle = \begin{pmatrix} 0 \\ v/\sqrt{2} \end{pmatrix} \ , \tag{2.5}$$

which implies that the SM gauge group is spontaneously broken to

$$G_{SM} \to SU(3)_C \times U(1)_{EM} \ . \tag{2.6}$$

This process is called *Electroweak Symmetry Breakdown* (EWSB).

The SM Lagrangian is the most general renormalizable one that fulfil these three conditions[3]. It can be divided in three pieces:

$$\mathcal{L} = \mathcal{L}_{\text{Kinetic}} + \mathcal{L}_{\text{Higgs}} + \mathcal{L}_{\text{Yukawa}} \ , \tag{2.7}$$

---

[2]The best that can be done is to impose additional global symmetries to the theory: this typically reduces the number of free parameters or puts some of them to zero.

[3]Actually, this statement is correct only if one forgets about the θ_{QCD} parameter. This caveat leads to the strong CP problem, already discussed in section 1.3.

with

$$\mathcal{L}_{\text{Kinetic}} = -\frac{1}{4}G^a_{\mu\nu}G^{a,\mu\nu} - \frac{1}{4}W^b_{\mu\nu}W^{b,\mu\nu} - \frac{1}{4}B_{\mu\nu}B^{\mu\nu} + \sum_f \bar{\Psi}_f i\slashed{D}\Psi_f \,, \qquad (2.8a)$$

$$\mathcal{L}_{\text{Higgs}} = (D_\mu\phi)^\dagger(D^\mu\phi) - \mu^2\phi^\dagger\phi - \lambda(\phi^\dagger\phi)^2 \,, \qquad (2.8b)$$

$$-\mathcal{L}_{\text{Yukawa}} = Y^d_{ij}\bar{Q}_{Li}\phi D_{Rj} + Y^u_{ij}\bar{Q}_{Li}\tilde{\phi}U_{Rj} + Y^e_{ij}\bar{L}_{Li}\phi E_{Rj} + \text{h.c.} \,, \qquad (2.8c)$$

where: $G^a_{\mu\nu}, W^b_{\mu\nu}$ and $B_{\mu\nu}$ are the field strength tensors of the eight gluon fields G^a_μ, the three weak interaction bosons W^b_μ and the hypercharge boson B_μ, respectively; Ψ_f is a collective symbol to denote all the fermions, with the index f running over all the fermion representations and families; D_μ is the covariant derivative; $\tilde{\phi} \equiv i\sigma^2\phi^*$ is the charge conjugate of the ϕ doublet; μ^2 and λ are real parameters and $Y^{u,d,e}$ are complex 3×3 matrices.

$\mathcal{L}_{\text{Kinetic}}$ include the kinetic terms for gauge bosons and fermions, as well as interaction terms among these fields. This part of the Lagrangian has three free parameters, g, g' and g_s, that are the gauge couplings associated with the three simple subgroups of G_{SM}.

$\mathcal{L}_{\text{Higgs}}$ is the Higgs doublet Lagrangian. It consists of the kinetic terms for this field (again with the gauge interaction terms) and its potential. In order for the ϕ field to acquire a VEV, we have to require $\mu^2 < 0$ and $\lambda > 0$. In addiction, the following relation between μ^2, λ and the VEV v (see Eq. (2.5)) holds:

$$v = \sqrt{\frac{-\mu^2}{\lambda}} \,. \qquad (2.9)$$

Then, this part of the Lagrangian involves two free parameters, say λ and μ. The implications of a dimensionful free parameter were already discussed in section 1.4.

Finally, $\mathcal{L}_{\text{Yukawa}}$ contains the Yukawa interactions between the fermions and the Higgs doublet. After the EWSB, these terms give rise to fermion masses. We will discuss in detail the structure of this piece of the Lagrangian in next sections, anticipating only that it has 13 (dimensionless) free parameters. Thus, the complete SM Lagrangian has 18 free parameters[4] to be determined by experiments, and 13 of them arise in the Yukawa sector.

2.1.2 The flavor structure of the Standard Model

The term *flavor physics* refers to interactions that distinguish between flavors, where we have already discussed that with *flavor* one means the several copies of fermion fields carrying the same quantum charges (i.e. belonging to the same representation of G_{SM}). In the SM all the source of flavor physics is in the Yukawa interactions, as can be seen directly in Eqs. (2.7) and (2.8), where $\mathcal{L}_{\text{Yukawa}}$ is the only part that distinguish between families, through the Yukawa matrices $Y^{u,d,e}$.

In the absence of the Yukawa interactions (namely $Y^{u,d,e} = 0$), the SM Lagrangian has a large $U(3)^5$ global symmetry:

$$G_{flavor} = U(3)^3_q \times U(3)^2_l \,, \qquad (2.10a)$$

---

[4]They really are 19, if one again include θ_{QCD}, see note 3.

$$U(3)_q^3 = U(3)_Q \times U(3)_U \times U(3)_D \ , \tag{2.10b}$$

$$U(3)_l^2 = U(3)_L \times U(3)_E \ , \tag{2.10c}$$

under which the fermion fields mixes between families in this way:

$$
\begin{aligned}
Q_{Li} &\to (V_Q)_{ij} Q_{Lj} \ , & L_{Li} &\to (V_L)_{ij} L_{Lj} \ , \\
U_{Ri} &\to (V_U)_{ij} U_{Rj} \ , & E_{Ri} &\to (V_E)_{ij} E_{Rj} \ , \\
D_{Ri} &\to (V_D)_{ij} D_{Rj} \ .
\end{aligned}
\tag{2.11}
$$

where in our notation $V_Q \in U(3)_Q$ and so on.

Since[5] $U(3) \cong SU(3) \times U(1)$, we can split G_{flavor} into Abelian and non-Abelian parts:

$$G_f = SU(3)_q^3 \times SU(3)_l^2 \times U(1)_B \times U(1)_L \times U(1)_Y \times U(1)_{PQ} \times U(1)_E \ , \tag{2.12}$$

where $U(1)_B$ and $U(1)_L$ are the invariances associated with the baryon and lepton number conservation, $U(1)_Y$ is the gauge invariance (then is actually a local symmetry), $U(1)_{PQ}$ rotates both D_R and E_R in the same way and $U(1)_E$ rotates only E_R.

When considering $Y^{u,d,e} \neq 0$, the flavor symmetry G_f is broken down to a smaller group:

$$G_f \to U(1)_B \times U(1)_e \times U(1)_\mu \times U(1)_\tau \ , \tag{2.13}$$

that is the well-known global accidental symmetry group of the SM (we have no longer considered the $U(1)_Y$ gauge symmetry, that of course is not an accidental global symmetry). Actually, one of the $U(1)$ factors, namely $B + L_e + L_\mu + L_\tau$, is anomalous. Thus the conserved quantum numbers of the SM, deriving from exact accidental global symmetries, are

$$\frac{1}{3}B - L_f, \qquad f = \{e, \mu, \tau\} \ . \tag{2.14}$$

We are now able to count the number of free physical parameters contained in the three $Y^{u,d,e}$ matrices, that is the free parameters of $\mathcal{L}_{\text{Yukawa}}$. Each matrix has 18 parameters (9 real numbers and 9 phases), then giving 54 parameters overall. However, every generator of G_f broken by the Y matrices imply an arbitrariness in the choice of the fermion basis, that reduce by one the number of physical parameters. In other words, if we use a broken generator to perform a rotation (2.11), then $\mathcal{L}_{\text{Yukawa}}$ will go through the transformation

$$\mathcal{L}_{\text{Yukawa}}(Y^u, Y^d, Y^e) \to \mathcal{L}_{\text{Yukawa}}(\tilde{Y}^u, \tilde{Y}^d, \tilde{Y}^e) \ , \tag{2.15}$$

with:

$$Y^u \to \tilde{Y}^u = V_Q^\dagger Y^u V_U \ , \tag{2.16a}$$

$$Y^d \to \tilde{Y}^d = V_Q^\dagger Y^d V_D \ , \tag{2.16b}$$

---

[5]Actually, the exact relation would be $U(3) \cong SU(3) \times U(1)/\mathbb{Z}_3$, but this subtlety does not play any role in the following discussion and we have stated it here only for completeness.

$$Y^e \to \tilde{Y}^e = V_L^\dagger Y^e V_E \ , \tag{2.16c}$$

while the rest of the Lagrangian (2.7) remains unchanged. But this means that the two sets $\{Y^u, Y^d, Y^e\}$ and $\{\tilde{Y}^u, \tilde{Y}^d, \tilde{Y}^e\}$, being related simply by a change of basis, are different representations of the same physical theory. Thus, the parameter associated with this change of basis is non-physical.

Then, being $\dim(G_f) = 45$ (corresponding to 15 real parameters and 30 phases), while the residual symmetry group[6] has dimension 4 (all phases), we can think of 41 parameters of the Y matrices as non-physical, leaving us with 13 physical one (12 real constants and 1 phase), as anticipated.

To understand the meaning of the free parameters of $\mathcal{L}_{\text{Yukawa}}$ it is useful to distinguish between the quark and the leptonic sector, starting from the latter, that has a simpler structure. For leptons, the pattern of flavor symmetry breaking is

$$U(3)_L \times U(3)_E \to U(1)_e \times U(1)_\mu \times U(1)_\tau \ . \tag{2.17}$$

Carrying on the same argument outlined above, this time for leptons only, we find that Y^e has 3 physical parameters, all real; these are nothing but the charged lepton masses.

Indeed, it is always possible to perform a change of basis (2.11) that makes the Y^e matrix diagonal; in other words, they always exist two unitary matrices V_L and V_E such that, according to Eq. (2.16c), $\tilde{Y}^e$ is diagonal, a procedure known as biunitary diagonalization. In such a basis, after EWSB and considering only the Higgs VEV contribution, this term becomes:

$$\mathcal{L}_{mass}^e = \sum_{i=1}^{3} \frac{v}{\sqrt{2}} \tilde{Y}_{ii}^e \bar{E}_{Li} E_{Ri} \ , \tag{2.18}$$

that is exactly a mass term for the charged fermions; the three eigenvalues of $\tilde{Y}^e$ being related to the masses of each family.

The discussion for the quark sector is more involved, since this time we are dealing with two Yukawa matrices, for the up-type and for the down-type quarks respectively. All the difficulties arise because, as can be easily seen looking at the transformation properties (2.16a) and (2.16b), this time it is not generally possible to simultaneously diagonalize both Y^u and Y^d with a transformation belonging to G_f, since the same matrix V_Q appear twice.

Instead, the best that can be done within G_f is to reach a basis of this kind:

$$Y^d = y^d \ , \quad Y^u = V_{CKM}^\dagger y^d \ , \tag{2.19}$$

where $y^{d,u}$ are diagonal,

$$y^d = \text{diag}(y^d, y^s, y^b) \ , \quad y^u = \text{diag}(y^u, y^c, y^t) \ , \tag{2.20}$$

---

[6]Why we does not count $U(1)_Y$ among the unbroken generators, allowing it to act as a change of basis instead, is a subtle point. The reason is that if we refer to $U(1)_Y$ as a rotation of only the fermion fields (not rotating the ϕ doublet), then the Yukawas breaks this "fake" $U(1)_Y$ symmetry, that thus can be used to reduce the physical parameters.

and V_{CKM} is a unitary matrix, known as the Cabibbo-Kobayashi-Maskawa (CKM) matrix:

$$V_{CKM} = \begin{pmatrix} Vud & Vus & Vub \\ Vcd & Vcs & Vcb \\ Vtd & Vts & Vtb \end{pmatrix} . \qquad (2.21)$$

The CKM matrix is of crucial importance for flavor physics because, in a certain manner, this matrix contains all the information about the flavor structure of the quark sector. We can also see it as a parametrization of the misalignment between Y^u and Y^d, since for $Y^u = Y^d$ we would have $V_{CKM} = \mathbb{1}$.

If we analyse the structure of the quark part of $\mathcal{L}_{\text{Yukawa}}$ in this basis, we see that after EWSB the mass terms for the up sector are not diagonal in flavor space. Indeed, again focusing only on the Higgs VEV contribution, we have:

$$\mathcal{L}^q_{mass} = \sum_{i=1}^{3} \frac{v}{\sqrt{2}} y_i^d \bar{D}_{Li} D_{Ri} + \sum_{i,j=1}^{3} \frac{v}{\sqrt{2}} (V^\dagger_{CKM})_{ij} y_j^u \bar{U}_{Li} U_{Rj} . \qquad (2.22)$$

However, we are often interested in dealing with mass eigenstates, since they are the experimentally detectable and distinguishable ones. As already discussed, to reach a mass-diagonal basis we are forced to perform a rotation that should still be unitary (in order to preserve the canonical kinetic terms) but explicitly breaks the flavor symmetry G_f:

$$U_{Li} \to (V_{CKM})^\dagger{}_{ij} U_{Lj} , \qquad (2.23)$$

in particular, this rotation (often referred to as the switch from the *interaction basis* to the *mass basis*) violates what we have called $SU(3)_Q$, because we are rotating only one component of the $SU(2)_L$ doublet. As a consequence, this change of basis affects only the interactions that distinguish between doublet components, that are the electroweak interactions and the Yukawa interactions. Since the latter (that are the interactions between the fermions and the Higgs boson) are made flavor-diagonal by the above change of basis, in the mass basis only weak interactions can mediate flavor violating processes.

In the interaction basis, the electroweak interaction terms in the quarks sector are described by the following Lagrangian:

$$\mathcal{L}_{\text{int}} = \mathcal{L}_{\text{CC}} + \mathcal{L}_{\text{NC}} , \qquad (2.24)$$

where the *charged current* interactions are described by:

$$\mathcal{L}_{\text{CC}} = \frac{g}{\sqrt{2}} (J_\mu^+ W^{+\mu} + \text{h.c.}) , \qquad (2.25)$$

$$J_\mu^{I+} = \sum_{i=1}^{3} \bar{U}_{Li} \gamma_\mu D_{Li} , \qquad (2.26)$$

and the *neutral current* interactions by:

$$\mathcal{L}_{\text{NC}} = e J_\mu^{em} A^\mu + \frac{g}{\cos\theta_W} J_\mu^0 Z^\mu , \qquad (2.27)$$

$$J_\mu^{I,em} = \sum_f Q_f \bar{\Psi}_f \gamma_\mu \Psi_f \ , \tag{2.28}$$

$$J_\mu^{I0} = \sum_f \bar{\Psi}_f \gamma_\mu (v_f - a_f \gamma_5) \Psi_f \ , \tag{2.29}$$

$$v_f = \frac{1}{2} T_3^f - Q_f \sin^2 \theta_W \ , \qquad a_f = \frac{1}{2} T_3^f \ , \tag{2.30}$$

where Q_f and T_3^f are the charge and the third component of the weak isospin, and θ_W is the Weinberg angle. The superscript 'I' reminds that these expressions are valid in the interaction basis.

An inspection of the above Lagrangian leads to the conclusion that only charged current interactions feels the change of basis (2.23), i.e. the misalignment between the mass basis and the interaction basis; in other words, at tree level only *Flavor Changing Charged Currents* (FCCC) are admitted in the SM, while *Flavor Changing Neutral Currents* (FCNC) can only appear at one-loop order. In the mass basis, the new $\mathcal{L}_{\text{CC}}$ reads:

$$\mathcal{L}_{\text{CC}} = \frac{g}{\sqrt{2}} \left((V_{CKM})_{ij} \bar{U}_{Li} \slashed{W}^+ D_{Lj} + (V_{CKM})_{ij}^\dagger \bar{D}_{Li} \slashed{W}^- U_{Lj} \right) \ , \tag{2.31}$$

where a sum over flavor indices is understood.

If the SM description of flavor physics is correct, the Lagrangian (2.31) is the only source of all flavor changing processes and the CKM matrix fully parametrize this behaviour. Further, this is also the only Lagrangian term that could in principle violate the CP symmetry, if V_{CKM} is not real (as it is the case). Then in the SM it also happens that CP and flavor violations are connected, in the sense that CP violation occurs only in flavor violating processes. This is not true in generic NP models, where new flavor-blind CP violating phases can be inserted.

2.1.3 The CKM matrix

Coming back to parameter counting, applying it to the quark sector gives us 9 real constants and one phase. According to Eq. (2.20), six real parameters are associated with the masses of the six quarks (i.e. to the eigenvalues of the Yukawa matrices $Y^{u,d}$); thus the CKM matrix can be parametrized through three real numbers and a complex phase. There is not a unique way to perform this parametrization, the most used are the standard parametrization [25] and the Wolfenstein parametrization [26].

The standard parametrization of the CKM matrix in terms of three rotational angles (θ_{ij}) and one complex phase (δ) is

$$V_{CKM} = \begin{pmatrix} c_{12}c_{13} & s_{12}c_{13} & s_{13}e^{-i\delta} \\ -s_{12}c_{23} - c_{12}s_{23}s_{13}e^{i\delta} & c_{12}c_{23} - s_{12}s_{23}s_{13}e^{i\delta} & s_{23}c_{13} \\ s_{12}s_{23} - c_{12}c_{23}s_{13}e^{i\delta} & -s_{23}c_{12} - s_{12}c_{23}s_{13}e^{i\delta} & c_{23}c_{13} \end{pmatrix} \ , \tag{2.32}$$

where $c_{ij} = \cos \theta_{ij}$ and $s_{ij} = \sin \theta_{ij}$ ($i,j = 1,2,3$). Their values are approximately $s_{12} \simeq 0.22$, $s_{23} \simeq 0.042$, $s_{13} \simeq 0.0041$ and $\delta \simeq 69°$ [22].

Given the above values, the off-diagonal elements of the CKM matrix show a strongly hierarchical pattern: $|V_{us}|$ and $|V_{cd}|$ are close to 0.22, the elements $|V_{cb}|$

and $|V_{ts}|$ are of order 4×10^{-2} whereas $|V_{ub}|$ and $|V_{td}|$ are of order 5×10^{-3}. The Wolfenstein parametrization, being an approximate expansion of the CKM matrix elements as a power series in the small parameter $\lambda \equiv |Vus| \simeq 0.22$, is a convenient way to exhibit this hierarchy in a more explicit way. At the third order it gives:

$$V_{CKM} = \begin{pmatrix} 1 - \frac{\lambda^2}{2} & \lambda & A\lambda^3(\rho - i\eta) \\ -\lambda & 1 - \frac{\lambda^2}{2} & A\lambda^2 \\ A\lambda^3(1 - \rho - i\eta) & -A\lambda^2 & 1 \end{pmatrix} + \mathcal{O}(\lambda^4) , \qquad (2.33)$$

and then the four free parameters in this representation of V_{CKM} are

$$\lambda, \quad A, \quad \rho, \quad \eta , \qquad (2.34)$$

where the $\{\rho, \eta\}$ pair gives rise to the physical complex phase. Sometimes the following redefinitions of these last two parameters are used [3]:

$$\bar{\rho} = \rho \left(1 - \frac{\lambda^2}{2}\right) + \mathcal{O}(\lambda^4) , \qquad \bar{\eta} = \eta \left(1 - \frac{\lambda^2}{2}\right) + \mathcal{O}(\lambda^4) , \qquad (2.35)$$

the reason being convenience when extending the Wolfenstein parametrization to higher orders.

For what discussed above, in the SM all the flavor physics in the quark sector is described by the Lagrangian (2.31) and then by the CKM matrix. This in turn implies severe constraints on flavour changing processes, that can be experimentally tested in order to verify the correctness of the SM description.

A first class of such constraints comes from the unitarity of V_{CKM}. Indeed, from the very definition of a unitary matrix, the following relations should hold:

$$\sum_{k=1,2,3} V_{ik}^* V_{ki} = 1 , \qquad (2.36a)$$

$$\sum_{k=1,2,3} V_{ik}^* V_{kj} = 0 \qquad \text{for } i \neq j , \qquad (2.36b)$$

These relations are a distinctive feature of the SM, therefore every deviation from them would be a clean signal of new physics. Among the relations (2.36b), the one obtained for $i = 1$ and $j = 3$, namely

$$V_{ud}V_{ub}^* + V_{cd}V_{cb}^* + V_{td}V_{tb}^* = 0 \qquad (2.37)$$

$$\text{or} \quad \frac{V_{ud}V_{ub}^*}{V_{cd}V_{cb}^*} + \frac{V_{td}V_{tb}^*}{V_{cd}V_{cb}^*} + 1 = 0 ,$$

is particularly interesting since it involves the sum of three terms all of the same order in λ. This relation can be represented as a triangle in the complex plane, as shown in Fig. 2.1, and indeed Eq. (2.36b) is often referred to as the CKM unitarity triangle. Its sides R_t and R_b, as well as its angles α, β and γ (see Fig. 2.1) are accessible in many flavor changing observables, thus the consistency of Eq. (2.37) can be experimentally tested.

Moreover, since the CKM matrix depends only on four parameters, four independent physical observables are sufficient to completely determine it; after this procedure
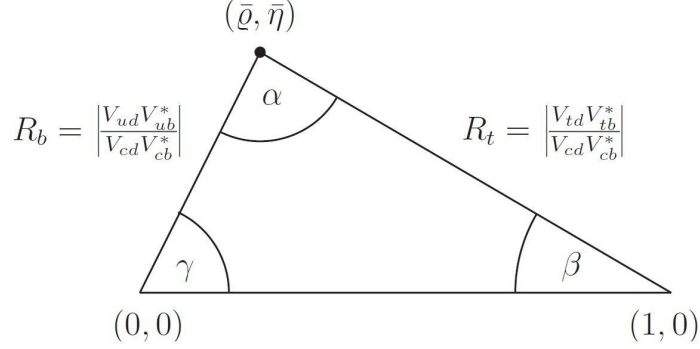
Figure 2.1: The CKM unitarity triangle.

is carried out, the theory becomes predictive and any other observable in flavor physics can be theoretically evaluated and compared with the experiments. The consistency of all these theoretical predictions with experiments represents another severe test of the SM description of flavor physics.

The numerical value of the first two parameters, λ and A, are known rather accurately [27] from, respectively, $K \to \pi l \nu$ and $b \to c l \nu$ decays:

$$\lambda = 0.22457^{+0.00186}_{-0.00014}\,, \qquad A = 0.823^{+0.012}_{-0.042}\,. \tag{2.38}$$

One can then express all the relevant observables as a function of the two remaining parameters, ρ and η, and check if there is a region in the $\rho - \eta$ plane that is consistent with all measurements. Among the most sensitive observables used to determine ρ and η are:

- The rates of inclusive and exclusive charmless semileptonic B decays depend on $|V_{ub}|^2 \propto \rho^2 + \eta^2$;

- The CP asymmetry in $B \to \psi K_S$, $S_{\psi K_S} = \sin 2\beta = \frac{2\eta(1-\rho)}{(1-\rho)^2+\eta^2}$;

- The rates of various $B \to DK$ decays depend on the phase γ, where

$$e^{i\gamma} = \frac{\rho + i\eta}{\sqrt{\rho^2 + \eta^2}}\;;$$

- The rates of various $B \to \pi\pi, \rho\pi, \rho\rho$ decays depend on the phase

$$\alpha = \pi - \beta - \gamma\;;$$

- The ratio between the mass splitting in the neutral B_d and B_s systems is sensitive to $|V_{td}/V_{ts}|^2 = \lambda^2[(1 - \rho)^2 + \eta^2]$;

- The CP violation in $K \to \pi\pi$ decays, ϵ_K, depends in a complicated way on ρ and η.
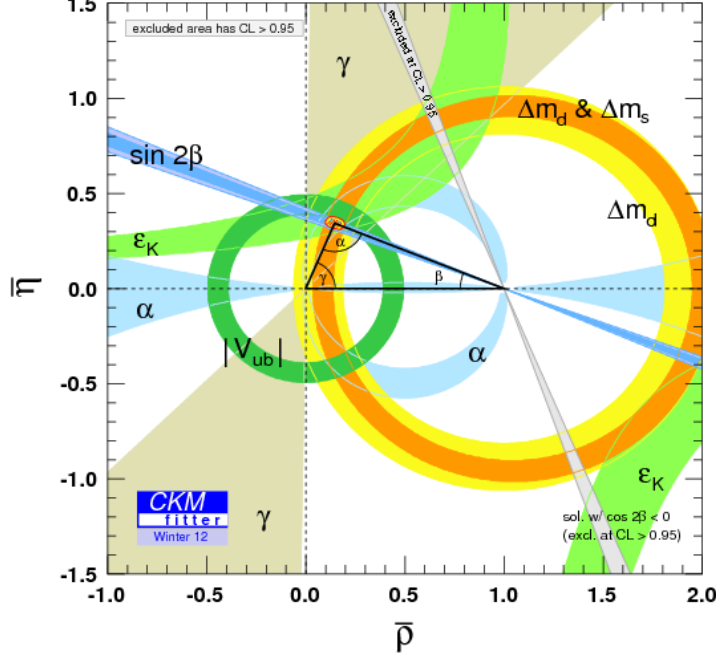
Figure 2.2: Allowed region in the $\rho - \eta$ plane [27]. Superimposed are the individual constraints from charmless semileptonic B decays ($|V_{ub}|$), mass differences in the B_d (Δm_d) and B_s (Δm_s) systems, CP violation in the neutral kaon (ε_K) and in the B_d systems ($\sin 2\beta$), the combined constrains on α and γ from various B decays.

The resulting constraints are shown in Fig. 2.2.

The consistency of the various constraints is impressive. In particular, the following numerical values for the $\bar{\rho}$ and $\bar{\eta}$ parameters can account for all the measurements [22]:

$$\bar{\rho} = 0.131^{+0.026}_{-0.013}, \qquad \bar{\eta} = 0.345^{+0.013}_{-0.014} \, . \tag{2.39}$$

From the above picture it is clear that the SM is very successful in describing flavor physics and we can come to the conclusion that very likely the CKM mechanism is the dominant source of flavor and CP violation in flavor changing processes. A compelling question is then if there exist still room for NP contributions and, if it is the case, why they are so suppressed with respect to the SM. The rest of this chapter will discuss these questions in detail.

2.2 Effective field theories

In order to describe NP effects in flavor physics, we can follow two main strategies: (i) to build an explicit UV completion of the model, or (ii) to analyse the NP effects using an EFT approach. The former approach is more predictive, but also more model-dependent and it will be used in next chapters. The latter has the advantage of furnishing a very general description of NP effects at low energies using a limited

number of parameters, but it has the drawback to shed much less light on the NP scenarios at high energies that could arise. We will use the second approach for the rest of this chapter.

While building an UV completion, one has to specify which are the new fields beyond the SM ones. Instead, in an EFT approach one assumes the new heavy fields to have been integrated-out as dynamical degrees of freedom, this giving rise to new terms in the Lagrangian. We can then parametrize NP contributions using the coefficients associated with these new Lagrangian terms:

$$\mathcal{L}_{\text{eff}} = \mathcal{L}_{\text{SM}} + \sum C_i^{(d)} Q_i^{(d)}(\text{SM fields}) , \qquad (2.40)$$

where $Q_i^{(d)}$ are generic operators of dimension d and $C_i^{(d)}$ are their associated coefficients, referred to as the *Wilson coefficients*, whose mass dimension is $[C_i^{(d)}] = 4 - d$. Since $\mathcal{L}_{\text{SM}}$ is the most general Lagrangian (compatible with the SM symmetries and using SM fields) with operators of dimension $d \leq 4$, the operators $Q_i^{(d)}$ should have $d > 4$.

Since there always exists an infinite number of such operators, the question of whether such a theory could be predictive or not naturally arises. This is where the simple, but powerful trick of "naive dimensional analysis" comes to play. Calling Λ the mass scale of the underlying physics generating the effective operator $Q_i^{(d)}$, we can decompose its Wilson coefficient in the following way:

$$C_i^{(d)} = \frac{c_i}{\Lambda^{d-4}} , \qquad (2.41)$$

where c_i is a dimensionless coefficient, that can be thought of $\mathcal{O}(1)$, according to the naturalness concept of section 1.3. Then, Eq. (2.40) can be recast as:

$$\mathcal{L}_{\text{eff}} = \mathcal{L}_{\text{SM}} + \sum \frac{c_i}{\Lambda^{d-4}} Q_i^{(d)}(\text{SM fields}) . \qquad (2.42)$$

Eq. (2.42) allows us to implement a perturbative approach that makes the EFT predictive as long as we are studying low energy processes, i.e. processes at energies $E \ll \Lambda$. Indeed, in that case we can associate with the contribution of the operator $Q_i^{(d)}$ a suppression factor $(\frac{E}{\Lambda})^{d-4} \ll 1$; then, the higher the dimension of an effective operator, the higher the suppression factor arising from dimensional analysis. Consequently, we can restrict ourself to considering only the operators of lowest dimension contributing to the process under study, since they give rise to the bigger corrections to the SM predictions.

It is important to stress that an EFT approach is justified (and then predictive) only as long as this perturbative analysis holds. But, in the low energy regime, an EFT is usable and useful exactly as a renormalizable theory. The only difference being that in the first case we already know that the theory has an ultimate cutoff at which an UV completion is needed, whereas in the second case the theory, from the mathematical point of view, is consistent at every energy scale.

2.2.1 Generalities on EFT

Already within the SM, i.e. when the full renormalizable theory is known and understood, it can be useful to adopt an EFT approach. In that case, the main advantage

is a practical one, since typically in EFTs the computations are simpler with respect to the full theory.

The most notable examples of such a situation are weak mediated decay and flavor oscillation processes. In these cases, the use of an effective approach is naturally suggested by the presence of two different energy scales: the weak interactions scale (~ 100 GeV), which mediate the processes, and the mass scale of the particles under analysis, either leptons (e.g. $m_\mu \simeq 100$ MeV) or hadrons (e.g. $m_K \simeq 500$ MeV).

According to this technique, when considering low energy processes ($E \ll M_W$), we can integrate out the $W^\pm$ bosons from the SM Lagrangian, and work out the observables with the new theory obtained, that is nothing but the well-known Fermi theory of weak interactions:

$$\mathcal{L}_{\text{weak}}^{\text{eff}} = -\frac{4G_F}{\sqrt{2}}\, J_\mu^+ J^{-\mu} \,, \tag{2.43}$$

$$J_\mu^+ = (V_{CKM})_{ij}\, \bar{u}_{Li}\gamma_\mu d_{Lj} + \bar{\nu}_{Li}\gamma_\mu l_{Li} \,, \qquad J_\mu^- = (J_\mu^+)^\dagger \,, \tag{2.44}$$

with G_F the Fermi constant ($G_F = 1.16639 \cdot 10^{-5}$ GeV^{-2}). The Lagrangian (2.43) can then be used to calculate tree level amplitudes in substitutions to the SM Lagrangian.

Thus, at the tree level, EFTs provide a simpler framework for performing computations. But, beyond the tree approximation, the question arises of how to account for the effects of the strong interactions in the derivation of the effective Lagrangian.

To overcome this difficulty, a general procedure called "matching" is used [4]. It consists of the following steps:

1. To list all possible gauge-invariant operators of a given dimension allowed by the symmetries and the quantum numbers associated with a given problem. Generally, for calculations in flavor physics ones consider only $d = 6$ operators.

2. To write down the effective Lagrangian with undetermined Wilson coefficients C_i:

$$\mathcal{L}_{\text{weak}}^{\text{eff}} = \sum C_i Q_i^{(6)} \,. \tag{2.45}$$

3. To determine the values of the coefficients C_i such that

$$\mathcal{M}_n = \langle f_n | \mathcal{L}_{\text{SM}} | i_n \rangle \overset{!}{=} \sum C_i \langle f_n | Q_i | i_n \rangle + \text{higher order terms} \,, \tag{2.46}$$

by computing a sufficient number of amplitudes $\mathcal{M}_n$ to a given order in perturbation theory, both using the full theory and the EFT.

With the above procedure, one determines the Wilson coefficients C_i that makes the predictions of the effective Lagrangian (2.45) merge at a given order with the SM ones.

If the underlying theory is weakly coupled, it is obvious that all these computations can be carried out using perturbation theory. But QCD becomes strongly coupled at low energies, thus we have to further justify the use of perturbation theory also in this case.

The crucial point is that the we can still determine the C_i perturbatively if the theory is weakly coupled at high energy (asymptotic freedom at short distances).

To understand this point, one has to think about the meaning of the expansions (2.42) and (2.45): the operators Q_i represent the long-distance processes that we want to describe, while the Wilson coefficients C_i parametrize our ignorance of the underlying short-distance physics mediating these processes; the discriminant between long-distance (i.e. small momentum) and short-distance (i.e. high momentum) effects being the energy scale Λ. Thus, the coefficients C_i are influenced only by the physics above the cutoff scale; as long as the theory is weakly coupled at and above the scale Λ, the Wilson coefficients are calculable perturbatively.

In particular, regarding the QCD corrections to weak hadronic processes, they influence the computations of the r.h.s. of the matching conditions (2.46) in two different ways: long-distance, non-perturbative QCD effects enter in the computations of $\langle f_n | Q_i | i_n \rangle$ (in the form of hadronic matrix elements), while only short-distance, perturbative loop effects modify the C_i values. The perturbative approach is then justified.

Once defined how to consistently perform the calculations for the matching conditions (2.46), another problem arises: since (2.45) define no more a renormalizable theory, generally the standard renormalization procedure of the SM does not completely eliminate the divergences from the physical amplitudes of the theory. Therefore, an additional renormalization, referred to as *operator renormalization* [4, 3], is necessary:

$$Q_i^{(0)} = Z_{ij} Q_j \ , \tag{2.47}$$

where, here and after, the '0' index indicates unrenormalized (bare) quantities. Two remarks are in order:

First, we can see that in the general case the renormalization constant Z_{ij} is a matrix. This means that, even when starting with a Lagrangian with only one operator, after the renormalization procedure we could possibly find non vanishing C_i coefficients even for others operators different from the starting one. This effect is referred to as *operator mixing*. In principle, every operator could mix with every other operator with the same dimension[7], but certain mixings could be forbidden by symmetries.

Second, it is useful to point out that one can think of the operator renormalization, which sounds like a new concept, in terms of the completely equivalent, but more customary, renormalization of the coupling constants C_i. This is clear, since the bare terms appearing in the (2.45) Lagrangian are of the form:

$$C_i^{(0)} Q_i^{(0)} = Z_{ij} C_i Q_j \ , \tag{2.48}$$

and we can as well think of them as the result of the renormalization procedure

$$C_i^{(0)} = Z_{ji} C_j \tag{2.49}$$

carried on the Wilson coefficients.

At this point, it seems that the procedure leading from the generic Lagrangian (2.45) to a predictive theory has been completely settled. However, in our justification

---

[7]This is because, in the $\overline{\text{MS}}$ scheme, Z_{ij} is dimensionless. In a general mass-dependent scheme, operators can also mix with operators of lower dimension.

of the perturbative approach to the matching conditions, we have neglected one detail that could in principle spoil all that argument.

Indeed, while computing in perturbation theory amplitudes of processes involving different energy scales, typically large logarithms appear. For example, for weak hadronic processes, at the leading order we always meet the quantity

$$\alpha_s \log \frac{M_W}{\mu} \sim \mathcal{O}(1) \ , \tag{2.50}$$

where μ is a mass characteristic of the process under study, such as the mass of the decaying particle (then $\mu \ll M_W$). But thus, a perturbative expansion in the small parameter $\alpha_s = g_s^2/4\pi$ is undermined by the presence of this large logarithm.

The solution to this problem, already present in ordinary QFT, is employing the method of the *renormalization group* (RG). The renormalization group equations (RGEs) describe the change of renormalized quantities, Green functions and parameters, with the renormalization scale μ in a differential form. Solving at the leading (i.e. one-loop) order these equations allows to sum up the terms $(\alpha_s \log \frac{M_W}{\mu})^n$ to all order in perturbation theory. For this reasons, this approximation is referred to as leading logarithmic approximation (LLA). In this framework, the next-to-leading order approximation (referred to as next-to-leading logarithmic approximation, NLLA) would be to sum up, again via RGEs, all the terms of the kind $\alpha_s(\alpha_s \log \frac{M_W}{\mu})^n$ [3].

The employment of the RG method allows to restore a perturbative approach, the so-called RG improved perturbation theory. First, the matching conditions are computed at the cutoff scale, then in our case we would have $\mu \sim M_W$. This prevents the appearance of large logarithms, and the ordinary perturbation theory can be applied at the desired order, say k. Only after the matching procedure is carried out, the RGEs are used to "run" the Wilson coefficients from their high energy to their low energy value, where they can be used to compute physical observables. This last procedure corresponds to sum all the contributions of the kind $\alpha_s^i(\alpha_s \log \frac{M_W}{\mu})^n$, to all order in n and for $i \leq k$.

We have already discussed the generalities about the matching procedure, we now briefly describe how to perform the running of the Wilson coefficients using the RGEs [3, 4]. The RGEs for the C_i follows from the fact that the bare Wilson coefficients $C_i^{(0)}$ are independent from the renormalization scale μ. Then, recasting Eq. (2.49) writing explicitly the μ dependence of the quantities, we have:

$$\vec{C}^{(0)} = Z^T(\mu)\vec{C}(\mu) \ , \tag{2.51}$$

and, differentiating this equation, we get

$$\frac{\mathrm{d}}{\mathrm{d} \log \mu}\vec{C}(\mu) = \gamma^T \vec{C}(\mu) \ , \tag{2.52}$$

where we have defined the anomalous dimension $\gamma(\alpha_s)$ as:

$$\gamma = Z^{-1}\frac{\mathrm{d}}{\mathrm{d} \log \mu}Z \ , \tag{2.53}$$

Note that, in the absence of QCD loop corrections, the couplings $\vec{C}$ would be μ-independent. The non-trivial μ-dependence of $\vec{C}$ expressed in (2.52) is a genuine

quantum effect, that imply an anomalous scaling behaviour of $\vec{C}$. For this reason, the factor γ is called anomalous (scale) dimension.

The renormalization constant Z, and then the anomalous dimension γ, can be computed using ordinary perturbation theory. Once these quantities are found, the differential equation (2.52) can be solved:

$$C_i(\mu) = P \exp \left[\int_{g(M_W)}^{g(\mu)} \frac{\gamma^T(g)}{\beta(g)} \mathrm{d}g \right]_{ij} C_j(M_W) \,, \tag{2.54}$$

where P denotes "coupling constant ordering" of the anomalous dimension matrices, and $C_j(M_W)$ are the values of the Wilson coefficients found via the matching procedure.

In conclusion, we have seen that the employment of the RG improved perturbation theory allows to consistently implement a perturbative procedure that leads to an effective low-energy Lagrangian, giving an easier framework for phenomenological computations in substitution to the SM one.

2.2.2 EFT, new physics and flavor physics

Even though they can be useful also within the SM, as discussed above, EFTs show their full potentialities when studying NP scenarios, where the UV completion of the theory is unknown. In those cases, one can fully parametrize NP contributions by a limited number of parameters, the Wilson coefficients c_i associated with the higer-dimensional operators. Recalling Eq. (2.42):

$$\mathcal{L}_{\mathrm{eff}} = \mathcal{L}_{\mathrm{SM}} + \sum \frac{c_i}{\Lambda^{d-4}} Q_i^{(d)}(\text{SM fields}) \,.$$

As already discusses at the beginning of this section, the higher the dimension of an effective operator, the higher the suppression factor arising from dimensional analysis. Then, what is usually done is to focus on dimension six operators, that are often the lowest-dimension operators giving rise to corrections to the process under study[8]. For this reason, all dimension six operators compatible with the SM symmetries had been studied and a complete list of them can be found in literature ([20, 28]).

The procedure, when dealing with EFTs parametrizing NP, is usually the following:

1. To take from the complete list of $d = 6$ operators the ones that contribute to the process of interest. To associate with any of them an unknown Wilson coefficient and to build up the effective Lagrangian (2.42).

2. To compute physical observables using the obtained Lagrangian, expressing the result as a function of the c_i and the NP scale Λ.

---

[8]As already pointed out in section 1.2, there exists only one dimension 5 operator compatible with the SM symmetries, see Eq. (1.2), and it usually does not give contribution to processes of interest.

3. To compare the results with present experimental bounds, in order to derive constraints about either the Wilson coefficients c_i or the NP scale Λ. In the former case, one assumes NP to arise at a certain energy scale (typically the TeV scale, as argued in section 1.4), deriving an upper limit for the c_i. In the latter case, one assumes $c_i \sim \mathcal{O}(1)$ (on the ground of naturalness considerations) and derive a lower limit for Λ.

It is clear that, in order to improve the experimental constraints on NP parameters, it is worthwhile to focus on physical observables that are highly suppressed within the SM, in order to reduce the background noise arising from SM-mediated processes when looking for NP effects.

This request strongly suggests to use FCNC processes as NP probes. Indeed, for this class of processes the corresponding amplitudes are suppressed for many reasons:

- First, as discussed in section 2.1, all flavor changing processes can only be mediated by weak interactions, then their associated amplitudes are suppressed by the weakness of such interactions at low energies.

- Second, all flavor changing processes must involve at least one off-diagonal element of the CKM matrix. Being this matrix hierarchical, its off-diagonal elements introduce a suppression factor, referred to as CKM suppression.

- FCNC are further suppressed for two reasons. First, they are absent at tree level and only appear at the one-loop order, then their amplitudes are loop-suppressed. Also, the unitarity of the CKM matrix implies a further cancellation of the leading one-loop contributions to these amplitudes, as a direct consequence of the relations (2.36b). This additional suppression is known as GIM mechanism.

- In the leptonic sector, flavor violating transitions are completely forbidden by the accidental symmetries of the SM[9].

The phenomenology of flavor violating processes is very various and many means of classification can be used. We have already introduced the distinction between FCCC and FCNC (section 2.1). Another common method of classification made use of the amount by which the flavor quantum numbers are violated. According to this notation, a $\Delta F = 1$ transition involves a violation by one unit of one flavor quantum number (e.g. a weak decay such as $K^+ \to \pi^+\pi^0$), while $\Delta F = 2$ denotes processes with an overall violation of flavor quantum numbers by two units (e.g. neutral meson oscillations such as $K^0 \to \bar{K}^0$ transitions).

All these considerations make the flavor violating processes an hard test for the SM predictions and a sensitive probe of NP contributions. As discussed in section 2.1, until now the SM picture completely fits experiments; thus, the flavor physics phenomenology is a powerful tool to impose severe constraints to NP scenarios, via EFTs.

---

[9]To be fair, anomalies arising at the one-loop level spoils these symmetries, but the corresponding amplitudes are absolutely negligible.

Operator	Bounds on Λ		Bounds on c_i		Observables
	Re (TeV)	Im (TeV)	Re	Im	
$(\bar{s}_L \gamma^\mu d_L)^2$	9.8×10^2	1.6×10^4	9.0×10^{-7}	3.4×10^{-9}	ΔM_K; ϵ_K
$(\bar{s}_R d_L)(\bar{s}_L d_R)$	1.8×10^4	3.2×10^5	6.9×10^{-9}	2.6×10^{-11}	ΔM_K; ϵ_K
$(\bar{c}_L \gamma^\mu u_L)^2$	1.2×10^3	2.9×10^3	5.6×10^{-7}	1.0×10^{-7}	ΔM_D; $|q/p|$
$(\bar{c}_R u_L)(\bar{c}_L u_R)$	6.2×10^3	1.5×10^4	5.7×10^{-8}	1.1×10^{-8}	ΔM_D; $|q/p|$
$(\bar{b}_L \gamma^\mu d_L)^2$	6.6×10^2	9.3×10^2	2.3×10^{-6}	1.1×10^{-6}	ΔM_{B_d}; $S_{\psi K_S}$
$(\bar{b}_R d_L)(\bar{b}_L d_R)$	2.5×10^3	3.6×10^3	3.9×10^{-7}	1.9×10^{-7}	ΔM_{B_d}; $S_{\psi K_S}$
$(\bar{b}_L \gamma^\mu s_L)^2$	1.4×10^2	2.5×10^2	5.0×10^{-5}	1.7×10^{-5}	ΔM_{B_s}; $S_{\psi\phi}$
$(\bar{b}_R s_L)(\bar{b}_L s_R)$	4.8×10^2	8.3×10^2	8.8×10^{-6}	2.9×10^{-6}	ΔM_{B_s}; $S_{\psi\phi}$

Table 2.1: Bounds on representative dimension six $\Delta F = 2$ operators, assuming an effective coupling c_i/Λ^2 [29]. The bounds are quoted on Λ, setting $|c_i| = 1$, or on c_i, setting $\Lambda = 1$ TeV. The right column denotes the main observables used to derive these bounds, all to be discussed in appendix A.1.

Summarising what outlined above, we can use dimension six operators in an EFT approach to derive bounds either on the Wilson coefficients of the effective Lagrangian or on the NP scale. The flavor physics, providing processes highly suppressed within the SM, furnishes an important framework where these constrains can be enhanced by many orders of magnitude.

In Table 2.1 are summarised the constraints, derived using flavor physics observables, for representative $\Delta F = 2$ dimension six operators. A detailed description of the physical processes and the corresponding observables used to derive such constraints is given in appendix A.1. For the time being, let us just present an overview of the general conclusions that can be drawn by a thorough analysis. Reading the table, a tension between a natural choice for the c_i and the assumption $\Lambda \sim$ TeV is evident. As a consequence, NP models with generic (anarchical) flavor structures ($c_i \sim \mathcal{O}(1)$) at the TeV scale are definitely ruled out. This situation is sometimes called the *new physics flavor problem* (or puzzle): it is problematic to accommodate NP at the TeV scale when considering the constraints derived from flavor physics.

The only solution to readmit the existence of NP at the TeV scale, also preserving the validity of naturalness considerations regarding the Wilson coefficients, is to assume that BSM physics has an highly non-generic flavor structure, such that its contributions to flavor physics observables are sufficiently suppressed in order not to create tensions with the nowadays experimental bounds. In sections 2.3 and 3.2, we will discuss and compare in detail two different proposals of how this suppression could be achieved.

2.3 Minimal flavor violation

A very reasonable set up which solves the NP flavor problem is the so-called *Minimal Flavor Violation* (MFV) hypothesis. Under this assumption, the Yukawa couplings are the only source of flavor violating interactions also beyond the SM. As a result,

NP contributions to flavor violating transitions turn out to be suppressed to a level consistent with experiments even for $\Lambda \sim$ few TeV. One of the most interesting aspects of the MFV hypothesis is that it can be naturally implemented within the generic effective Lagrangian in Eq. (2.42). Furthermore, SM extensions where the flavor hierarchy is generated at a scale much higher than other dynamical scales tend to flow to the MFV class of models in the infrared.

The MFV hypothesis consists of two ingredients [6]: (i) a flavor symmetry and (ii) a set of symmetry-breaking terms. The symmetry is nothing but the large global symmetry G_{flavor} (2.10), which is the flavor symmetry of the SM Lagrangian in absence of the Yukawa couplings. As discussed in section 2.1, this symmetry is already broken within the SM, giving rise to flavor violating processes. Thus, it would be unreasonable to promote it to be an exact symmetry of the NP sector, and further such an imposed symmetry would be spoiled at the quantum level because of the SM contributions. Therefore, the best that can be done to protect in a consistent way flavor violating transitions from excessive TeV scale NP contributions is to assume that Y^u and Y^d are the only sources of flavor symmetry breaking also in the NP sector.

It is now necessary to implement in a mathematical manner the MFV concept. We start by recalling the notation of section 2.1 about the flavor symmetry, focusing on the quark sector. The flavor group is

$$U(3)_q^3 = SU(3)_q^3 \times U(1)^3 \ ,$$
$$SU(3)_q^3 = SU(3)_Q \times SU(3)_U \times SU(3)_D \ ,$$

under which the quark fields transform in the following way:

$$Q_{Li} \to (V_Q)_{ij} Q_{Lj} \ , \qquad U_{Ri} \to (V_U)_{ij} U_{Rj} \ , \qquad D_{Ri} \to (V_D)_{ij} D_{Rj} \ .$$

The symmetry $U(3)_q^3$ is broken by the Yukawa interactions (2.8c)

$$\mathcal{L}_{\text{Yukawa}} = -Y_{ij}^d \bar{Q}_{Li} \phi D_{Rj} - Y_{ij}^u \bar{Q}_{Li} \tilde{\phi} U_{Rj} + \text{h.c.} \ .$$

Watching the expression of $\mathcal{L}_{\text{Yukawa}}$, we notice that the flavor symmetry can be restored if we promote the Yukawa matrices Y^u and Y^d to be non-dynamical fields (*spurions*) with non-trivial transformation properties under $SU(3)_q^3$:

$$Y^u \sim (3, \bar{3}, 1) \ , \qquad\qquad Y^d \sim (3, 1, \bar{3}) \ , \tag{2.55}$$
$$Y^u \to V_Q Y^u V_u^\dagger \ , \qquad\qquad Y^d \to V_Q Y^d V_d^\dagger \ . \tag{2.56}$$

The SM Yukawa couplings can then be thought of as the background values of these spurionic fields. We can still perform a basis redefinition, and in particular from now on we will work in the basis with Yukawa backgrounds given by Eq. (2.19):

$$Y^d = y^d \ , \qquad\qquad y^d = \text{diag}(y^d, y^s, y^b) \ ,$$
$$Y^u = V^\dagger y^u \ , \qquad\qquad y^u = \text{diag}(y^u, y^c, y^t) \ .$$

All the above observations suggest a solution for implementing the MFV hypothesis directly on the effective Lagrangian (2.42): we will say that an effective theory

satisfies the MFV criterion in the quark sector[10] if all higher dimensional operators
are formally invariant under the flavor group $SU(3)_q^3$, under which the SM fields and
Yukawas transforms according to Eqs. (2.11) and (2.56), respectively.

This criterion is very effective in suppressing NP contributions to flavor violating
processes. Indeed, to satisfy the MFV prescription while building a flavor violating
operator, at least one insertion of the CKM matrix is needed; this is clear since in
our basis Y^u is the only flavor mixing spurion. But then, the leading amplitudes
generated by such operator will benefit of a CKM suppression, exactly as the SM
amplitudes.

Furthermore, working in the "minimal" case, where the two spurions $Y^{d,u}$ are
assumed to be the only sources also of CP violation (CPV), NP corrections to some
observables are completely cancelled by an alignment mechanism [5]. This is the case
e.g. for CP violating phases in neutral meson mixing. In that case, since both SM
and NP contributions have the same dependence on the CKM complex phase δ, they
clearly give the same CPV phase, that can be factored out, with no distinction from
the SM-alone case.

According to the MFV criterion, one should in principle consider operators with
arbitrary powers of the (dimensionless) Yukawa fields. However, a strong simplifi-
cation arises by the observation that all the eigenvalues of the Yukawa matrices are
small, but for the top one, and that the off-diagonal elements of the CKM matrix
are very suppressed. Thus, in our basis and neglecting the light quark masses with
respect to the top mass, we have:

$$\left[Y^u(Y^u)^\dagger\right]_{i\neq j}^n \simeq (y^t)^{2n} V_{ti}^* V_{tj} \ . \tag{2.57}$$

Consequently, at the leading order, including higher powers of the Yukawa matrices
leads only to a redefinition of the overall factor following the CKM suppression $V_{ti}^* V_{tj}$
(remember that $y^t \sim \mathcal{O}(1)$). This consideration makes more clear what argued above,
i.e. that the MFV hypothesis transfer the CKM suppression also to the NP sector.

The approximation (2.57) furnishes a great simplification for calculations, and
allows a simple framework to predict the suppression factor associated with a generic
higher dimension operator. To be specific, once identified the spurionic structure of
the operator under analysis, one can follow the Wolfenstein parametrization of the
CKM matrix elements (2.33), and carry out an expansion in power series of λ (the
sine of the Cabibbo angle). This procedure gives as a result the CKM suppression
associated with that operator.

Here follows an example of how these techniques can be used in practice. We will
work on a particular dimension six $\Delta F = 1$ operator, the so-called *electromagnetic
dipole operator*:

$$Q_{7\gamma} = \frac{em_b}{16\pi^2} F_{\mu\nu} \, \bar{s}_L \sigma^{\mu\nu} b_R \ . \tag{2.58}$$

Notice that this is really a dimension six operator, since its gauge-invariant form
should involve an additional Higgs doublet:

$$Q_{7\gamma} \propto eF_{\mu\nu} \, \phi \, \bar{Q}_L \sigma^{\mu\nu} D_R \ , \tag{2.59}$$

---

[10]The notion of MFV can be extended also to the lepton sector. However, in this case there is not
a unique way to define the minimal sources of flavour symmetry breaking if we want to keep track
of the non-vanishing neutrino masses [30].

but, after EWSB, the Higgs VEV combined with the Yukawa coupling for D_R (arising from the spurionic analysis we are about to carry out) becomes a mass term for the right-handed field, exactly as expresses in Eq. (2.58).

The first step is to identify the lowest order combination of spurionic fields $Y^{d,u}$ that makes $Q_{7\gamma}$ formally invariant under $SU(3)_q^3$; for this purpose, it is better to use the covariant expression (2.59). It is easy to verify that the sought combination is

$$Q_{7\gamma} \propto e F_{\mu\nu}\, \phi\, \bar{Q}_L Y^u Y^{u\dagger} Y^d \sigma^{\mu\nu} D_R \; . \tag{2.60}$$

After EWSB and using explicitly the b and s fields, we are left with

$$Q_{7\gamma} \propto e F_{\mu\nu}\, v \sum_k \bar{s}_L (Y^u Y^{u\dagger})_{2k} (Y^d)_{k3} \sigma^{\mu\nu} b_R \; . \tag{2.61}$$

Once identified the (leading order) spurionic structure of the operator, we can go further and calculate the suppression factor arising from such structure. In the case we are studying, applying Eqs. (2.19) and (2.57) we find:

$$Q_{7\gamma} \propto e F_{\mu\nu}(v y^b)(y^t)^2 V_{ts}^* V_{tb}\, \bar{s}_L \sigma^{\mu\nu} b_R \sim \lambda^2\, m_b \bar{s}_L \sigma^{\mu\nu} b_R \; . \tag{2.62}$$

In Eq. (2.62) we have recovered the m_b coefficient inserted in the definition (2.58). Furthermore, we have found the predicted suppression factor in the SM and in all NP models satisfying the MFV hypothesis. If we now consider the operator with opposite chiralities, namely:

$$Q_{7\gamma}' = \frac{e m_b}{16\pi^2} F_{\mu\nu}\, \bar{s}_R \sigma^{\mu\nu} b_L \; , \tag{2.63}$$

it is straightforward to verify that now one has:

$$Q_{7\gamma}' \sim \lambda^2\, m_s \bar{s}_R \sigma^{\mu\nu} b_L \; , \tag{2.64}$$

and thus the "wrong chirality" operator $Q_{7\gamma}'$ receives in MFV the same suppression factor m_s/m_b that one finds in the SM.

In an analogous manner, we can predict the suppression factor in MFV for the contribution of every higher dimension operator. Consequently, one can actually revise Tab. 2.1 by taking into account such suppressions.

The result of this analysis, carried out for some representative dimension six operators, can be seen in Tab. 2.2. The general result is that NP at the TeV scale satisfying the MFV paradigm is still consistent with nowadays experimental bounds. In section 3.2, we will return on this analysis to compare it with other paradigms used to suppress NP contributions to flavor physics.

Although MFV seems to be a natural solution to the flavor problem, it should be stressed that (i) it is not a theory of flavor (there is no explanation for the observed hierarchical structure of the Yukawas), and (ii) we are still far from having proved the validity of this hypothesis from data (in the effective theory language we can say that there is still room for sizeable new sources of flavor symmetry breaking beside the SM Yukawa couplings [33]). Confirmation or falsification of MFV hypothesis can be achieved only with evidence of BSM physics, checking if it presents or not the flavor-universality pattern predicted by the MFV assumption.

Operator	Bound on Λ	Observables
$\phi^\dagger \left(\bar{D}_R Y^{d\dagger} Y^u Y^{u\dagger} \sigma_{\mu\nu} Q_L \right) (e F_{\mu\nu})$	6.1 TeV	$B \to X_s \gamma$, $B \to X_s \ell^+ \ell^-$
$\frac{1}{2} (\bar{Q}_L Y^u Y^{u\dagger} \gamma_\mu Q_L)^2$	5.9 TeV	ϵ_K, ΔM_{B_d}, ΔM_{B_s}
$\left(\bar{Q}_L Y^u Y^{u\dagger} \gamma_\mu Q_L \right) (\bar{E}_R \gamma_\mu E_R)$	2.7 TeV	$B \to X_s \ell^+ \ell^-$, $B_s \to \mu^+ \mu^-$
$i \left(\bar{Q}_L Y^u Y^{u\dagger} \gamma_\mu Q_L \right) \phi_U^\dagger D_\mu \phi_U$	2.3 TeV	$B \to X_s \ell^+ \ell^-$, $B_s \to \mu^+ \mu^-$
$\left(\bar{Q}_L Y^u Y^{u\dagger} \gamma_\mu Q_L \right) (\bar{L}_L \gamma_\mu L_L)$	1.7 TeV	$B \to X_s \ell^+ \ell^-$, $B_s \to \mu^+ \mu^-$
$\left(\bar{Q}_L Y^u Y^{u\dagger} \gamma_\mu Q_L \right) (e D_\mu F_{\mu\nu})$	1.5 TeV	$B \to X_s \ell^+ \ell^-$

Table 2.2: Spurionic structure and bounds on the scale of new physics (at 95% C.L.) for some representative $\Delta F = 1$ [31] and $\Delta F = 2$ [32] MFV operators (assuming effective coupling $\pm 1/\Lambda^2$) and the corresponding observables used to set the bounds.

The MFV idea has become a very popular concept in recent literature and has been implemented and discussed in several works. Here we have presented its formulation based on a renormalization-group-invariant symmetry argument, with the further assumptions that no other sources of CP violation are present and that there exist only one Higgs doublet. Relaxing the latter assumption, one can build up theories where the bottom Yukawa y^b is of $\mathcal{O}(1)$ (e.g. MSSM with large $\tan\beta$, see [34]), thus giving rise to new order-one contributions. Alternatively, different definitions or modifications of the MFV hypothesis can be proposed, such as constrained MFV (CMFV, [35]) or general MFV (GMFV, [34]).

Further, since the connection between flavor and CP violation in the SM can be thought of as accidental, one can add flavor-diagonal CPV phases to generic MFV models [36]. However, because of the experimental constraints on electric dipole moments, which are generally sensitive to such flavour-diagonal phases, in these more general cases the bounds on the scale of new physics are substantially higher with respect to the "minimal" case, where the Yukawa couplings are assumed to be the only breaking sources of both symmetries.

Composite Higgs models

3.1 Possible solutions to the hierarchy problem

3.1.1 Overview on proposed models

In section 1.4 we have discussed about hierarchy problem, that is the naturalness problem concerning the small value of the Higgs mass, compared with the fundamental (planckian) mass scale, a fine tuning that does not have any explanation within the SM. In the last decades different solutions has been suggested to explain the Higgs mass, and we can group the main proposals in the following classes:

- Supersymmetry. In section 1.3 we have explained why a small value for the fermion masses can be thought of as natural. We have also seen that the same argument does not hold for a scalar boson mass (that is the Higgs mass). Supersymmetry (SUSY, [37]) is a symmetry that relates boson fields with fermion fields: in the limit of exact SUSY, the masses of the boson and the fermion fields must be equal, and the contribution from fermions to the quadratic divergence of the boson mass exactly cancels the contribution of bosons, and only a logarithmic dependence remains. In other words, this new symmetry allows to extent the 't Hooft condition to boson masses, solving the hierarchy problem.

  However, exact SUSY is clearly unrealistic, then SUSY breaking terms must be added to the theory, these introducing new quadratic divergences to the Higgs mass. For approximate SUSY (with soft breaking terms and R-parity conservation), Λ^2 of Eq. (1.3) is essentially replaced by the splitting of SUSY multiplets: $\Lambda^2 \sim m_{\mathrm{SUSY}}^2 - m_{\mathrm{ord}}^2$. Then in most realistic SUSY models a little hierarchy problem still survives, since the mass corrections induced by Λ^2 requires a little fine tuning to be adjusted.

- Strongly interacting EWSB sector. The archetypal idea of this class of models was the so-called Technicolor theory, where the EWSB was dynamically realized by a new strong interaction and new particles at the TeV scale, and no additional scalar bosons have to be introduced. In this class of models, the EWSB scale is dynamically generated by the RG evolution of the technicolor coupling constant,

that becomes non-perturbative (resulting in a strong interacting sector) at the Fermi scale.

Since its first formulation, many extensions of the original Technicolor model have been proposed, in order to introduce a naturally light Higgs boson, explain the Fermion masses, satisfy the increasingly tight experimental constraints. These ameliorated models sometimes are referred to as technicolor theories, with the lower case, in order to distinguish them from the original Technicolor theory (with capital T). We will discuss in detail these modifications through this chapter.

- Extra dimensions. The existence of extra, compactified dimension(s) is a fascinating physical idea. In last decades, QFT models in five (or even more) dimensions have been studied, resulting in several interesting results and analogies with ordinary QFT in four flat dimensions. Within this very rich framework, the hierarchy problem could possibly be addressed using models with one curved extra dimension, such as Randall-Sundrum models [38]. In these models, the background metric of the "warped" extra dimension can generate exponential mass hierarchies.

  In appendix A.2 models with one flat extra dimension are briefly described and the analogies of these models with composite Higgs models are shown.

- Multiverse reformulation of the problem. The concept of Multiverse, realizable e.g. in chaotic inflation models, is the idea that our Universe is just one of infinitely many bubbles continuously created from the vacuum by quantum fluctuations [39]. Further, each Universe could present its peculiar set of fundamental constants, according to the multitude of string theory solutions ($\sim 10^{500}$ [40]). Within this picture, the hierarchy problem can be reformulated in the following way: why, among all the possible sets of fundamental constants, our Universe has its peculiar one, that looks so unlikely with all those hierarchies? Two possible solutions have been proposed so far to solve the hierarchy problem using this point of view.

  One is the anthropic evasion of the problem, that is the idea that our Universe, although unlikely, is the only one that allows our existence as conscious observers. This idea has become popular since Weinberg used it in 1987 to predict the range of allowed values for the cosmological constant, on the ground of consideration concerning the galaxies formation [41] (actually, the predicted value is just a factor $10 \div 100$ times larger than the measured one). However, at present days it is unclear how this principle could work for certain SM parameters, that does not seems to affect in any way our existence (such as the mixing angles and the mass hierarchies among fermions).

  The second proposal arise from the observation that the SM parameters seems to lie, in the parameter space, in the vicinity of specific critical points, on the border of transitions between different phases. For example, the values of Higgs and top-quark masses lie in the vacuum metastability region for the Higgs potential [42]. This could lead to the speculation that, within the multiverse,

critical points are attractors. Thus, maybe our Universe actually is a likely one, despite our naturalness considerations.

- Disregard for naturalness argumentations. Electroweak precision tests and flavor physics experiments have not revealed the existence of TeV physics yet, even though a natural solution to the hierarchy problem apparently predicts it. Since the naturalness concept is not supported by any mathematical theorem, there has been in the last years a revival of models that simply ignore the fine tuning problem while trying to accommodate the known facts.

3.1.2 Early Technicolor models, credits and problems

To introduce the basic ideas of Technicolor (TC) models, it is worthwhile to start using an analogy with a better understood situation: the QCD chiral symmetry breakdown. It is well-known that, when considering only the first family of quarks, the QCD theory has an approximate global symmetry $SU(2)_L \times SU(2)_R$ (chiral symmetry), that undergoes a dynamically realized symmetry breaking:

$$SU(2)_L \times SU(2)_R \to SU(2)_V , \tag{3.1}$$

being the pions the associated pseudo Nambu–Goldstone (pNG) bosons.

In the chiral limit (quark masses set to zero), the QCD chiral symmetry becomes an exact symmetry and the breaking pattern (3.1) generates massless NG bosons (the pions). In this limit, interesting considerations can be made when also the electroweak gauge group $SU(2)_L \times U(1)_Y$ is taken into account. In this case, the dynamical symmetry breaking (3.1) represents a spontaneous breaking of the local (gauge) symmetry $SU(2)_L$. In other words, in the chiral limit QCD dynamically breaks the $SU(2)_L$ invariance and the (massless) pions are eaten to give mass to the W and the Z bosons.

To see how the weak bosons get mass, let us consider e.g. the W propagator in the Landau gauge ($\xi = 0$):

$$\mathord{\sim}\mathord{\sim}\mathord{\sim}\mathord{\sim} = \frac{-i}{q^2}(P_T)_{\mu\nu}, \qquad (P_T)_{\mu\nu} = \eta_{\mu\nu} - \frac{q_\mu q_\nu}{q^2} , \tag{3.2}$$

To compute the loop correction to such propagator, one have to sum to all orders its one-particle-irreducible contributions:

then, with

$$\mathord{\sim}\!\!\fbox{1PI}\!\!\mathord{\sim} = i\Pi_{\mu\nu}(q) = iq^2 \left(\frac{g}{2}\right)^2 \Pi(q^2)(P_T)_{\mu\nu} , \tag{3.3}$$

we have

$$\sim\!\!\!\!\sim\!\!\boxed{}\!\!\sim\!\!\!\!\sim = G_{\mu\nu}(q) = \frac{-i}{q^2[1 - g^2\Pi(q^2)/4]}(P_T)_{\mu\nu} \ . \tag{3.4}$$

Thus, a mass for the W arises only if $\Pi(q^2)$ has a pole at $q^2 = 0$. The pole in fact exists as a result of the symmetry breaking, due to the exchange of a massless pion:

$$\sim\!\!(\text{1PI})\!\!\sim \quad \Longrightarrow \quad \sim\!\!\!\!\sim\!\!\ast\!-\!-\!\!\overset{\pi}{-}\!-\!\ast\!\!\sim\!\!\!\!\sim \quad \Longrightarrow \quad \Pi(q^2) = \frac{f_\pi^2}{q^2} \ , \tag{3.5}$$

where f_π is the pion decay constant.

Substituting Eq. (3.5) in Eq. (3.4), we finally find

$$G_{\mu\nu}(q) = \frac{-i}{q^2 - g^2 f_\pi^2/4}(P_T)_{\mu\nu} \ , \tag{3.6}$$

that implies a mass for the W boson:

$$M_W = \frac{g f_\pi}{2} \simeq 29 \text{ MeV} \ . \tag{3.7}$$

Although the predicted mass for the W is completely wrong, this example shows how EWSB could in principle be achieved with a dynamical symmetry breaking mechanism and without the necessity for an Higgs boson.

Another important feature of this model, that will become an important request for realistic technicolor models, is the presence of a residual $SU(2)_V$ global symmetry (see Eq. (3.1)). In the absence of the $U(1)_Y$ gauge group (or, equivalently, in the limit $g' \to 0$) this symmetry is preserved and imposes the same mass for both $W^\pm$ and Z. In other words, in the limit $g' \to 0$ the residual $SU(2)_V$ symmetry imposes, at tree level:

$$\frac{M_W^2}{M_Z^2} = 1 \ . \tag{3.8}$$

When we turn on the gauge group $U(1)_Y$ ($g' \neq 0$), the $SU(2)_V$ symmetry is broken, because W^3 now mixes with B. But, since this is the only source of symmetry breaking (at tree level), it is easy to see that Eq. (3.8) is modified into

$$\rho \equiv \frac{M_W^2}{M_Z^2 \cos^2 \theta_W} = 1 \ . \tag{3.9}$$

Thus the residual $SU(2)_V$ global symmetry guarantees at tree level that $\rho = 1$, protecting this SM prediction. This is important because electroweak precision tests (EWPT) on ρ have confirmed until now this relation[1].

---

[1] At one-loop level, the ρ parameter receives other contributions that spoil the $\rho = 1$ relation in generic renormalization schemes. Until now, even considering loop corrections, the SM prediction is consistent with experiments.

For this reason, $SU(2)_V$ is sometimes called *custodial* symmetry, since it prevents NP models from giving too strong (i.e. experimentally incompatible) corrections to the ρ parameter.

The way the above example fails in describing realistically the EWSB suggests a simple solution to overcome the difficulty. The above predicted W mass was $M_W \sim 29$ MeV, more that three order of magnitude smaller than the actual W mass, $M_W \simeq 80$ GeV. One could then imagine that the actual EWSB dynamics could be just a scaled-up version of QCD, with

$$f_\pi \longrightarrow F_\pi \sim v = 256 \text{ GeV} . \tag{3.10}$$

In general, one can think of an $SU(N_{TC})$ "Technicolor" gauge group, together with a certain number of "technifermions" charged under this gauge group and a global symmetry breaking pattern $SU(2)_L \times SU(2)_R \to SU(2)_V$ triggered by confinement[2].

Such models behave in the same way as the QCD example above, and further they predict the correct values for the W and Z bosons. The hierarchy problem is then solved by dimensional transmutation: the electroweak scale v is generated dynamically as the scale at which the Technicolor coupling constant g_{TC} grows strong in the infrared, according to its RG evolution.

Since we can think of the would-be NG bosons as "technipions", they will have heavy resonances, such as the "techni-ρ" particles ρ_{TC} (in the same way as the first heavy resonances of the pions are the ρ mesons), that should be detectable particles. Actually, the global symmetry breaking pattern could be bigger than the minimal one of Eq. (3.1). In this case, together with the would-be NG, other pNGs arise and again these should be detectable.

What are the masses of these light technimesons? A simple argument based on the QCD analogy can be adduced: since we are thinking of $SU(N_{TC})$ as a scaled up version of QCD, we can suppose that such scaling is roughly valid also for the masses of the bound states[3]:

$$m_{\rho_{TC}} \sim \frac{F_\pi}{f_\pi} m_\rho \simeq 2.1 \text{ TeV} . \tag{3.11}$$

Similar values can be found for the masses of the pNG arising from bigger symmetry breaking patterns. Thus, a general prediction of TC theories is a whole spectrum of new particles, starting roughly at the TeV scale.

Having discussed the features of the original TC theories that makes them interesting candidates for EWSB, we now turn on predictions in conflict with experimental data, that require more sophisticated models to be solved. The two main problems of early TC theories were a parametrically too large correction to the Peskin-Takeuchi S parameter and too fast FCNC processes. Referring to the literature for a discussion of the first problem [43], we now concentrate to the second one.

To understand the problem of FCNC in Technicolor theories, it is first necessary to explain how in these models the SM fermions become massive. In order for the

---

[2]To be fair, the assumption that a generic $SU(N)$ gauge theory with $N > 2$ presents the phenomenon of confinement is, until now, only a conjecture.

[3]A little less naïve argument, that takes into account also the fact that it could be $N_{TC} \neq 3$, gives an extra factor $\sqrt{3/N_{TC}}$ [9].

ordinary fermions to feel the EWSB, some interaction must exist between fermions and technifermions. A simple solution is to assume that both the color group $SU(3)_C$ and the Technicolor $SU(N_{TC})$ are embedded in a larger Extended Technicolor (ETC) group,

$$SU(N_{ETC}) \supset SU(3)_C \times SU(N_{TC}) , \tag{3.12}$$

which is assumed to be spontaneously broken at the scale Λ_{ETC}. Now the fermions are allowed to interact with technifermions via the exchange of the broken ETC gauge bosons. Such interactions generate, at energy scales lower than Λ_{ETC}, effective four-fermion operators with two SM fermions (ψ) and two technifermions (ψ_{TC}):

$$\mathcal{L}_{\text{int}} = \frac{g_{ETC}^2}{\Lambda_{ETC}^2} (\bar{\psi}\psi) (\bar{\psi}_{TC}\psi_{TC}) . \tag{3.13}$$

At the lower scale $\Lambda_{TC} \simeq F_\pi \simeq v$ the $SU(N_{TC})$ group condenses giving rise to effective fermion mass terms:

$$\mathcal{L}_{\text{int}} = \frac{g_{ETC}^2}{\Lambda_{ETC}^2} (\bar{\psi}\psi) \langle \bar{\psi}_{TC}\psi_{TC} \rangle \sim \Lambda_{TC} \left(\frac{\Lambda_{TC}}{\Lambda_{ETC}} \right)^2 (\bar{\psi}\psi) . \tag{3.14}$$

This is the general mechanism that was proposed to generate mass terms for the SM fermions in TC models. This proposal gives rise to two main difficulties:

- In order to explain the hierarchy of fermion masses, it is clear that the generation of the four-fermion interactions (3.13) for different flavors cannot happen just at one single scale Λ_{ETC}. Thus, a complicated (and awkward) cascade of symmetry breakdowns is needed. Alternatives solutions (such as the tumbling mechanism [44]) does not seem to gracefully solve this point.

  Anyway, it is clear that, to reproduce the correct SM fermion masses, the Λ_{ETC} scale(s) cannot be too large. For example, if $\Lambda_{TC} \simeq v$ one needs $\Lambda_{ETC} \simeq 10$ TeV in order to reproduce the s quark mass. This will go into conflict with the next point.

- A more serious problem, as anticipated, arises when considering FCNC processes. The observation is that the exchange of a broken ETC gauge boson also generates operators with four SM fermions:

$$\mathcal{L}'_{int} = \frac{g_{ETC}^2}{\Lambda_{ETC}^2} (\bar{\psi}\psi)^2 . \tag{3.15}$$

  Generically, these operators are flavor anarchic since different SM flavors have to be embedded into the same ETC multiplet; this gives rise to various tree level FCNC amplitudes. As already discussed in section 2.2, FCNC are highly suppressed in the SM; thus to satisfy the experimental bounds on NP contributions to FCNC, one needs to assume $\Lambda_{ETC} \gtrsim 10^3 \div 10^5$ TeV (see Tab. 2.1). However, this last assumption generates a great friction with the previous point, since such lower bound on Λ_{ETC} leads to exceedingly too small masses for the SM fermions.
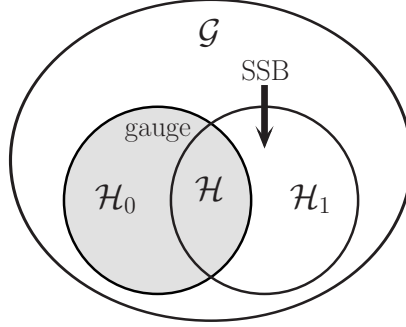
Figure 3.1: The pattern of symmetry breaking in a generic CH model.

One mechanism that has been proposed to resolve this tension is that of Walking Technicolor (for references, see [9]). The basic idea of this proposal is to drift from the above naïve dimensional analysis (NDA) arguments for the running behaviour of the ETC operators exploiting large anomalous dimensions, that could arise e.g. if the TC coupling constant has an IR non-perturbative fixed point. Referring to the literature for a thorough discussion, we just add that generally this solution can lead to a milder disagreement, but cannot solve the above problem.

From the above discussion, it should be now clear that these early TC models, although they suggest interesting mechanisms that can be alternatives to the SM ones, need deep improvements in order to be able to represent a plausible theory of EWSB. Last but not least, they also does not account for the by now confirmed existence of the Higgs boson.

3.2 Composite Higgs models

3.2.1 Generalities

There is an interesting variation of the strong symmetry breaking paradigm presented above that interpolates between simple TC theories and the Higgs model. In this class of theories the Higgs boson, rather that being an elementary scalar, is one among the strongly interacting sector bound states (that we will for now on call composite particles): this is the basic idea of *Composite Higgs* (CH) models [8]. The hierarchy problem is then solved as in TC theories: the compositeness scale of the new strong interaction (i.e. the EWSB scale) is dynamically generated by the RG evolution of its coupling constant.

Within this new scenario, the Higgs could naturally be lighter than the other resonances if it emerges as the pNG boson of a global symmetry breaking pattern characteristic of the strong dynamics under study; this further assumption allows these models to solve in a simple way the little hierarchy problem.

A specific CH model is then characterized by its peculiar symmetry structure. In the most general case, represented in Fig. 3.1, the strong interacting sector has a global $\mathcal{G}$ symmetry group dynamically broken to $\mathcal{H}_1$ at the scale f, while the subgroup

$\mathcal{H}_0 \subset \mathcal{G}$ is gauged by external vector bosons. The global symmetry breaking $\mathcal{G} \to \mathcal{H}_1$ implies $n = \dim(\mathcal{G}) - \dim(\mathcal{H}_1)$ Goldstone bosons, $n_0 = \dim(\mathcal{H}_0) - \dim(\mathcal{H})$ of which are eaten to give mass to as many vector bosons, so that $\mathcal{H} = \mathcal{H}_0 \cap \mathcal{H}_1$ is the unbroken gauge group. The remaining $n - n_0$ are either NG or (as in our case) pNG bosons, according to whether the broken symmetry associated with them is an exact or approximated one.

We now specialize the outlined general structure to a realistic theory of EWSB, specifying the features that it should have:

1. The SM electroweak gauge group G_{SM} must be embeddable in the unbroken subgroup $\mathcal{H}_1$. One should notice that this does not necessarily implies $G_{SM} \subset \mathcal{H}_1$, as it will soon be clear;

2. Since the Goldstone bosons live in the coset $\mathcal{G}/\mathcal{H}_1$, in order to have a composite pNG Higgs boson such coset must contains at least one $SU(2)$ doublet, to be identified with the $SU(2)_L$ Higgs doublet;

3. Even if it is not mandatory, it is desirable to furnish the unbroken subgroup $\mathcal{H}_1$ also of a custodial symmetry, to prevent too large corrections to the ρ parameter;

4. The global symmetry $\mathcal{G}$ is assumed to be explicitly broken by the interactions between SM fields and the strong sector. If it is the case, the Higgs doublet becomes a pNG bosons and it acquires a non-vanishing potential (and ergo a mass) at one-loop order. This, in turns, triggers the EWSB and the SM electroweak gauge group, previously unbroken, go through an Higgs-mediated spontaneous breakdown.

The fourth condition already explains the SSB dynamics in these models, that can be illustrated in two different passages. At tree level, the strong dynamics mediates the $\mathcal{G} \to \mathcal{H}_1$ symmetry breaking, which occurs at the energy scale f. At this point, the Higgs is a NG massless doublet and $G_{SM} \subset \mathcal{H}_1$.

However, an interaction between SM fermions and composite sector is needed in order to explain fermion masses, as illustrated in the previous section. If we assume these interactions to explicitly breaks the $\mathcal{G}$ symmetry, we encounter the second passage of the SSB: at one-loop order the Higgs, now a pNG boson, acquires a non-vanishing mass and a VEV, and the latter triggers the EWSB. In other words, at one-loop level a misalignment between G_{SM} and $\mathcal{H}_1$ ($G_{SM} \not\subset \mathcal{H}_1$) arises from the non-vanishing Higgs potential. As a consequence of such misalignment, now G_{SM} feels the global symmetry breaking $\mathcal{G} \to \mathcal{H}_1$, resulting in the EWSB process.

The dynamics described above is illustrated in Fig. 3.2. It is important to stress that, in this picture, the energy scale of EWSB is the Higgs VEV v, that is different from the scale f of the global $\mathcal{G} \to \mathcal{H}_1$ SSB. The ratio $\xi = v/f$ is determined by the vacuum misalignment between G_{SM} and $\mathcal{H}$ discussed above. A mild fine tuning over ξ can then explain why the Higgs boson is lighter that the other (so far unobserved) composite particles, as expected from a pNG boson.

As an example, we now briefly comment on the minimal set satisfying the above
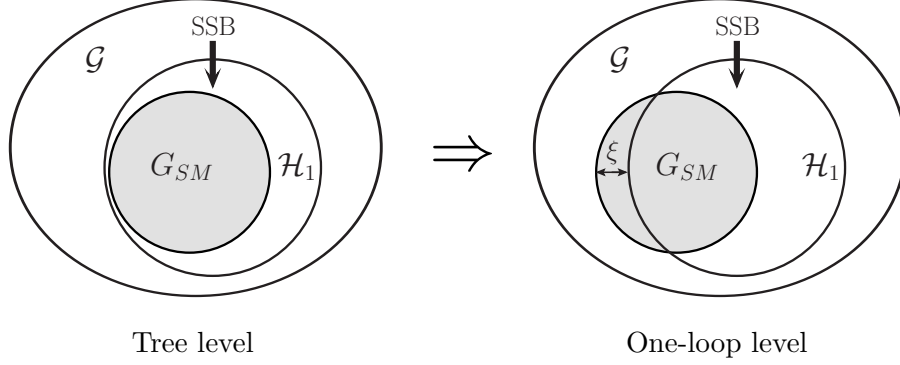
Figure 3.2: Realization of the EWSB in a CH model. At one-loop level, the vacuum misalignment ξ between the Higgs VEV v and the unbroken $\mathcal{H}_1$ group triggers the symmetry breaking of the electroweak gauge group.

conditions, that is the $SO(5)/SO(4)$ model[4], where $\mathcal{G} = SO(5)$ and $\mathcal{H}_1 = SO(4)$. Indeed, with this pattern:

- Since $SO(4) \cong SU(2)_L \times SU(2)_R \supset SU(2)_L \times U(1)_Y$, the unbroken $\mathcal{H}_1$ group includes G_{SM}, and furthermore it has the required custodial symmetry;

- The Goldstones of the coset $SO(5)/SO(4)$ can be parametrized in terms of four real fields, or equivalently of a complex doublet ϕ. Such doublet transforms under $SO(4) \cong SU(2)_L \times SU(2)_R$ as a bidoublet:

$$(\tilde{\phi}, \phi) \to V_L(\tilde{\phi}, \phi)V_R^\dagger \,, \tag{3.16}$$

where $\tilde{\phi} = i\sigma^2\phi^*$. This behaviour encapsulates the right transformation properties of the Higgs doublet (to be identified with ϕ) under the $SU(2)_L \times U(1)_Y$ gauge group (the generator of $U(1)_Y$ is defined as $Y = T^{3R}$).

This configuration can be slightly ameliorated to include an extra $U(1)_X$ symmetry, required to accommodate composite fermions with the correct quantum numbers to interact with the SM fermions.

For all the above reasons, the $SO(5) \times U(1)_X \to SO(4) \times U(1)_X$ pattern is called *minimal composite Higgs model* (MCHM) [45]. Of course, also less minimal sets can be considered, such as the $SO(6)/SO(5)$ pattern [46].

Until now, we have discussed the differences that improve the CH models with respect to simple TC models. We have seen in the previous section that the latter fails in explaining the SM fermion masses, basically because of the FCNC experimental constraints. We now discuss if and how the CH models can address those tensions.

A first possible mechanism to explain SM fermion masses is essentially the repetition of the argument adduced in TC models: assuming an ETC broken gauge group that leads to some fermion-technifermion interaction, the theory generates effective four-fermion terms:

$$\mathcal{L}_{\text{int}} = \frac{g_{ETC}^2}{\Lambda_{ETC}^2}(\bar{\psi}\psi)\left(\bar{\psi}_{TC}\psi_{TC}\right). \tag{3.17}$$

---

[4]Of course, an extra $SU(3)$ gauge group has to be added to the following model in order to describe also QCD. It can be simply added to the unbroken $\mathcal{H}$ group.

Below the scale f, the strong dynamics condenses resulting in an interpolated Higgs field. After EWSB, it takes a VEV leading to:

$$\mathcal{L}_{\text{int}} = \frac{g_{ETC}^2}{\Lambda_{ETC}^2} (\bar{\psi}\psi)\langle\bar{\psi}_{TC}\psi_{TC}\rangle \simeq \left(\frac{f}{\Lambda_{ETC}}\right)^2 (\bar{\psi}\phi\psi) \simeq v \left(\frac{f}{\Lambda_{ETC}}\right)^2 (\bar{\psi}\psi) \ . \quad (3.18)$$

Again, we have to admit the existence of generic flavor violating four-fermion operators generated by the ETC interactions:

$$\mathcal{L}'_{int} = \frac{g_{ETC}^2}{\Lambda_{ETC}^2} (\bar{\psi}\psi)^2 \ , \quad (3.19)$$

but, this time, we can conciliate both sufficiently high SM fermion masses and sufficiently suppressed FCNC contributions by assuming $\Lambda_{ETC} \simeq f \gg v$. In other words, we can completely solve the tension between contributions of (3.18) and (3.19), but at the price of an high tuning over ξ, namely $\xi \simeq 10^{-3} \div 10^{-5}$.

The fine tuning of the ξ parameter is not the only problem of this explanation of the SM fermion masses. The difficulties related to the reproduction of the mass hierarchies of fermions discussed in the previous section still hold. All these reasons motivate the introduction of a different mechanism that can transmit the EWSB to the SM fermions.

Suppose that some UV physics generates a linear coupling between a composite operator O and one SM fermion [7]:

$$\mathcal{L}_{\text{int}} = \lambda \bar{\psi} O + \text{h.c.} \ , \quad (3.20)$$

where O must be a fermionic composite operator, made for example, but not necessarily, of three technifermions. It is important to notice that every SM fermionic representation needs a different composite operator O, with the correct quantum numbers to make the Lagrangian (3.20) invariant under G_{SM}.

At low energy the composite Higgs field is interpolated by pairs of composite operators $O_L O_R$, and the effective low energy Lagrangian generated from the Wick contraction of two O operators becomes

$$\mathcal{L}_{\text{eff}} = \lambda_L \lambda_R \langle(\bar{\psi}_R O_L)(\bar{\psi}_L O_R)\rangle + \text{h.c.} \sim v \lambda_L \lambda_R \bar{\psi}\psi + \text{h.c.} \ , \quad (3.21)$$

then producing a mass term for the SM fermions. As discussed in Ref. [9], in this case it is also possible, through a RG argument and using quite general assumptions, to generate hierarchical mass terms exploiting different evolutions under the RGEs of the different couplings λ, due to their peculiar anomalous dimensions.

3.2.2   Partial compositeness paradigm

Linear couplings have an interesting phenomenological consequence, already noticed in Ref. [7]: at energies below f, at which the strong dynamics is assumed to condense, the composite operator O can excite a heavy fermionic resonance (i.e. a composite fermion that can be thought of as the analogous of a "technibarion" in Technicolor

theories). More exactly, there will be a full tower of composite Dirac fermions χ_n of increasing mass that can be excited by the operator O. In formulas:

$$\langle 0|O|\chi_n\rangle = \Delta_n u_{\chi_n}. \tag{3.22}$$

where u_{χ_n} is the Dirac spinor associated with χ_n. From this relation follows that one can generate the same Green functions of the Lagrangian (3.20) with the following Lagrangian:

$$\mathcal{L}'_{\text{mix}} = \sum_n \Delta_n(\bar{\psi}\chi_n + \text{h.c.}) \ . \tag{3.23}$$

The Lagrangian (3.23) can be thought of a mass mixing term between the elementary (ψ) and the composite (χ) fermions.

Similarly, a conserved current J_μ associated with the global symmetry $\mathcal{G}$ of the strong sector will excite a tower of spin-1 resonances ρ_n, which will mix with the elementary gauge fields A_μ:

$$\mathcal{L}'_{\text{mix}} = \sum_n m_{\rho_n} f_{\rho_n} A_\mu \rho_n^\mu \ , \qquad \langle 0|J_\mu|\rho_n(\varepsilon_r)\rangle = \varepsilon_r m_{\rho_n} f_{\rho_n} \ . \tag{3.24}$$

From the mixing terms (3.23) and (3.24) follows that the SM fields (that is the physical fields) are an admixture of elementary and composite fields. In this case one speaks of *partial compositeness* of the SM particles.

To clarify the above concepts, we first focus on a simple example, considering one elementary chiral field with only one composite resonance, namely:

$$\mathcal{L} = \bar{\psi}_L i\slashed{\partial}\psi + \bar{\chi}(i\slashed{\partial} - m)\chi + (\Delta_L \bar{\psi}_L \chi_R + \text{h.c.}) \ . \tag{3.25}$$

The Lagrangian (3.25) can be easily diagonalized by rotating the left-handed fields:

$$\begin{pmatrix} \psi_L \\ \chi_L \end{pmatrix} \rightarrow \begin{pmatrix} \cos\varphi_L & \sin\varphi_L \\ -\sin\varphi_L & \cos\varphi_L \end{pmatrix} \begin{pmatrix} \psi_L \\ \chi_L \end{pmatrix} \ , \qquad \tan\varphi_L = \frac{\Delta_L}{m} \ . \tag{3.26}$$

The mass eigenstates resulting from this rotation are a massless left-handed fermion (to be identified with the SM field) and a heavy Dirac fermion of mass $m_* = \sqrt{\Delta_L^2 + m^2}$ (to be identified with the first heavy resonance):

$$\begin{aligned} |\text{SM}_L\rangle &= \cos\varphi_L|\psi_L\rangle + \sin\varphi_L|\chi_L\rangle \ , \\ |\text{heavy}_L\rangle &= -\sin\varphi_L|\psi_L\rangle + \cos\varphi_L|\chi_L\rangle \ , \\ |\text{heavy}_R\rangle &= |\chi_R\rangle \ . \end{aligned} \tag{3.27}$$

The above procedure can be straightforwardly extended to the case where a right-handed elementary field is added. To be definite, for now on we will use the elementary/composite terminology when talking about the field basis before the mass diagonalization, while we will use the SM/heavy terminology referring to the mass basis, as done here.

As it can be seen in the example, at the moment the SM fermions are still massless. This is clear since, in the language developed before, the first step of SSB,

but not the second (that is the EWSB), has been carried out. Although the explicit implementation of the EWSB is a model-dependent issue, some far-reaching and model-independent consequences can be derived using general assumptions of CH models.

First, it is important to notice that the mass mixing parameters Δ_L, again as a result of a RG evolution argument, can be naturally much smaller than the masses m of the composite fermions. From this fact follows that the mixing angles are $\varphi \ll 1$ and then the SM fields are a linear combination of almost elementary fields and a small amount of composite fields. Also, one should recall that it is a general feature of CH models that only the composite sector interacts with the Higgs boson and feels the EWSB.

As a consequence of the above observations, we can identify two different contributions that determine the strength with which a SM field feels the EWSB. It depends upon the interaction of the corresponding composite field with the Higgs doublet (determined by the unknown strong dynamics), and upon the degree of partial compositeness of the SM field (parametrized by the mixing angle φ). In formulas, we can express the Yukawa couplings of the SM fields as:

$$y^{SM} = y^{\text{comp}} \sin\varphi_L \sin\varphi_R \ . \tag{3.28}$$

Plugging this argument into a realistic three-families description, we conclude that the Yukawa matrices for the SM fields have the following structure:

$$(Y^{SM})_{ij} = (Y^{\text{comp}})_{ij} \sin\varphi_{Li} \sin\varphi_{Rj} \ , \tag{3.29}$$

where we are not summing over the i, j indices. It is preferable to choose the composite Yukawa matrix Y^{comp} to be flavor anarchic, in order to avoid fine tuning. In this picture, the hierarchies of both the SM fermion masses and the CKM matrix can be explained by a hierarchical structure of the mixing angles φ_i, which in turn can arise from a different RG evolution for the mixing parameter Δ_i. Then, partial compositeness furnishes a fascinating mechanism to solve the SM flavor puzzle.

From all the above considerations, we can work out a method to compute the predicted suppression factor arising from partial compositeness for a generic operator [63]. As a final result of the following analysis, we will be able to compare the suppression generated by the partial compositeness paradigm with the one generated by the MFV paradigm developed in section 2.3.

First, we define an unambiguous notation for the degrees of partial compositeness of the SM fields. Clearly, we will focus here on the quark sector, as done in section 2.3. Calling ϵ the sine of the generic mixing angle, we set the following associations:

$$Q_{Li} \rightarrow \epsilon_i^q \qquad i = \{1, 2, 3\} \ , \tag{3.30a}$$

$$U_{Ri} \rightarrow \epsilon_i^u \qquad i = \{1, 2, 3\} = \{u, d, t\} \ , \tag{3.30b}$$

$$D_{Li} \rightarrow \epsilon_i^d \qquad i = \{1, 2, 3\} = \{d, s, b\} \ . \tag{3.30c}$$

As explained above, we assume the composite sector to be flavor anarchic, thus all the hierarchies of the SM arise from the hierarchies among the ϵ's, where $\epsilon_1 < \epsilon_2 < \epsilon_3$.

In particular, according to Eq. (3.29), the SM Yukawa matrices can be parametrized as follows:

$$(Y^u)_{ij} \sim \epsilon_i^q \epsilon_j^u \,, \qquad\qquad (Y^d)_{ij} \sim \epsilon_i^q \epsilon_j^d \,. \qquad (3.31)$$

Keeping only the leading terms in the expansion, it is easy to see that the Yukawa matrices can be diagonalized by these unitary matrices:

$$(L^u)_{ij} \sim (L^d)_{ij} \sim \min\left(\frac{\epsilon_i^q}{\epsilon_j^q}\,, \frac{\epsilon_j^q}{\epsilon_i^q}\right) \,, \quad (R^{u,d})_{ij} \sim \min\left(\frac{\epsilon_i^{u,d}}{\epsilon_j^{u,d}}\,, \frac{\epsilon_j^{u,d}}{\epsilon_i^{u,d}}\right) \,, \qquad (3.32)$$

resulting in:

$$(L^{u\dagger}Y^uR^u)_{ij} \sim \epsilon_i^q \epsilon_i^u \delta_{ij} \sim y_i^u \delta_{ij} \,, \quad (L^{d\dagger}Y^dR^d)_{ij} \sim \epsilon_i^q \epsilon_i^d \delta_{ij} \sim y_i^d \delta_{ij} \,. \qquad (3.33)$$

The above relations imply:

$$\frac{\epsilon_i^{u,d}}{\epsilon_j^{u,d}} \simeq \frac{y_i^{u,d}}{y_j^{u,d}} \frac{\epsilon_j^q}{\epsilon_i^q} \,. \qquad (3.34)$$

Furthermore, observing that $V_{CKM} = L^{d\dagger}L^u \sim L^{u,d}$, to reproduce the correct CKM hierarchies we should have

$$\frac{\epsilon_1^q}{\epsilon_2^q} \simeq V_{12} \sim \lambda \,, \qquad \frac{\epsilon_1^q}{\epsilon_3^q} \simeq V_{13} \sim \lambda^3 \,, \qquad \frac{\epsilon_2^q}{\epsilon_3^q} \simeq V_{23} \sim \lambda^2 \,, \qquad (3.35)$$

where λ is the sine of the Cabibbo angle.

Assuming the approximate equalities (3.34) and (3.35) to hold exactly, we have fixed the ϵ coefficients up to two renormalization factors. Thus, we can choose that the only two free parameters of this description are e.g. ϵ_3^q and ϵ_3^u, that can be both roughly thought of as $\mathcal{O}(1)$ quantities (since they are the degrees of partial compositeness for the top quark).

The set of relations (3.33), (3.34) and (3.35) furnishes a method to predict the suppression factor due to the partial compositeness of any operator. As an example, we work out an explicit calculation taking the electromagnetic dipole operator (2.58) as in section 2.3, namely:

$$Q_{7\gamma} = \frac{em_b}{16\pi^2}F_{\mu\nu}\,\bar{s}_L\sigma^{\mu\nu}b_R \,.$$

From Eqs. (3.30) we can immediately associate with this operator the suppression factor

$$Q_{7\gamma} \sim \epsilon_2^q \epsilon_3^d \,, \qquad (3.36)$$

and the only thing left to do is to recast it in a more intelligible form, using known physical quantities. By elementary manipulations and using the above relations:

$$\epsilon_2^q \epsilon_3^d \sim \epsilon_2^q \frac{y_3^d}{\epsilon_3^q} \sim y_3^d \frac{\epsilon_2^q}{\epsilon_3^q} \sim m_b\lambda^2 \,. \qquad (3.37)$$

In this case, we have found the same suppression factor as in the MFV case (Eq. (2.62)), but this is not always the case. For example, let us now analyse the $Q'_{7\gamma}$ operator defined in Eq. (2.63):

$$Q'_{7\gamma} = \frac{e m_b}{16\pi^2} F_{\mu\nu}\, \bar{s}_R \sigma^{\mu\nu} b_L \ .$$

The PC paradigm predicts for $Q'_{7\gamma}$ a suppression factor:

$$Q'_{7\gamma} \sim \epsilon_2^d \epsilon_3^q \sim \frac{y_2^d}{\epsilon_2^q} \epsilon_3^q \sim y_2^d \frac{\epsilon_3^q}{\epsilon_2^q} \sim \frac{m_s}{\lambda^2} \ . \tag{3.38}$$

We can now appreciate that, this time, the MFV and PC paradigms give very different predictions:

$$\begin{aligned} \text{MFV} &\longrightarrow & Q'_{7\gamma} \sim m_s \lambda^2 \ , \\ \text{PC} &\longrightarrow & Q'_{7\gamma} \sim \frac{m_s}{\lambda^2} \ , \end{aligned} \tag{3.39}$$

and this leads to opposite conclusions for the two scenarios:

$$\frac{Q'_{7\gamma}}{Q_{7\gamma}} = \begin{cases} \dfrac{m_s}{m_b} \simeq 0.025 & \text{in MFV} \\[2mm] \dfrac{m_s}{m_b \lambda^4} \simeq 10 & \text{in PC} \end{cases} . \tag{3.40}$$

As can be directly seen, for the "wrong chirality" process (associated with $Q'_{7\gamma}$) the MFV predicts a considerable suppression factor, whereas the PC scenario predicts an enhancement with respect to $Q_{7\gamma}$. It turns out that this is a general feature of models with PC: "wrong chirality" processes are not suppressed as in the SM (and thus in MFV scenarios), instead sometimes they are even enhanced with respect to the "SM-like chirality" processes, such as in this case.

In Tab. 3.1 the suppression factors arising from MFV and PC are compared for the dipole operator and other representative $\Delta F = 1$ operators (considering both their chiralities), in order to fully appreciate this property of the PC scenarios.

Of course, the enhancement of the flavor coefficient associated to a definite operator is not the only factor that determines the relevance of that operator for phenomenological purposes. Indeed, the very important parameters are the ratio of such coefficient with the SM dominant one and possible enhancements of the operator matrix elements. The following two examples will make clearer these last points.

First, let us analyse again the dipole operator, but this time the one describing the underlying transition $s \to d\gamma$:

$$Q_{7\gamma} = \frac{e m_s}{16\pi^2} F_{\mu\nu}\, \bar{d}_L \sigma^{\mu\nu} s_R \ , \tag{3.41}$$

$$Q'_{7\gamma} = \frac{e m_s}{16\pi^2} F_{\mu\nu}\, \bar{d}_R \sigma^{\mu\nu} s_L \ . \tag{3.42}$$

We can straightforwardly generalize the results of the previous analysis to conclude that:

$$\text{MFV} \quad \longrightarrow \quad \begin{cases} Q_{7\gamma} \sim m_s V_{td}^* V_{ts} \sim m_s \lambda^5 \\ Q'_{7\gamma} \sim m_d V_{td}^* V_{ts} \sim m_d \lambda^5 \end{cases} \quad \longrightarrow \quad \frac{Q'_{7\gamma}}{Q_{7\gamma}} = \frac{m_d}{m_s} \simeq 0.046 \ , \tag{3.43a}$$

Operator	MFV	PC
$F_{\mu\nu}\,\bar{s}_L\sigma^{\mu\nu}b_R$	$y^b V_{ts}^* V_{tb} \sim y^b \lambda^2$	$\epsilon_2^q \epsilon_3^d \sim y^b \lambda^2\, \epsilon_3^u \epsilon_3^q$
$F_{\mu\nu}\,\bar{s}_R\sigma^{\mu\nu}b_L$	$y^s V_{ts}^* V_{tb} \sim y^s \lambda^2$	$\epsilon_2^d \epsilon_3^q \sim \frac{y^s}{\lambda^2}\, \epsilon_3^u \epsilon_3^q$
$F_{\mu\nu}\,\bar{d}_L\sigma^{\mu\nu}s_R$	$y^s V_{td}^* V_{ts} \sim y^s \lambda^5$	$\epsilon_1^q \epsilon_2^d \sim y^s \lambda\, \epsilon_3^u \epsilon_3^q$
$F_{\mu\nu}\,\bar{d}_R\sigma^{\mu\nu}s_L$	$y^d V_{td}^* V_{ts} \sim y^d \lambda^5$	$\epsilon_1^d \epsilon_2^q \sim \frac{y^d}{\lambda}\, \epsilon_3^u \epsilon_3^q$
$(\bar{d}_L\gamma_\mu s_L)(\bar{e}\gamma^\mu e)$	$V_{td}^* V_{ts} \sim \lambda^5$	$\epsilon_1^q \epsilon_2^q \sim \lambda^5 (\epsilon_3^q)^2$
$(\bar{d}_R\gamma_\mu s_R)(\bar{e}\gamma^\mu e)$	$y^d y^s V_{td}^* V_{ts} \sim y^d y^s \lambda^5$	$\epsilon_1^d \epsilon_2^d \sim \frac{y^d y^s}{\lambda^5}(\epsilon_3^u)^2$
$(\bar{c}_L\gamma_\mu u_L)(\bar{e}\gamma^\mu e)$	$(y^b)^2 V_{cb}^* V_{ub} \sim (y^b)^2 \lambda^5$	$\epsilon_1^q \epsilon_2^q \sim \lambda^5 (\epsilon_3^q)^2$
$(\bar{c}_R\gamma_\mu u_R)(\bar{e}\gamma^\mu e)$	$y^u y^c (y^b)^2 V_{cb}^* V_{ub} \sim y^u y^c (y^b)^2 \lambda^5$	$\epsilon_1^u \epsilon_2^u \sim \frac{y^u y^c}{\lambda^5}(\epsilon_3^u)^2$

Table 3.1: Comparison between the suppression factors arising from the MFV or the partial compositeness (PC) paradigm, computed for some representative $\Delta F = 1$ operators and their correspondent "wrong chirality" partners.

$$\text{PC} \quad \longrightarrow \quad \begin{cases} Q_{7\gamma} \sim \epsilon_1^q \epsilon_2^d \sim m_s \lambda \\ Q_{7\gamma}' \sim \epsilon_1^d \epsilon_2^q \sim \dfrac{m_d}{\lambda} \end{cases} \quad \longrightarrow \quad \frac{Q_{7\gamma}'}{Q_{7\gamma}} = \frac{m_d}{m_s \lambda^2} \simeq 0.95 \ . \quad (3.43\text{b})$$

It can be immediately appreciated that this time the enhancement for $Q_{7\gamma}'$ in PC is weaker that in the $b \to s\gamma$ case. However, as previously stated, the important parameter is the total enhancement with respect to the SM dominant contribution. Comparing such total enhancement for the dominant contribution in PC for the $b \to s\gamma$ and $s \to d\gamma$ processes, one finds:

$$b \to s\gamma \quad \longrightarrow \quad \frac{Q_{7\gamma}'^{PC}}{Q_{7\gamma}^{SM}} = \frac{m_s}{m_b \lambda^4} \simeq 10 \ , \tag{3.44}$$

$$s \to d\gamma \quad \longrightarrow \quad \frac{Q_{7\gamma}^{PC}}{Q_{7\gamma}^{SM}} \simeq \frac{Q_{7\gamma}'^{PC}}{Q_{7\gamma}^{SM}} = \frac{m_d}{m_s \lambda^6} \simeq 407 \ . \tag{3.45}$$

$$\tag{3.46}$$

Thus, the overall enhancement of the dipole operator in PC with respect to the SM is far more significant in the $s \to d\gamma$ process, despite the considerations regarding Eqs. (3.40) and (3.43).

To understand the importance also of the contribution from the matrix elements, let us analyse a $\Delta F = 2$ process, the $K^0 - \bar{K}^0$ mixing. In the SM, the most relevant operator is

$$Q_1 = (\bar{s}_L\gamma_\mu d_L)(\bar{s}_L\gamma^\mu d_L) \ , \tag{3.47}$$

since it is has the maximal chiral enhancement. The spurionic analysis gives:

$$Q_1 \propto \left[Y^u (Y^u)^\dagger \right]_{21}^2 \simeq (V_{ts}^* V_{td})^2 \simeq \lambda^{10} \ . \tag{3.48}$$

Switching to PC, the Q_1 operator has the suppression factor

$$Q_1 \propto (\epsilon_2^q \epsilon_1^q)^2 \simeq \lambda^{10}(\epsilon_3^q)^4 \simeq 2.5 \cdot 10^{-7} \, (\epsilon_3^q)^4 \ , \tag{3.49}$$

However, now there is another operator[5] with a similar suppression factor, namely

$$Q_4 = (\bar{s}_R d_L)(\bar{s}_L d_R) \, , \tag{3.50}$$

to which we can associate the coefficient

$$Q_4 \propto \epsilon_2^d \epsilon_1^q \epsilon_2^q \epsilon_1^d \sim y^d y^s (\epsilon_3^u \epsilon_3^q)^2 \sim 1.7 \cdot 10^{-8} \, (\epsilon_3^u \epsilon_3^q)^2 \, . \tag{3.51}$$

Considering now that the Q_4 matrix element has a chirality enhancement with respect to the matrix element of Q_1, in formulas

$$\frac{\langle K^0 | Q_4 | \bar{K}^0 \rangle}{\langle K^0 | Q_1 | \bar{K}^0 \rangle} \propto \left(\frac{M_K}{m_d + m_s} \right)^2 \simeq 20 \, , \tag{3.52}$$

and that the running due to QCD corrections further increases this enhancement, it turns typically out that Q_4 is the dominant operator.

In appendix A.1 the complete basis of $\Delta F = 2$ dimension six operators, Eq. (A.4), is introduced and the importance of neutral meson system observables in imposing constrains on NP contributions is discussed. It is interesting to systematically compare also for these operators the suppressions predicted by the two different paradigms in the light of the above considerations regarding "wrong chirality" processes. The result of this comparison can be appreciate in Tabs. 3.2 and 3.3: as anticipated, the enhancement of right currents contributions with respect to the MFV scenario is a general feature of the PC paradigm.

A conclusion that can be established from all the above considerations is that the CH models with partial compositeness generally use a different mechanism to suppress contributions to flavor physics observables, thus presenting a different path of flavor changing processes beyond the SM, alternative to the MFV scenario and then experimentally distinguishable.

---

[5]As can be appreciated in Tab. 3.3 and in Eq. (A.4), they really are two operators, related to the two different possible contractions of the color indecis. Here we consider for notational simplicity just one of them.

Operator	MFV	PC
$Q_1 = (\bar{u}_\alpha \gamma_\mu P_L c_\alpha)^2$	$(y^b)^4 (V_{ub} V_{cb}^*)^2$	$(\epsilon_1^q \epsilon_2^q)^2 \sim (V_{ub} V_{cb}^*)^2 (\epsilon_3^q)^4$
$\tilde{Q}_1 = (\bar{u}_\alpha \gamma_\mu P_R c_\alpha)^2$	$(y^u y^c)^2 (y^b)^4 (V_{ub} V_{cb}^*)^2$	$(\epsilon_1^u \epsilon_2^u)^2 \sim \left(\frac{y^u y^c}{V_{ub} V_{cb}^*} \right)^2 (\epsilon_3^u)^4$
$Q_2 = (\bar{u}_\alpha P_L c_\alpha)(\bar{u}_\beta P_L c_\beta)$	$(y^u)^2 (y^b)^4 (V_{ub} V_{cb}^*)^2$	$(\epsilon_1^u \epsilon_2^q)^2 \sim (y^u)^2 \left(\frac{V_{cb}^*}{V_{ub}} \right)^2 (\epsilon_3^u \epsilon_3^q)^2$
$\tilde{Q}_2 = (\bar{u}_\alpha P_R c_\alpha)(\bar{u}_\beta P_R c_\beta)$	$(y^c)^2 (y^b)^4 (V_{ub} V_{cb}^*)^2$	$(\epsilon_1^q \epsilon_2^u)^2 \sim (y^c)^2 \left(\frac{V_{ub}}{V_{cb}^*} \right)^2 (\epsilon_3^u \epsilon_3^q)^2$
$Q_3 = (\bar{u}_\alpha P_L c_\beta)(\bar{u}_\beta P_L c_\alpha)$	$(y^u)^2 (y^b)^4 (V_{ub} V_{cb}^*)^2$	$(\epsilon_1^u \epsilon_2^q)^2 \sim (y^u)^2 \left(\frac{V_{cb}^*}{V_{ub}} \right)^2 (\epsilon_3^u \epsilon_3^q)^2$
$\tilde{Q}_3 = (\bar{u}_\alpha P_R c_\beta)(\bar{u}_\beta P_R c_\alpha)$	$(y^c)^2 (y^b)^4 (V_{ub} V_{cb}^*)^2$	$(\epsilon_1^q \epsilon_2^u)^2 \sim (y^c)^2 \left(\frac{V_{ub}}{V_{cb}^*} \right)^2 (\epsilon_3^u \epsilon_3^q)^2$
$Q_4 = (\bar{u}_\alpha P_L c_\alpha)(\bar{u}_\beta P_R c_\beta)$	$y^u y^c (y^b)^4 (V_{ub} V_{cb}^*)^2$	$\epsilon_1^u \epsilon_2^u \epsilon_1^q \epsilon_2^q \sim y^u y^c (\epsilon_3^u \epsilon_3^q)^2$
$Q_5 = (\bar{u}_\alpha P_L c_\beta)(\bar{u}_\beta P_R c_\alpha)$	$y^u y^c (y^b)^4 (V_{ub} V_{cb}^*)^2$	$\epsilon_1^u \epsilon_2^u \epsilon_1^q \epsilon_2^q \sim y^u y^c (\epsilon_3^u \epsilon_3^q)^2$

Table 3.2: Comparison between the suppression factors arising from the MFV or the partial compositeness (PC) paradigm, computed for the complete basis of $\Delta F = 2$ dimension six operators for the $D^0 - \bar{D}^0$ system, Eq. (A.4). Greek letters denote color indices.

Operator	MFV	PC
$Q_1 = (\bar{D}_{i\alpha} \gamma_\mu P_L D_{j\alpha})^2$	$(V_{ti}^* V_{tj})^2$	$(\epsilon_i^q \epsilon_j^q)^2 \sim (V_{ti}^* V_{tj})^2 (\epsilon_3^q)^4$
$\tilde{Q}_1 = (\bar{D}_{i\alpha} \gamma_\mu P_R D_{j\alpha})^2$	$(y_i^d y_j^d)^2 (V_{ti}^* V_{tj})^2$	$(\epsilon_i^d \epsilon_j^d)^2 \sim \left(\frac{y_i^d y_j^d}{V_{ti}^* V_{tj}} \right)^2 (\epsilon_3^u)^4$
$Q_2 = (\bar{D}_{i\alpha} P_L D_{j\alpha})(\bar{D}_{i\beta} P_L D_{j\beta})$	$(y_i^d)^2 (V_{ti}^* V_{tj})^2$	$(\epsilon_i^d \epsilon_j^q)^2 \sim (y_i^d)^2 \left(\frac{V_{tj}}{V_{ti}^*} \right)^2 (\epsilon_3^u \epsilon_3^q)^2$
$\tilde{Q}_2 = (\bar{D}_{i\alpha} P_R D_{j\alpha})(\bar{D}_{i\beta} P_R D_{j\beta})$	$(y_j^d)^2 (V_{ti}^* V_{tj})^2$	$(\epsilon_i^q \epsilon_j^d)^2 \sim (y_j^d)^2 \left(\frac{V_{ti}^*}{V_{tj}} \right)^2 (\epsilon_3^u \epsilon_3^q)^2$
$Q_3 = (\bar{D}_{i\alpha} P_L D_{j\beta})(\bar{D}_{i\beta} P_L D_{j\alpha})$	$(y_i^d)^2 (V_{ti}^* V_{tj})^2$	$(\epsilon_i^d \epsilon_j^q)^2 \sim (y_i^d)^2 \left(\frac{V_{tj}}{V_{ti}^*} \right)^2 (\epsilon_3^u \epsilon_3^q)^2$
$\tilde{Q}_3 = (\bar{D}_{i\alpha} P_R D_{j\beta})(\bar{D}_{i\beta} P_R D_{j\alpha})$	$(y_j^d)^2 (V_{ti}^* V_{tj})^2$	$(\epsilon_i^q \epsilon_j^d)^2 \sim (y_j^d)^2 \left(\frac{V_{ti}^*}{V_{tj}} \right)^2 (\epsilon_3^u \epsilon_3^q)^2$
$Q_4 = (\bar{D}_{i\alpha} P_L D_{j\alpha})(\bar{D}_{i\beta} P_R D_{j\beta})$	$y_i^d y_j^d (V_{ti}^* V_{tj})^2$	$\epsilon_i^d \epsilon_j^q \epsilon_i^q \epsilon_j^d \sim y_i^d y_j^d (\epsilon_3^u \epsilon_3^q)^2$
$Q_5 = (\bar{D}_{i\alpha} P_L D_{j\beta})(\bar{D}_{i\beta} P_R D_{j\alpha})$	$y_i^d y_j^d (V_{ti}^* V_{tj})^2$	$\epsilon_i^d \epsilon_j^q \epsilon_i^q \epsilon_j^d \sim y_i^d y_j^d (\epsilon_3^u \epsilon_3^q)^2$

Table 3.3: Comparison between the suppression factors arising from the MFV or the partial compositeness (PC) paradigm, for the complete basis of $\Delta F = 2$ dimension six operators for the down type neutral meson systems, easily derivable from Eq. (A.4). Greek letters denote color indices, latin letters denote flavor indices.

Phenomenological computations

4.1 The two-site model

In this chapter we want to work out some phenomenological consequences regarding NP contributions, in CH models, to flavor violating processes in the leptonic sector. In particular we will focus on the muon decay mode $\mu \to e\gamma$, which is forbidden within the SM. To do this, we will use a simplified composite Higgs model.

Indeed, the problem is that in full CH theories (developed in section 3.2) the computations are often prohibitive. Thus, some kind of simplification should be carried out in order to obtain a model that still retains the important features of the CH phenomenology (such as partial compositeness), but at the same time provides a framework to perform simpler (and still reliable) explicit computations.

One interesting proposal, that has become popular in recent literature, is to consider a model where only the lowest-lying set of composite states arising from the strong dynamics is inserted in the Lagrangian [10]. Such minimal set is chosen in order to fully recreate the partial compositeness phenomenology, both for fermions and for gauge bosons. Due to the peculiar truncation carried out in these models, they are called *two-site models*. According to the analogy of CH models with extra dimension theories discussed in appendix A.2, this truncation can also be seen as the addiction to the SM Lagrangian of only the set of first KK modes of the 5D fields.

This simplification leads to a much simpler Lagrangian that still leads to reliable results. Indeed, the error due to this approximation is typically roughly around the 50% [10]. Even though this size of error may seems rather large, it implies that these models are able to furnish the correct order of magnitude for the corrections to the SM observables in CH theories. This is still an important information, in the context of searches for NP signals, and thus the usage of these simplified models is justified.

Once explained the origins and the reasons to use these kind of models, we are left with characterizing our considered one in detail. Following the general discussion about QFT at the beginning of chapter 2, we define the two-site model we will deal with from its three peculiar features[1]:

---

[1]Reading the properties of our two-site model, one can easily recognize them to be defined exactly in order to reproduce the CH phenomenology described in the previous chapter.

	Subgroup	Generator(s)	Field(s)	Coupling
el	$SU(3)_C$	$\lambda^{c,\,\text{el}}, \quad c = 1 \dots 8$	$G_\mu^{c,\,\text{el}}$	g_s^{el}
	$SU(2)_L$	$T^{aL,\,\text{el}}, \quad a = 1,2,3$	$W_\mu^{a,\,\text{el}}$	g_1^{el}
	$U(1)_Y$	Y	B_μ^{el}	g_2^{el}
comp	$SU(3)_C$	$\lambda^{c,\,\text{comp}}, \quad c = 1 \dots 8$	$G_\mu^{c,\,\text{comp}}$	g_s^{comp}
	$SU(2)_L$	$T^{aL,\,\text{comp}}, \quad a = 1,2,3$	$W_\mu^{a,\,\text{comp}}$	g_1^{comp}
	$SU(2)_R \times U(1)_X$	$(T^{3R,\,\text{comp}} + X)$	B_μ^{comp}	g_2^{comp}
		$T^{1R,\,\text{comp}}, \; T^{2R,\,\text{comp}}$	$\tilde{W}_\mu^{1,2,\,\text{comp}}$	g_2^{comp}
		$(T^{3R,\,\text{comp}} - X)$	$\tilde{B}_\mu^{\text{comp}}$	g_2^{comp}

Table 4.1: Gauge subgroups and their associated generators, boson fields and couplings.

(i) The gauge group is:

$$G^{\text{gauge}} = G^{\text{el}} \times G^{\text{comp}} , \tag{4.1}$$
$$G^{\text{el}} = [SU(3)_C \times SU(2)_L \times U(1)_Y]^{\text{el}} ,$$
$$G^{\text{comp}} = [SU(3)_C \times SU(2)_L \times SU(2)_R \times U(1)_X]^{\text{comp}} .$$

In Table 4.1 is summarized our notation for generators, boson fields and coupling constants associated with each simple subgroup. Purely for convenience, we have associated the same coupling both with $SU(2)_R$ and $U(1)_X$, the most general case being straightforward but computationally more involved and with no significant phenomenological differences.

Notice that G^{comp} has been chosen to be bigger that G^{el}, in order to provide a custodial symmetry, whose importance has been discussed in section 3.1.

(ii) Regarding the particle content, there are two different sets of fermions. We have a first set of chiral fermions, charged under the G^{el} gauge group in the same way as in the SM, and a second set of vector-like fermions, charged under G^{comp}; three families for each representation are considered and we will distinguish among them with an extra latin index as done in chapter 2. In addiction, we have a real bidoublet $(\tilde{\phi}, \phi)$ charged under $[SU(2)_L \times SU(2)_R]^{\text{comp}}$.

Focusing only on leptons, Table 4.2 summarises the quantum numbers for these particles. In our notation, lower case letters denote elementary fields, whereas capital letters denote composite fields. Further, the 'tilde' apex denotes $SU(2)_L$ singlets, in order to distinguish them from the doublets. Finally, the decomposition of the two $SU(2)_L$ doublets into their components reads:

$$\ell_L = \begin{pmatrix} \nu_L \\ e_L \end{pmatrix} ; \quad L = \begin{pmatrix} N \\ E \end{pmatrix} . \tag{4.2}$$

	Elementary		Composite		
	$SU(2)_L$	$U(1)_Y$	$SU(2)_L$	$SU(2)_R$	$U(1)_X$
ℓ_{Li}	**2**	$-\frac{1}{2}$	**1**	**1**	0
$\tilde{e}_{Ri}$	**1**	-1	**1**	**1**	0
L_i	**1**	0	**2**	**1**	$-\frac{1}{2}$
$\tilde{E}_i$	**1**	0	**1**	**1**	-1
$(\tilde{\phi}, \phi)$	**1**	0	**2**	**2**	0

Table 4.2: Particle content and quantum numbers of the two-site minimal model. The index $i = 1, 2, 3$ runs over three families for each representation.

(iii) We can divide the symmetry breaking pattern of the theory in two steps. The first step breaks G^{gauge} into the SM gauge group:

$$G^{\text{gauge}} \to [SU(3)_C \times SU(2)_L \times U(1)_Y]^{SM} . \tag{4.3}$$

And in particular:

$$\lambda^{c,\, SM} = \lambda^{c,\, \text{el}} + \lambda^{c,\, \text{comp}} , \tag{4.4a}$$

$$T^{aL,\, SM} = T^{aL,\, \text{el}} + T^{aL,\, \text{comp}} , \tag{4.4b}$$

$$Y^{SM} = Y + T^{3R,\, \text{comp}} + X . \tag{4.4c}$$

The gauge fields associated with G^{SM} are then a linear combination of elementary and composite fields:

$$G_\mu = \cos\theta_s G_\mu^{\text{el}} + \sin\theta_s G_\mu^{\text{comp}} , \qquad \tan\theta_s \equiv \frac{g_s^{\text{el}}}{g_s^{\text{comp}}} , \tag{4.5a}$$

$$W_\mu = \cos\theta_1 W_\mu^{\text{el}} + \sin\theta_1 W_\mu^{\text{comp}} , \qquad \tan\theta_1 \equiv \frac{g_1^{\text{el}}}{g_1^{\text{comp}}} , \tag{4.5b}$$

$$B_\mu = \cos\theta_2 B_\mu^{\text{el}} + \sin\theta_2 B_\mu^{\text{comp}} , \qquad \tan\theta_2 \equiv \frac{g_2^{\text{el}}}{g_2^{\text{comp}}} , \tag{4.5c}$$

this is exactly the partial compositeness scenario for gauge bosons, described in Eq. (3.24). The massive gauge fields associated with the broken generators can be divided into the combinations orthogonal to Eqs. (4.5):

$$G_\mu^* = -\sin\theta_s G_\mu^{\text{el}} + \cos\theta_s G_\mu^{\text{comp}} , \tag{4.6a}$$

$$W_\mu^* = -\sin\theta_1 W_\mu^{\text{el}} + \cos\theta_1 W_\mu^{\text{comp}} , \tag{4.6b}$$

$$B_\mu^* = -\sin\theta_2 B_\mu^{\text{el}} + \cos\theta_2 B_\mu^{\text{comp}} , \tag{4.6c}$$

and the fields that ultimately does not mix with the elementary bosons:

$$\tilde{W}_\mu^{\pm} \equiv \frac{1}{\sqrt{2}} (\tilde{W}_\mu^{1,\, \text{comp}} \mp i\, \tilde{W}_\mu^{2,\, \text{comp}}) , \tag{4.7a}$$

$$\tilde{B}_\mu \equiv \tilde{B}_\mu^{\text{comp}} \, . \tag{4.7b}$$

We assume this first symmetry breaking to be carried out by some unknown dynamics (perhaps a distinct Higgs mechanism at high energies) whose degrees of freedom are above the cutoff scale of our effective description. Thus no additional fields are inserted in the model to take account for this SSB.

The second step of symmetry breaking is the well-known EWSB in the SM, already discussed in section 2.1. We not review it here.

4.1.1   The model Lagrangian

We will for now on focus on the leptonic sector of the model. Therefore we will forget about not only the quark sector but also about the $SU(3)_C$ gauge groups and associated bosons; indeed all our particles will be singlets with respect to these subgroups of G^{gauge}. Under these premises, we first write down the Lagrangian of the model in the elementary/composite basis:

$$\mathcal{L} = \mathcal{L}_{\text{el}} + \mathcal{L}_{\text{comp}} + \mathcal{L}_{\text{mix}} \, , \tag{4.8}$$

with

$$\mathcal{L}_{\text{el}} = -\frac{1}{4}(F_{\mu\nu}^a)^2 + \sum_{i=1}^{3} \left(\bar{\ell}_{Li} i \slashed{D} \ell_{Li} + \bar{\tilde{e}}_{Ri} i \slashed{D} \tilde{e}_{Ri} \right) \, , \tag{4.9}$$

$$\begin{aligned}
\mathcal{L}_{\text{comp}} = {}& -\frac{1}{4}(\rho_{\mu\nu}^a)^2 + \frac{M_*^2}{2}(\rho_\mu^a)^2 + |D_\mu \phi|^2 - V(\phi) \\
&+ \sum_{i=1}^{3} \left(\bar{L}_i (i\slashed{D} - m_i) L_i + \bar{\tilde{E}}_i (i\slashed{D} - \tilde{m}_i) \tilde{E}_i \right) \\
&- \sum_{i,j=1}^{3} \left(Y_{L\,ij}^* \bar{L}_{Ri} \phi \tilde{E}_{Lj} + Y_{R\,ij}^* \bar{L}_{Li} \phi \tilde{E}_{Rj} \right) + \text{h.c.} \, ,
\end{aligned} \tag{4.10}$$

$$\begin{aligned}
\mathcal{L}_{\text{mix}} = {}& -M_{*1}^2 \frac{g_1^{\text{el}}}{g_1^{\text{comp}}} W^{a\mu} W_\mu^{*a} + \frac{M_{*1}^2}{2} \left(\frac{g_1^{\text{el}}}{g_1^{\text{comp}}} W_\mu^a \right)^2 \\
&- M_{*2}^2 \frac{g_2^{\text{el}}}{g_2^{\text{comp}}} B^\mu B_\mu^* + \frac{M_{*2}^2}{2} \left(\frac{g_2^{\text{el}}}{g_2^{\text{comp}}} B_\mu \right)^2 \\
&- \sum_{i,j=1}^{3} \left(\Delta_{ij} \bar{\ell}_{Li} L_{Rj} - \tilde{\Delta}_{ij} \bar{\tilde{e}}_{Ri} \tilde{E}_{Lj} \right) + \text{h.c.} \, .
\end{aligned} \tag{4.11}$$

Several comments are in order:

- $F_{\mu\nu}^a$ and $\rho_{\mu\nu}^a$ collectively denote the field strength tensors associated with the gauge field of table 4.1 for the elementary and composite bosons, respectively. Due to the particular choice of fields made for the $SU(2)_R \times U(1)_X$ subgroup, the field strength tensors associated with these two simple subgroups involve linear combinations of $\tilde{B}^{\text{comp}}$ and B^{comp} in order to build up the correct gauge invariant quantities.

- The elementary sector is completely analogous to the SM, with the notable exception of the Higgs field, that indeed is a composite particle. Thus, before introducing any interaction with the composite sector, the mass spectrum of the theory presents a set of massless chiral fermions.

- In the composite sector, we have inserted the mass terms $\frac{1}{2}M_*^2\rho_\mu^a\rho^{a\mu}$, where ρ_μ^a collectively denotes the composite gauge fields and thus in this expression a sum over the different bosons is understood. As already discussed, we assume that some high energy dynamics breaks the initial G^{gauge} group into G^{SM}, without exploring the underlying mechanism in detail. We just parametrize this SSB using the masses M_*^2 of the composite gauge fields, that then should respect a $[SU(3)_C \times SU(2)_L \times SU(2)_R \times U(1)_X]^{\text{comp}}$ global symmetry in order to provide the correct symmetry breaking pattern. For convenience, we further associate with the subgroup $SU(2)_R \times U(1)_X$ the same mass parameter M_{*2}^2.

  Again, the choice of the fields associated with the $SU(2)_R \times U(1)_X$ subgroup makes the explicit expression of these mass terms using $\tilde{B}^{\text{comp}}$ and B^{comp} a bit involved.

- The composite leptons are vector-like, thus each of them presents both chiralities, differently from the elementary sector. Also, without loss of generality, we can choose a basis where the mass matrices m and $\tilde{m}$ are diagonal in flavor space:

$$m = \text{diag}(m_i), \quad \tilde{m} = \text{diag}(\tilde{m}_i), \qquad i = \{1, 2, 3\}. \tag{4.12}$$

- The Higgs doublet ϕ appears in the composite sector. Together with its kinetic term and its potential (that triggers the EWSB), it also presents Yukawa interactions with composite fermions. An analogous coupling with elementary leptons is clearly impossible since it is not possible in that case to build up a gauge invariant interaction term.

  If no supplementary symmetries are inferred, it should be considered (as it is done here) the most general case in which two different Yukawa interactions with different couplings Y_L^* and Y_R^* can be build up, where Y_L^* and Y_R^* are 3×3 complex matrices in flavor space. Further, in the absence of supplementary symmetries, these matrices should be considered flavor-anarchic, this assumption resulting as we will see in more stringent experimental bounds. The term involving Y_L^* is sometimes called the "wrong" Yukawa interaction, since the lepton's singlet and doublet chiralities are inverted with respect to the usual SM Yukawa interaction.

- The mixing Lagrangian consists of two parts. The first part (corresponding to the first two lines on the r.h.s. of Eq. (4.11)) is responsible for the elementary/composite mixing between gauge bosons. It is straightforward to see that this part, together with the mass terms in Eq. (4.10), still preserve the gauge invariance under G^{SM}, as it is required by the model. Indeed, they give rise to mass terms only for the linear combinations (4.6) and not for the SM fields (4.5).

The third line on the r.h.s. of Eq. (4.11) is a mixing term between elementary
and composite leptons. This mixing is regulated by two 3×3 complex matrices
in flavor space, namely Δ and $\tilde{\Delta}$. These terms are fundamental features of
the model, since they allow the elementary sector to indirectly interact with
the Higgs doublet and then to feel the EWSB, giving mass to the elementary
leptons. Also these terms preserve the SM gauge invariance, since the chiral
fermions, before EWSB, remains massless (while a mass term for the heavy
Dirac fermions is allowed by the gauge symmetry).

Performing the fields redefinitions (4.5), (4.6) and (4.7), we switch to the mass
basis for the gauge bosons (before EWSB). It is easy to see that after these rota-
tions are performed, the SM gauge fields couple with the same strength to both the
elementary and the composite sector, with gauge couplings given by:

$$g_i^{SM} \equiv \frac{g_i^{\text{el}} g_i^{\text{comp}}}{\sqrt{(g_i^{\text{el}})^2 + (g_i^{\text{comp}})^2}} \ , \qquad i = s, 1, 2 \ . \tag{4.13}$$

while the same is not true for the heavy gauge bosons.

We now write down the Lagrangian in this new basis:

$$\mathcal{L} = \mathcal{L}_{\text{gauge}} + \mathcal{L}_{\text{fermion}} + \mathcal{L}_{\text{Higgs}} \ , \tag{4.14}$$

with

$$\begin{aligned}
\mathcal{L}_{\text{gauge}} = {}&- \frac{1}{4} F_{\mu\nu}^2 + \frac{1}{2} \left(D_\mu \rho_\nu D_\nu \rho_\mu - D_\mu \rho_\nu D_\mu \rho_\nu \right) + \frac{M_{*2}^2}{2} \tilde{\rho}_\mu^2 + \frac{M_*^2}{2 \cos^2 \theta} \rho_\mu^{*\,2} \\
&+ \frac{i g^{SM}}{2} F_{\mu\nu}[\rho_\mu, \rho_\nu] + 2 i g^{SM} \cot 2\theta \, D_\mu \rho_\nu^*[\rho_\mu^*, \rho_\nu^*] + \frac{i g_2^{SM}}{\sin \theta_2} D_\mu \tilde{\rho}_\nu [\tilde{\rho}_\mu, \tilde{\rho}_\nu] \\
&+ i g_2^{SM} \cot \theta_2 \, D_\mu \rho_\nu^*[\tilde{\rho}_\mu, \tilde{\rho}_\nu] + i g_2^{SM} \cot \theta_2 \, D_\mu \tilde{\rho}_\nu \left([\rho_\mu^*, \tilde{\rho}_\nu] + [\tilde{\rho}_\mu, \rho_\nu^*] \right) \\
&+ \frac{(g^{SM})^2}{4} \left(\frac{\sin^4 \theta}{\cos^2 \theta} + \frac{\cos^4 \theta}{\sin^2 \theta} \right) [\rho_\mu^*, \rho_\nu^*]^2 + \frac{(g_2^{SM})^2}{4 \sin^2 \theta_2} [\tilde{\rho}_\mu, \tilde{\rho}_\nu]^2 \\
&+ \frac{(g_2^{SM})^2}{4} \cot^2 \theta_2 \left([\rho_\mu^*, \tilde{\rho}_\nu] + [\tilde{\rho}_\mu, \rho_\nu^*] \right)^2 + (g_2^{SM})^2 \frac{\cos \theta_2}{\sin^2 \theta_2} [\tilde{\rho}_\mu, \tilde{\rho}_\nu][\rho_\mu^*, \rho_\nu^*] \ ,
\end{aligned}$$
$$\tag{4.15}$$

$$\begin{aligned}
\mathcal{L}_{\text{fermion}} = {}&\bar{\ell}_L i \slashed{D} \ell_L + \bar{\tilde{e}}_R i \slashed{D} \tilde{e}_R + + \bar{L}(i \slashed{D} - m) L + \bar{\tilde{E}}(i \slashed{D} - \tilde{m}) \tilde{E} \\
&- g^{SM} \tan \theta \, \bar{\ell}_L \gamma^\mu \rho_\mu^* \ell_L - g^{SM} \tan \theta \, \bar{\tilde{e}}_R \gamma^\mu \rho_\mu^* \tilde{e}_R \\
&+ g^{SM} \cot \theta \, \bar{L} \gamma^\mu \rho_\mu^* L + g^{SM} \cot \theta \, \bar{\tilde{E}} \gamma^\mu \rho_\mu^* \tilde{E} \\
&- \frac{g_2^{SM}}{2 \sin \theta_2} \bar{L} \gamma^\mu \tilde{B}_\mu L - \frac{g_2^{SM}}{\sin \theta_2} \bar{\tilde{E}} \gamma^\mu \tilde{B}_\mu \tilde{E} \\
&- \Delta \bar{\ell}_L L_R - \tilde{\Delta} \bar{\tilde{e}}_R \tilde{E}_L - Y_L^* \bar{L}_R \phi \tilde{E}_L - Y_R^* \bar{L}_L \phi \tilde{E}_R + \text{h.c.} \ ,
\end{aligned} \tag{4.16}$$

$$\begin{aligned}
\mathcal{L}_{\text{Higgs}} = {}&|D_\mu \phi|^2 - V(\phi) + \left(i g^{SM} \cot \theta \, \phi^\dagger \rho_\mu^* D^\mu \phi + \text{h.c.} \right) \\
&- i \frac{g_1^{SM}}{\sqrt{2} \sin \theta_1} \tilde{\phi}^\dagger \tilde{W}_\mu^- D^\mu \phi + i \frac{g_2^{SM}}{2 \sin \theta_2} \phi^\dagger \tilde{B}_\mu D^\mu \phi + \text{h.c.} \\
&- \frac{g_1^{SM}}{\sqrt{2} \sin \theta_1} g^{SM} \cot \theta \, \tilde{\phi}^\dagger \tilde{W}_\mu^- \rho^{*\mu} \phi + \frac{g_2^{SM}}{2 \sin \theta_2} g^{SM} \cot \theta \, \phi^\dagger \tilde{B}^\mu \rho_\mu^* \phi + \text{h.c.}
\end{aligned}$$

$$+ \phi^\dagger \left[(g^{SM} \cot\theta\, \rho_\mu^*)^2 + \frac{(g_1^{SM})^2}{2\sin^2\theta_1} |\tilde{W}_\mu^+|^2 + \frac{(g_2^{SM})^2}{4\sin^2\theta_2} (\tilde{B}_\mu)^2 \right] \phi \; . \qquad (4.17)$$

In order to simplify the final expressions, we have used a compact notation where $\rho_\mu^* \equiv \{W_\mu^*, B_\mu^*\}$, $\tilde{\rho}_\mu \equiv \{\tilde{W}_\mu, \tilde{B}_\mu\}$, $g^{SM} \equiv \{g_1^{SM}, g_2^{SM}\}$ and $\theta \equiv \{\theta_1, \theta_2\}$. Every time those collective symbols are used, a sum over the two possibilities is understood. Then, for example:

$$g^{SM} \cot\theta\, \bar{L}\gamma^\mu \rho_\mu^* L \equiv g_1^{SM} \cot\theta_1\, \bar{L}\gamma^\mu W_\mu^* L + g_2^{SM} \cot\theta_2\, \bar{L}\gamma^\mu B_\mu^* L \; .$$

All the covariant derivatives are with respect to the unbroken SM gauge group, using the couplings defined in Eq. (4.13). All vector fields in Eqs. (4.16) and (4.17) (including those in the covariant derivatives) are to be considered in a matrix notation, i.e. each gauge component multiplies its corresponding generator T^a, normalized according to the standard convention ($\mathrm{Tr}(T^a T^b) = \delta^{ab}/2$ for the non-Abelian generators). The only exception is for $\tilde{W}^\pm$ and $\tilde{\mathcal{B}}$ in Eq. (4.17), which are component fields. This complication arises as a result of the subtle transformation of the Higgs under $SU(2)_R$. In the gauge Lagrangian (4.15) we adopt a different notation: gauge fields are still in matrix notation, with an implicit trace operation over the whole Lagrangian, but with the following normalization: $\mathrm{Tr}(T^a T^b) = \delta^{ab}$ for non-Abelian generators, $T = 1$ for the Abelian ones. This choice leads to a more compact and simple-to-read expression, compared to the standard normalization or the use of component fields.

4.1.2 The mass insertion approximation

To reach the correct mass basis for all the fields, starting from the Lagrangian (4.14), two more steps should be carried out. First, also the fermion fields before EWSB should be diagonalized, switching to the SM/heavy basis. Second, and more difficult, the EWSB should be taken into account.

When considering the Higgs VEV contribution, off-diagonal mass terms appear both for bosons and for fermions. Further, the new basis rotation needed to diagonalize the mass matrices typically cannot be performed analytically. Here we are interested in charged leptons, thus we now work out a strategy to take into account the above effects for them. The mass matrix for charged leptons after EWSB becomes:

$$M_E = \begin{array}{c} \begin{array}{ccc} \tilde{e}_R & \quad E_R & \quad \tilde{E}_R \end{array} \\ \left(\begin{array}{ccc} 0 & \Delta & 0 \\ 0 & m & \frac{v}{\sqrt{2}} Y_R^* \\ \tilde{\Delta}^\dagger & \frac{v}{\sqrt{2}} Y_L^{*\dagger} & \tilde{m} \end{array} \right) \end{array} \begin{array}{c} e_L \\ E_L \\ \tilde{E}_L \end{array} \; , \qquad (4.18)$$

where one should keep in mind that all the blocks in this matrix are 3×3 matrices, and then M_E is actually a 9×9 complex matrix. Consequently, even though a biunitary transformation that diagonalizes (4.18) exists for sure, its exact analytical expression is overwhelmingly difficult to find in the general case.

A possible solution to the problem could be to perform such diagonalization in a perturbative fashion. The consideration that leads to a perturbative approach is

that, since the composite sector is conjectured to appear at the TeV scale, it is fair to assume $vY^*_{L,R} \ll m, \tilde{m}$ (where we are actually comparing the $vY^*_{L,R}$ matrix elements with the eigenvalues $m_i, \tilde{m}_i$). Further, as discussed in section 3.2, it is also licit to assume $\Delta, \tilde{\Delta} \ll m, \tilde{m}$ (again using this short notation to mean the comparison between eigenvalues).

These observations lead to the idea of setting up a perturbative expansion, where v, Δ and $\tilde{\Delta}$ are order-one quantities while m and $\tilde{m}$ are zero order quantities. From this perspective, M_E is diagonal at the zero order (remember that we are working in a basis where m and $\tilde{m}$ are diagonal) and its off-diagonal elements are all quatities of the first order.

Actually, a further condition must be satisfied in order to fully legitimate the above expansion. To be definite, not only m_i and $\tilde{m}_i$, but also $m_i - \tilde{m}_j$ should be zero order quantities. Intuitively, this is because in calculations such quantities could possibly appear (in the numerator or, worst, in the denominator), and without the above additional assumption they would spoil the perturbative power counting settled above.

Using the approach just described, approximate expressions for the unitary matrices that perform the mass diagonalization can be explicitly computed. For example, up to the second order the unitary matrices that makes M_E block-diagonal are

$$
V_L \simeq \begin{pmatrix} \mathbb{1} - \frac{1}{2}\Delta m^{-2}\Delta^\dagger & \Delta m^{-1} & -\Delta m^{-1}\left(J^\dagger + \frac{v}{\sqrt{2}}Y^*_R\tilde{m}^{-1}\right) \\ -m^{-1}\Delta^\dagger & \mathbb{1} - \frac{1}{2}m^{-1}\Delta^\dagger\Delta m^{-1} - \frac{1}{2}J^\dagger J & -J^\dagger \\ \frac{v}{\sqrt{2}}\tilde{m}^{-1}Y^{*\dagger}_R m^{-1}\Delta^\dagger & J & \mathbb{1} - \frac{1}{2}JJ^\dagger \end{pmatrix} ,
$$

$$(4.19)$$

$$
V_R \simeq \begin{pmatrix} \mathbb{1} - \frac{1}{2}\tilde{\Delta} m^{-2}\tilde{\Delta}^\dagger & \tilde{\Delta}\tilde{m}^{-1}\left(K - \frac{v}{\sqrt{2}}Y^{*\dagger}_R m^{-1}\right) & \tilde{\Delta}\tilde{m}^{-1} \\ \frac{v}{\sqrt{2}}m^{-1}Y^*_R\tilde{m}^{-1}\tilde{\Delta}^\dagger & \mathbb{1} - \frac{1}{2}K^\dagger K & -K^\dagger \\ -\tilde{m}^{-1}\tilde{\Delta}^\dagger & K & \mathbb{1} - \frac{1}{2}\tilde{m}^{-1}\tilde{\Delta}^\dagger\tilde{\Delta}\tilde{m}^{-1} - \frac{1}{2}KK^\dagger \end{pmatrix} ,
$$

$$(4.20)$$

where J and K are implicitly defined via the following Sylvester equations:

$$
\begin{cases} Jm^2 - \tilde{m}^2 J = \frac{v}{\sqrt{2}}(Y^{*\dagger}_L m + \tilde{m}Y^{*\dagger}_R) \\ Km^2 - \tilde{m}^2 K = \frac{v}{\sqrt{2}}(Y^{*\dagger}_R m + \tilde{m}Y^{*\dagger}_L) \end{cases} ,
$$

$$(4.21)$$

that can be solved analytically since m and $\tilde{m}$ are diagonals, resulting in

$$
(J)_{ij} = \frac{1}{m_j^2 - m_i^2}\frac{v}{\sqrt{2}}(Y^{*\dagger}_L m + \tilde{m}Y^{*\dagger}_R)_{ij} ,
$$

$$(4.22a)$$

$$
(K)_{ij} = \frac{1}{m_j^2 - m_i^2}\frac{v}{\sqrt{2}}(Y^{*\dagger}_R m + \tilde{m}Y^{*\dagger}_L)_{ij} .
$$

$$(4.22b)$$

The resulting diagonalized mass matrix becomes:

$$
M_E^{\text{diag}} = V_L^\dagger M_E V_R = \begin{pmatrix} 0 & 0 & 0 \\ 0 & A & 0 \\ 0 & 0 & B \end{pmatrix} + \text{third order terms} ,
$$

$$(4.23)$$

$$
A \equiv m + \frac{v}{\sqrt{2}}(Y^*_R K + J^\dagger Y^{*\dagger}_L) + \frac{1}{2}m^{-1}\Delta^\dagger\Delta - \frac{1}{2}mK^\dagger K - \frac{1}{2}J^\dagger Jm + J^\dagger\tilde{m}K ,
$$

$$(4.24)$$

$$B \equiv \tilde{m} - \frac{v}{\sqrt{2}}(JY_R^* + Y_L^{*\dagger}K^\dagger) + \frac{1}{2}\Delta^\dagger\Delta\tilde{m}^{-1} - \frac{1}{2}\tilde{m}K^\dagger K - \frac{1}{2}J^\dagger J\tilde{m} + J\tilde{m}K^\dagger \,, \quad (4.25)$$

where one can appreciate that, at the second order, the SM leptons are still massless, implying that the SM lepton masses are at least third order quantities. In fact, they first arise at the third order.

The solutions (4.22) are valid only in the case of non degeneracy between doublets and singlets masses (i.e. $m_i \neq \tilde{m}_j \; \forall i, j$). Remarkably, they also show in a clear way why, if the hypothesis $m_i - \tilde{m}_j \gg v$ failed, all the analysis above would be spoiled. Indeed, in that case J and K would not be anymore order-one quantities and all the perturbative expansions made to consistently compute the above expressions would be ruined.

Through the matrices $V_{L,R}$ one can infers the rotation to the mass basis (for the SM charged leptons) into the Lagrangian (4.16). Introducing a nine-component vector ξ to represent all the nine charged lepton fields of a definite chirality

$$\xi_L = \begin{pmatrix} e_L \\ E_L \\ \tilde{E}_L \end{pmatrix}, \qquad \xi_R = \begin{pmatrix} \tilde{e}_R \\ E_R \\ \tilde{E}_R \end{pmatrix}, \qquad (4.26)$$

the rotation from the interaction to the mass basis can be written as:

$$\xi_L^{\text{int}} = V_L \xi_L^{\text{mass}} \,, \qquad \xi_R^{\text{int}} = V_R \xi_R^{\text{mass}} \,, \qquad (4.27)$$

and hereafter we will shorten the 'mass' apex simply to 'm'. Using this compact notation, the Lagrangian (4.16) after the basis rotation becomes:

$$\mathcal{L}_{\text{fermion}} = \bar{\xi}^{\text{m}} i \slashed{D} \xi^{\text{m}} + \bar{\nu}_L i \slashed{D} \nu_L + \bar{N} i \slashed{D} N - \left(\bar{\xi}_L^{\text{m}} M_E^{\text{diag}} \xi_R^{\text{m}} + \text{h.c.} \right)$$

$$- \frac{1}{\sqrt{2}}(h + i\varphi_Z)\bar{\xi}_L^{\text{m}} \Upsilon \xi_R^{\text{m}} - \varphi^+ \bar{N}_R \Sigma_L \xi_L^{\text{m}} - \varphi^+ \bar{N}_L \Sigma_R \xi_R^{\text{m}} + \text{h.c.}$$

$$+ \text{heavy boson interactions} \,, \qquad (4.28)$$

$$\Upsilon = V_L^\dagger \begin{pmatrix} 0 & 0 & 0 \\ 0 & 0 & Y_R^* \\ 0 & Y_L^{*\dagger} & 0 \end{pmatrix} V_R \,, \qquad (4.29)$$

$$\Sigma_{L,R} = \begin{pmatrix} 0 & 0 & Y_{L,R}^* \end{pmatrix} V_{L,R} \,. \qquad (4.30)$$

where we have expressed the Higgs doublets in terms of its components:

$$\phi = \begin{pmatrix} \varphi^+ \\ (v + h + i\varphi_Z)/\sqrt{2} \end{pmatrix} \,. \qquad (4.31)$$

The Lagrangian (4.28) allows to compute the Higgs doublet contribution in an exact manner as functions of the Υ and Σ matrices and then to introduce the perturbative approach only in the end, deriving an approximate expression for Υ and Σ using Eqs. (4.19), (4.20), (4.29) and (4.30).

The approach developed so far will be used only in this work only once to check one obtained result. In all the other computations, we will adopt a different strategy:

retaining the perturbative approach settled before (with the same caveat regarding the composite fermions mass differences), we will perform calculations directly using the Lagrangian (4.14), without changing the field basis. This can be done using the so called *mass insertion approximation*: the off-diagonal terms of the mass matrices (that, as already observed, are all perturbative quantities) are interpreted as interaction vertices, that have to be considered when building up the possible Feynman diagrams. The Feynman rules involving leptons arising from the Lagrangian (4.14) using the mass insertion approximation are listed in appendix A.3.

Clearly, one should keep in mind that the physical states are the mass eigenstates. Thus, in order to find the correct physical amplitude, one should coherently sum up all the contributions arising from the various components that make up the physical admixture. This procedure is equivalent to the rotation to the mass basis; the difference is that, in this case, such rotation is performed after the evaluation of the amplitudes.

In particular, such final basis rotation cancels tree level contributions to FCNC processes. Indeed in this approximation, using the Feynman rules listed in appendix A.3, one can in principle build up tree level FCNC diagrams exploiting the off-diagonal elements of M_E. However, one can easily verify that such amplitudes will become flavor-diagonal when the rotation to the mass basis is performed.

In what follows, we have assumed that the perturbative approach is fully justified; in particular, no quasi-degeneracy of the spectrum is supposed to occur. Thus, a mass insertion approximation will be used to perform phenomenological computations of FCNC leptonic processes.

4.2 The dipole operator

4.2.1 Generalities

The search for charged lepton flavor violation (cLFV) is one major goal of flavour physics in the next years. Indeed, the observation of neutrino oscillations has clearly demonstrated that lepton flavour is not conserved, then the question is whether LFV effects can be visible also for charged leptons.

The most promising LFV low-energy channels are probably $\mu \to e\gamma$, $\mu \to eee$, $\mu \to e$ conversion in Nuclei and τ LFV processes. Since, in the SM with massive neutrinos, LFV effects are loop suppressed and proportional to the GIM factor $(m_\nu/M_W)^4$ (therefore completely negligible), any observation of such processes would clearly point toward NP signal. Present bounds and future sensitivities of next-generation experiments for these processes are collected in table 4.3.

Adopting the EFT approach described in section 2.2, examples of dimension six operators contributing to the above processes are

$$\left(\bar{e}_L\gamma^\mu\mu_L\right)\left(\bar{f}_L\gamma^\mu f_L\right) \;, \qquad \left(\bar{e}_L\mu_R\right)\left(\bar{f}_L f_R\right) \;, \qquad F_{\mu\nu}\phi\,\bar{e}_L\sigma^{\mu\nu}\mu_R \;, \qquad (4.32)$$

where f are either lepton or quark fields. All the operators in (4.32) lead to processes like $\mu \to eee$ and $\mu \to e$ conversion in Nuclei. However, only the third one generates, at the leading order, also the LFV decay $\mu \to e\gamma$; this operator is nothing but the electromagnetic dipole operator already introduced in the quark sector, Eq. (2.58).

LFV Process	Present Bound	Future Experiments and Sensitivities		Year (expected)
$BR(\mu \to e\gamma)$	$5.7 \cdot 10^{-13}$ [48]	MEG [49]	$\approx 6 \cdot 10^{-14}$	~ 2019
		Project X [50]	$\mathcal{O}(10^{-15})$	> 2021
$BR(\mu \to eee)$	$1.0 \cdot 10^{-12}$ [51]	Mu3e [52]	$\mathcal{O}(10^{-15})$	~ 2017
		"	$\mathcal{O}(10^{-16})$	> 2017
		Project X [50]	$\mathcal{O}(10^{-17})$	> 2021
$CR(\mu^- N \to e^- N)$	$\sim \mathcal{O}(10^{-12})$ [53]	COMET [54]	$\mathcal{O}(10^{-17})$	~ 2017
		MuSIC [54]	$\mathcal{O}(10^{-16})$	~ 2017
		Mu2e [55]	$\mathcal{O}(10^{-17})$	~ 2020
		Project X [50]	$\mathcal{O}(10^{-19})$	> 2021
$BR(\tau \to \mu\gamma)$	$4.4 \cdot 10^{-8}$ [56]	Belle II [57]	$\mathcal{O}(10^{-9})$	> 2020
$BR(\tau \to e\gamma)$	$3.3 \cdot 10^{-8}$ [56]	Belle II [57]	$\mathcal{O}(10^{-9})$	> 2020
$BR(\tau \to \mu\mu\mu)$	$2.1 \cdot 10^{-8}$ [58]	Belle II [57]	$\mathcal{O}(10^{-10})$	> 2020

Table 4.3: Present bounds for cLFV processes and future sensitivities of next-generation experiments.

Which operators give the dominant LFV contributions in specific NP models determines which are the observable most sensitive to NP effects. In CH models it turns out that one of the most sensitive operator to NP contribution is the dipole operator. Further, among the various dipole-mediated processes, it can be shown that the most sensitive ones are the LFV decays $\ell \to \ell'\gamma$. For this reason, in the following, we will focus our attention to these class of processes and in particular to the muon decay mode:

$$\mu \to e\,\gamma\,, \tag{4.33}$$

describing the peculiar features of this process, and then evaluating the contribution to this decay arising from the two-site model described in the previous section.

First, we consider the amplitude associated with the process (4.33):

$$= \quad \mathcal{M}(p,p')\,, \tag{4.34}$$

where, being all the three external momenta on-shell, it is clear that only two of them are linearly independent, the third fixed by the momentum conservation $p = p' + q$; thus $\mathcal{M}$ depends only upon two of them.

We now want to find how $\mathcal{M}(p,p')$ can be cast. As we will see, our result will be immediately generalizable to the more generic process $\ell \to \ell'\gamma$. We then start by writing the most general expression that it can assume:

$$\mathcal{M}(p,p') = \varepsilon_\mu(q)\bar{e}(p')\big[(A + B\gamma^5)(p+p')^\mu + (C + D\gamma^5)(p-p')^\mu$$
$$+ (E + F\gamma^5)\gamma^\mu\big]\mu(p)$$

$$= \varepsilon_\mu(q)\bar{e}(p') \left[(A + B\gamma^5)(p + p')^\mu + (E + F\gamma^5)\gamma^\mu \right] \mu(p) , \qquad (4.35)$$

where we have already used the relation $(p - p') \cdot \varepsilon = q \cdot \varepsilon = 0$, that is the transversality of the photon polarizations. A, B, E, F are understood to be Lorentz scalars, thus they can only be functions of $m_{\mu,e}$. Indeed, given the momentum conservation $p = p' + q$:

$$\begin{cases} p \cdot p' = \frac{1}{2}(m_\mu^2 + m_e^2) \\ p \cdot q = p' \cdot q = \frac{1}{2}(m_\mu^2 - m_e^2) \end{cases} . \qquad (4.36)$$

The expression (4.35) can be further simplified if one imposes the Ward identity, namely:

$$\begin{aligned} 0 &\stackrel{!}{=} q_\mu \, \bar{e}(p') \left[(A + B\gamma^5)(p + p')^\mu + (E + F\gamma^5)\gamma^\mu \right] \mu(p) \\ &= (m_\mu^2 - m_e^2) \, \bar{e}(A + B\gamma^5)\mu + m_\mu \, \bar{e}(E + F\gamma^5)\mu - m_e \, \bar{e}(E - F\gamma^5)\mu \\ &= (m_\mu - m_e) \left[(m_\mu + m_e)A + E \right] \bar{e}\mu + (m_\mu + m_e) \left[(m_\mu - m_e)B + F \right] \bar{e}\gamma^5\mu , \end{aligned} \qquad (4.37)$$

thus:

$$\begin{cases} E = -(m_\mu + m_e)A \\ F = -(m_\mu - m_e)B \end{cases} . \qquad (4.38)$$

Plugging (4.38) into (4.35) we get

$$\mathcal{M} = 2\varepsilon \cdot pA \, \bar{e}\mu - (m_\mu + m_e)A \, \bar{e}\gamma \cdot \varepsilon\mu + 2\varepsilon \cdot pB \, \bar{e}\gamma^5\mu - (m_\mu - m_e)B \, \bar{e}\gamma^5\gamma \cdot \varepsilon\mu . \qquad (4.39)$$

Now we exploit the Gordon identities:

$$\begin{cases} 2 \, \varepsilon \cdot p \, \bar{e}_L\mu_R - m_\mu \, \bar{e}_L\gamma \cdot \varepsilon\mu_L - m_e \, \bar{e}_R\gamma \cdot \varepsilon\mu_R = i\varepsilon_\mu q_\nu \, \bar{e}_L\sigma^{\mu\nu}\mu_R \\ 2 \, \varepsilon \cdot p \, \bar{e}_R\mu_L - m_\mu \, \bar{e}_R\gamma \cdot \varepsilon\mu_R - m_e \, \bar{e}_L\gamma \cdot \varepsilon\mu_L = i\varepsilon_\mu q_\nu \, \bar{e}_R\sigma^{\mu\nu}\mu_L \end{cases} , \qquad (4.40)$$

that can be equivalently written as:

$$\begin{cases} (p + p')^\mu \, \bar{e}\mu - (m_\mu + m_e) \, \bar{e}\gamma^\mu\mu = i(p - p')_\nu \, \bar{e}\sigma^{\mu\nu}\mu \\ 2p^\mu \, \bar{e}\gamma^5\mu - (m_\mu - m_e) \, \bar{e}\gamma^5\gamma^\mu\mu = i(p - p')_\nu \, \bar{e}\sigma^{\mu\nu}\gamma^5\mu \end{cases} , \qquad (4.41)$$

where $\sigma^{\mu\nu} \equiv \frac{i}{2}[\gamma^\mu\gamma^\nu]$. We finally get:

$$\begin{aligned} \mathcal{M} &= iA \, \varepsilon_\mu q_\nu \, \bar{e}\sigma^{\mu\nu}\mu + iB \, \varepsilon_\mu q_\nu \, \bar{e}\sigma^{\mu\nu}\gamma^5\mu \\ &= iC_1 \, \varepsilon_\mu q_\nu \, \bar{e}_L\sigma^{\mu\nu}\mu_R + iC_2 \, \varepsilon_\mu q_\nu \, \bar{e}_R\sigma^{\mu\nu}\mu_L , \end{aligned} \qquad (4.42)$$

where in the last line we have recast the expression making explicit the two different chirality structures. It is easy to verify that $C_{1,2} = A \pm B$.

As a result of the above analysis, we can conclude that the effective Lagrangian

$$\mathcal{L}_{\text{eff}} = \frac{m_\ell}{2} eF_{\mu\nu} \left[\left(C_{\ell\ell'} \, \bar{\ell}'_L\sigma^{\mu\nu}\ell_R + C^*_{\ell\ell'} \, \bar{\ell}_R\sigma^{\mu\nu}\ell'_L \right) + \ell \leftrightarrow \ell' \right] \qquad \ell, \ell' = e, \mu, \tau , \quad (4.43)$$

built up using the two different chiralities of the dipole operator in Eq. (4.32), completely accounts for the processes $\ell \to \ell'\gamma$, and then in particular for the decay (4.33).

We are thus able to completely parametrize NP contributions to $\ell \to \ell'\gamma$ using the Wilson coefficients $C_{\ell\ell'}$ and $C_{\ell'\ell}$.

Using Eq. (4.43), we can express the branching ratio for the LFV $\ell \to \ell'\gamma$ process as [59]

$$\frac{\text{BR}(\ell \to \ell'\gamma)}{\text{BR}(\ell \to \ell'\nu_\ell\bar{\nu}_{\ell'})} = \frac{48\pi^3\alpha}{G_F^2}\left(|C_{\ell\ell'}|^2 + |C_{\ell'\ell}|^2\right) . \tag{4.44}$$

If we assume $C_{\ell\ell'} = c_{\ell\ell'}/\Lambda^2$, where Λ refers to the NP scale, we can evaluate which are the values of Λ probed by $\mu \to e\gamma$. We find that

$$\text{BR}(\mu \to e\gamma) \simeq 10^{-12}\left(\frac{500 \text{ TeV}}{\Lambda}\right)^4\left(|c_{\mu e}|^2 + |c_{e\mu}|^2\right) . \tag{4.45}$$

Considering $c_{\ell\ell'} \sim 1$ on the ground of naturalness considerations, and comparing Eq. (4.45) with the current experimental bound (see Tab. 4.3), we can conclude that $\Lambda > 500$ TeV. Thus, a NP flavor problem arises also in the leptonic sector.

Furthermore, the underlying $\ell \to \ell'\gamma$ transition can generate also lepton flavor conserving processes ($\ell = \ell'$) like the anomalous magnetic moments Δa_ℓ as well as leptonic electric dipole moments (EDMs, d_ℓ). In terms of the effective Lagrangian of Eq. (4.43), we can write Δa_ℓ and d_ℓ as [59]

$$\Delta a_\ell = 2m_\ell^2 \, \text{Re}(C_{\ell\ell}) , \qquad \frac{d_\ell}{e} = -m_\ell \, \text{Im}(C_{\ell\ell}) . \tag{4.46}$$

On general grounds, one then would expect that, in concrete NP scenarios, Δa_ℓ, d_ℓ and $\text{BR}(\ell \to \ell'\gamma)$, are correlated. In practice, their correlations depend on the unknown flavor and CP structure of the NP couplings and thus we cannot draw any firm conclusion. Nevertheless, interesting considerations can be made comparing the different experimental results for NP contributions to these observables.

For example, taking into account the claimed $\sim 3.5\sigma$ discrepancy between SM prediction and experimental value for a_μ, $\Delta a_\mu = a_\mu^{\text{EXP}} - a_\mu^{\text{SM}} = (2.90 \pm 0.90) \cdot 10^{-9}$ [60], and further assuming that such a discrepancy is due to NP, we find a theoretical prediction for $\text{BR}(\mu \to e\gamma)$ of:

$$\text{BR}(\mu \to e\gamma) \simeq 10^{-12}\left(\frac{\Delta a_\mu}{3 \times 10^{-9}}\right)^2\left(\frac{\theta_{e\mu}}{2 \times 10^{-5}}\right)^2 , \tag{4.47}$$

where $\theta_{e\mu} = \sqrt{|c_{e\mu}|^2 + |c_{\mu e}|^2}/|c_{\mu\mu}|$. From the comparison between Eq. (4.47) and the current experimental constraint we learn that the a_μ anomaly can be accommodated while satisfying the $\text{BR}(\mu \to e\gamma)$ bound only for an extremely small flavor mixing angle $\theta_{e\mu}$. Thus, trusting the a_μ anomaly, this can be seen as another clue for a NP flavor problem in the leptonic sector.

An analogous problem arises when considering the electron EDM. This quantity has a very strict experimental bound [61]:

$$d_e < 8.7 \cdot 10^{-29} \, e \, \text{cm} , \tag{4.48}$$

that, assuming naïve scaling [59], is again incompatible with the assumption of a NP contribution to a_μ of order $\sim 3 \cdot 10^{-9}$, unless some highly non trivial flavor suppression

is at work. Indeed one finds:

$$d_e \simeq \left(\frac{\Delta a_\mu}{3 \times 10^{-9}} \right) \cdot 10^{-24} \tan \phi_e \ e \, \mathrm{cm} \,, \tag{4.49}$$

and thus $\tan \phi_e \equiv \mathrm{Arg}(C_{ee}) \lesssim 10^{-4}$.

For completeness, let us consider also the experimental bound for d_μ [22],

$$d_\mu \lesssim 10^{-18} \ e \, \mathrm{cm} \,, \tag{4.50}$$

and compare it with its prediction using the a_μ anomaly,

$$d_\mu \simeq \left(\frac{\Delta a_\mu}{3 \times 10^{-9}} \right) 2 \cdot 10^{-22} \tan \phi_\mu \ e \, \mathrm{cm} \,, \tag{4.51}$$

where again $\tan \phi_\mu = \mathrm{Arg}(C_{\mu\mu})$. This time, no evident friction arises, and there is still room for sizeable values for d_μ compatible with the a_μ anomaly in an anarchic scenario.

Now that we have briefly discussed the importance, for present and future researches, of cLFV contributions in NP scenarios, let us return on the process (4.33), in order to develop a strategy to perform the computations in our two-site model. There is a first important conclusion that can be immediately drawn from our previous discussion. When computing the Feynman diagrams associated with $\mathcal{M}$, both operators that flip chirality ($\varepsilon \cdot p \, \bar{e}\mu$ and $\varepsilon_\mu q_\nu \, \bar{e}\sigma^{\mu\nu}\mu$) and that conserve chirality ($\bar{e}\gamma \cdot \varepsilon \mu$) can occur. However, the coefficients associated with all these operators should satisfy Eqs. (4.40) and (4.42). As a result, only four over the six mentioned operators have linearly independent coefficients, needed to compute the two parameters $C_{1,2}$ (or equivalently $C_{e\mu}$ and $C_{\mu e}$).

As a consequence, we can arbitrarily make the choice of considering as independent only the four chirality flipping operators $\varepsilon \cdot p \, \bar{e}\mu$ and $\varepsilon_\mu q_\nu \, \bar{e}\sigma^{\mu\nu}\mu$ (each of these two operators indeed can appear with two different chiralities). This choice allows us, in the calculation of the amplitude $\mathcal{M}$, to consider only chirality-flipping contributions (neglecting chirality-conserving ones) and still obtain the full, correct amplitude in virtue of the above argument.

Now we have to embed the above discussion into the two-site model in mass insertion approximation we are using. Indeed, all the three particles involved in the process (4.33) are a compound of both elementary and composite fields and this could in principle complicate the calculations, in the basis we are using. However, as already observed, the SM fields admixture is made up of almost elementary fields. In other words, the elementary fields give a zero order contribution to such admixture, while the composite fields give an order-one contribution (using the power-counting introduced in the previous section). Since we will perform the computations at the first non-vanishing order, only the elementary components of the SM fields will give their contribution.

Thus, in the elementary/composite basis, the process (4.33) at the leading order can be written as

$$e_i \to e_j \, \gamma \,, \tag{4.52}$$

where we will express the flavor indices i, j in an implicit form for generality, but for the process under study one should at the end put $i = 2$ and $j = 1$.

In addiction, according to the previous discussion regarding the chiralities structures to be considered, we can further reduce ourselves to study the two chirality-flipping processes, with which we will associate the following amplitudes and operators:

$$\tilde{e}_{Ri} \to e_{Lj}\, \gamma \qquad \longrightarrow \qquad \mathcal{M}_L \propto Q_{\gamma L} \equiv i\varepsilon_\mu q_\nu\, \bar{e}_{Li}\sigma^{\mu\nu}\tilde{e}_{Rj}\ , \tag{4.53a}$$

$$e_{Li} \to \tilde{e}_{Rj}\, \gamma \qquad \longrightarrow \qquad \mathcal{M}_R \propto Q_{\gamma R} \equiv i\varepsilon_\mu q_\nu\, \bar{\tilde{e}}_{Ri}\sigma^{\mu\nu}e_{Lj}\ . \tag{4.53b}$$

4.2.2 Spurionic analysis

Now that we have completely characterized the decay we are considering, we will soon start the explicit computations of the associated amplitude. However, it is worthwhile to first carry out a spurionic analysis of the amplitudes for the processes (4.53).

As a first step, we have to identify the flavor symmetry group of the Lagrangian (4.14) and its breaking terms. Given the leptonic content Tab. 4.2 of the theory, we can assume the following flavor group (focusing only on the non-Abelian part):

$$\begin{aligned} G_{flavor} &= SU(3)^6 \\ &= SU(3)_\ell \times SU(3)_{\tilde{e}} \times SU(3)_{L_L} \times SU(3)_{L_R} \times SU(3)_{\tilde{E}_L} \times SU(3)_{\tilde{E}_R}\ , \end{aligned} \tag{4.54}$$

under which the lepton fields rotate in generation space in the following way:

$$\begin{aligned} \ell_{Li} &\to (V_\ell)_{ij}\ell_{Lj}\ , & \tilde{e}_{Ri} &\to (V_{\tilde{e}})_{ij}\tilde{e}_{Rj}\ , \\ L_{Li} &\to (V_{L_L})_{ij}L_{Lj}\ , & \tilde{E}_L &\to (V_{\tilde{E}_L})_{ij}\tilde{E}_{Lj}\ , \\ L_{Ri} &\to (V_{L_R})_{ij}L_{Lj}\ , & \tilde{E}_R &\to (V_{\tilde{E}_R})_{ij}\tilde{E}_{Rj}\ . \end{aligned} \tag{4.55}$$

It is straightforward to verify that the interaction terms between leptons and gauge bosons preserve this flavor symmetry group[2]. The only flavor violating parameters are then the composite leptons masses $m, \tilde{m}$, the mass mixing parameters between elementary and composite leptons $\Delta, \tilde{\Delta}$ and the Yukawa matrices Y_L^*, Y_R^*.

Once found the symmetry breaking terms, we have to promote them to spurions in order to recover the flavor symmetry. It is again easy to see that the symmetry under G_{flavor} can be restored assuming the following spurionic transformation properties for the above parameters:

$$\begin{aligned} m &\to V_{L_L} m V_{L_R}^\dagger\ , & \Delta &\to V_\ell \Delta V_{L_R}^\dagger\ , & Y_R^* &\to V_{L_L} Y_R^* V_{\tilde{E}_R}^\dagger\ , \\ \tilde{m} &\to V_{\tilde{E}_L} \tilde{m} V_{\tilde{E}_R}^\dagger\ , & \tilde{\Delta} &\to V_{\tilde{e}} \tilde{\Delta} V_{\tilde{E}_L}^\dagger\ , & Y_L^* &\to V_{L_R} Y_L^* V_{\tilde{E}_L}^\dagger\ . \end{aligned} \tag{4.56}$$

We are now ready to deduce the spurionic structure of the two amplitudes associated with the $Q_{\gamma L}$ and $Q_{\gamma R}$ operators defined in Eqs. (4.53). Considering $Q_{\gamma L}$, we want to obtain a G_{flavor} invariant quantity starting from

$$\bar{e}_L(\ldots)\bar{\tilde{e}}_R \to \bar{e}_L V_\ell^\dagger(\ldots)V_{\tilde{e}}\tilde{e}_R\ , \tag{4.57}$$

---

[2]Actually, one could consider a bigger flavor group, $SU(6)^2 \times SU(3)^2$, that mixes among ℓ_L and L_L fields, and among $\tilde{e}_R$ and $\tilde{E}_R$ fields. The discussion would become more involved since heavy bosons interactions breaks this bigger flavor group and further a new formalism should be introduced. For our present purposes, the flavor group (4.54) is sufficient.

where $(\ldots)$ stands for the spurionic structure we have to build up. A first possible solution could be:

$$\bar{e}_L \Delta Y_L^* \tilde{\Delta}^\dagger \tilde{e}_R \ , \tag{4.58}$$

but this is not a valid combination, since it has the wrong mass dimension. Indeed we have $[Q_{\gamma L}] = 2$ and $[\mathcal{M}] = 1$; since possible additional v factors in the expression of $\mathcal{M}$ can occur, the spurionic structure should have mass dimension lower or equal to -1.

The next possible invariant spurions combinations are

$$\bar{e}_L \Delta m^\dagger Y_R^* \tilde{m}^\dagger \tilde{\Delta}^\dagger \tilde{e}_R \ , \tag{4.59}$$

$$\bar{e}_L \Delta m^\dagger Y_R^* \tilde{m}^\dagger Y_L^{*\dagger} m^\dagger Y_R^* \tilde{m}^\dagger \tilde{\Delta}^\dagger \tilde{e}_R \ , \tag{4.60}$$

that again have both the wrong dimension. However, this time, a licit configuration is found if, in the expression (4.60), we replace $m^\dagger, \tilde{m}^\dagger$ with $m^{-1}, \tilde{m}^{-1}$ respectively, that have the same spurionic transformation properties. We then find the allowed spurionic structure:

$$\bar{e}_L \Delta m^{-1} Y_R^* \tilde{m}^{-1} Y_L^{*\dagger} m^{-1} Y_R^* \tilde{m}^{-1} \tilde{\Delta}^\dagger \tilde{e}_R \ . \tag{4.61}$$

Since it has mass dimension -2, a v factor in the final amplitude will appear to fix the dimensional analysis. Thus, also remembering Eq. (4.12), we can write the lowest-order contribution to the process (4.53a) as

$$\mathcal{M}_L = c_L v \sum_{a,b,c,d} \frac{1}{m_d \tilde{m}_c m_b \tilde{m}_a} (\Delta)_{jd} (Y_R^*)_{dc} (Y_L^{*\dagger})_{cb} (Y_R^*)_{ba} (\tilde{\Delta}^\dagger)_{ai} \ Q_{\gamma L} \ , \tag{4.62}$$

where c_L is an unknown numerical coefficient.

The introduction of a negative power for the mass matrices in Eq. (4.61), supported above using a simple dimensional argument, can receive a further explanation. Indeed, following the EFT discussion of section 2.2, we already know that for a dimension six operator (as the dipole operator $Q_{7\gamma}$) a decoupling $\sim 1/\Lambda_{\mathrm{NP}}^2$ is expected, where clearly $\Lambda_{\mathrm{NP}} \sim m, \tilde{m}$. Further, according to the PC paradigm of these kind of models (see section 3.2), the complete amplitude is expected to present a suppression factor related to two tiny mixing angles (representing the composite state contribution to the SM particles admixture). According to Eq. (3.26), we can then conclude that:

$$\mathcal{M}_L \sim \frac{1}{\Lambda_{\mathrm{NP}}^2} \varphi_L \varphi_R \sim \frac{1}{m \tilde{m}} \frac{\Delta}{m} \frac{\tilde{\Delta}}{\tilde{m}} \ . \tag{4.63}$$

Using this general argument, we have explained the appearance of four masses at the denominator and partially reconstructed the correct spurionic structure (4.62).

To complete the argument above, we have to justify one subtlety: if in Eq. (4.60) we perform the substitution $Y_{L,R}^* \to Y_{L,R}^* (Y_{L,R}^{*\dagger} Y_{L,R}^*)^n$, we still have a correct spurionic structure apparently with the same mass dimension, but we have not considered this possibility. This is because one has to consider how a Yukawa matrix can appear in the amplitude: it can be either as a mass insertion, and this does modify the dimension through a VEV factor, or either as an interaction vertex with an Higgs

boson (or a would-be Goldstone boson, if not in unitary gauge), and then the spurion $(Y_{L,R}^{*\dagger} Y_{L,R}^*)$ arise from an extra loop (since we are looking for one-loop contributions, we neglect also this case).

An identical reasoning can be carried out for the (4.53b) process. The result is then:

$$\mathcal{M}_R = c_R v \sum_{a,b,c,d} \frac{1}{\tilde{m}_d m_c \tilde{m}_b m_a} (\tilde{\Delta})_{jd} (Y_R^{*\dagger})_{dc} (Y_L^*)_{cb} (Y_R^{*\dagger})_{ba} (\Delta^\dagger)_{ai} \, Q_{\gamma R} \, , \qquad (4.64)$$

where again c_R is an unknown numerical coefficient.

4.3 Explicit computations

After having deduced the expected structure of the amplitudes from spurionic considerations, we are now ready to perform an explicit computation, using the mass insertion approximation.

We have already discussed how FCNC processes arise first at the one-loop order. In this section, we will evaluate the contribution to the process (4.52) given by the exchange of a SM boson (either an Higgs or a gauge boson) in the loop.

Even though this outlined calculation is clearly incomplete, as one should in principle take into account also the contribution from the heavy bosons, it is nevertheless meaningful, as the result will give a reasonable approximation of the order of magnitude for the expected contribution of our NP scenario to the dipole operator.

4.3.1 Higgs boson contribution

We start with computing the contribution from an Higgs boson circulating in the loop. We carry out explicit computations for the process (4.53a),

$$\tilde{e}_{Ri} \rightarrow e_{Lj} \gamma \, ,$$

and then we will exploit simple analogies and similarities to deduce the corresponding amplitude for the process (4.53b).

We start building the possible Feynman diagrams with finding the possible flavor structure(s) of the fermionic line, limiting ourselves to the one(s) with the lowest number of mass insertions (according to the perturbative approach chosen to perform the calculation).

The steps needed to find the lowest order fermionic line are represented in Fig. 4.1. First, we impose the correct external fermionic lines, corresponding to the elementary charged leptons with the correct chiralities. The step 2 is a forced one, since we need to switch to the composite sector in order to interact with the Higgs boson and there is only one way to do that. Now, to connect the two composite fermions $\tilde{E}_a$ and E_d, an odd number of Yukawa insertions (either Yukawas interactions or mass mixings) are required. But we need at least two Yukawa insertions in order to build an Higgs loop. Then the lowest order solution has three Yukawa insertions, as represented in the third step of Fig. 4.1.

Among the three Yukawa insertions, two of them are associated with the interaction vertex between the composite leptons and the Higgs, while the third one is a
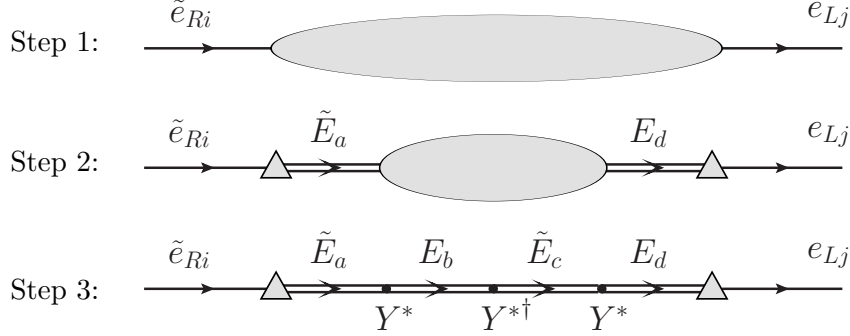
Figure 4.1: Steps of construction of the lowest order fermionic line leading to FCNC at one-loop order.

mass insertion (i.e. an interaction between the two leptons and the Higgs VEV). It is then clear that there are only three possibilities of creating the Higgs loop.

We are then left only with inserting the outgoing photon. In principle, this could be done at any point of the fermionic line; however, a very general argument can be adduced to prove that only if the photon is attached inside the loop, the amplitude would not vanish. Indeed, if this would not be the case, the loop could only produce a contribution proportional to γ^μ; but then the total amplitude would become $\bar{e}_{Lj}\gamma \cdot \varepsilon\, \tilde{e}_{Ri}$, that clearly vanishes. Thus, imposing the photon line to be inserted inside the loop, we find the four Feynman diagrams in Fig. 4.2. These are the amplitudes to be evaluated in order to calculate the Higgs contribution to the $\mathcal{M}_L$ amplitude.

The $\mathcal{M}_L$ amplitude.

We now evaluate explicitly the diagrams of Fig. 4.2, using the Feynman rules listed in appendix A.3. We start from the A_1 amplitude, and for this first calculation we will perform in great detail all the steps, in order to make them clear. In Fig. 4.3 are represented the conventions adopted for the loop momenta, while for the flavor indices we use the same convention as in Fig. 4.2. We have:

$$A_1 = \bar{e}_{Lj}(p')\,(-i(\Delta)_{jd}P_R)\,\frac{i(\slashed{p}' + m_d)}{p'^2 - m_d^2}\left[\frac{-i}{\sqrt{2}}\left((Y_L^*)_{dc}P_L + (Y_R^*)_{dc}P_R\right)\right] \times$$

$$\times \left\{\int \frac{\mathrm{d}^4 k}{(2\pi)^4}\,\frac{i(\slashed{k} + \tilde{m}_c)}{k^2 - \tilde{m}_c^2}\left[\frac{-iv}{\sqrt{2}}\left((Y_L^{*\dagger})_{cb}P_R + (Y_R^{*\dagger})_{cb}P_L\right)\right] \times$$

$$\times \frac{i(\slashed{k} + m_b)}{k^2 - m_b^2}\,(-ie\gamma^\alpha\varepsilon_\alpha(q))\,\frac{i(\slashed{k} + \slashed{q} + m_b)}{(k+q)^2 - m_b^2}\,\frac{i}{(k-p')^2 - M_h^2}\right\} \times$$

$$\times \left[\frac{-i}{\sqrt{2}}\left((Y_L^*)_{ba}P_L + (Y_R^*)_{ba}P_R\right)\right]\frac{i(\slashed{p} + \tilde{m}_a)}{p^2 - \tilde{m}_a^2}\left(-i(\tilde{\Delta}^\dagger)_{ai}P_R\right)\tilde{e}_{Ri}(p)\,. \quad (4.65)$$

where a sum over all flavor indices a, b, c, d is understood.

There are several tricks that can be used to simplify this expression. First, since we are working in a basis where the elementary fermions are massless, it immediately
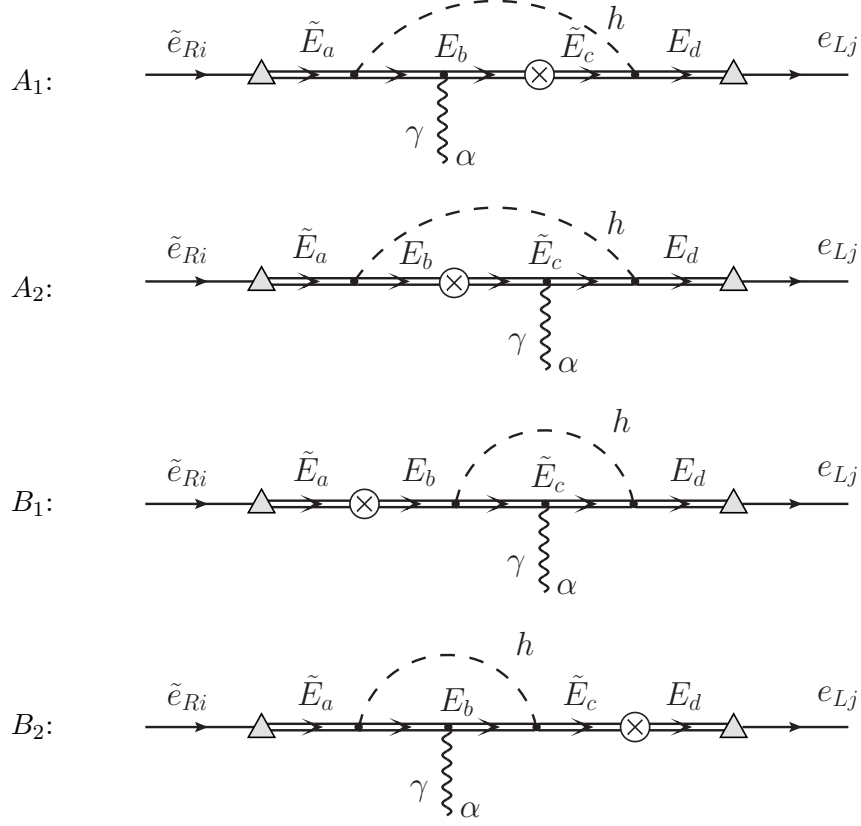
Figure 4.2: Higgs mediated dipole one-loop diagrams.

follows from the Dirac equation that:

$$\begin{cases} \not{p}\, \tilde{e}_{Ri}(p) & = & 0 \\ \bar{e}_{Lj}(p')\, \not{p}' & = & 0 \end{cases} .$$
(4.66)

In addiction, in this basis the elementary fermions are massless and then $p^2 = p'^2 = 0$. The last two assumptions allow us to "shrink" the propagators of the composite fermions that are outside the loop. Namely, for our present calculation:

$$\frac{i(\not{p} + \tilde{m}_a)}{p^2 - \tilde{m}_a^2} \simeq -\frac{i}{\tilde{m}_a} ,$$
(4.67)

$$\frac{i(\not{p}' + m_d)}{p^2 - m_d^2} \simeq -\frac{i}{m_d} .$$
(4.68)

Once these shrinking are performed, we can further simplify the expression (4.65)
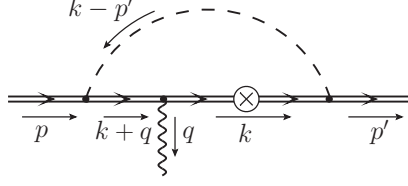
Figure 4.3: Convention for the loop momenta in the calculation of the amplitude A_1.

by using simple projector algebra. Carrying on this simplification, we find:

$$
A_1 = \frac{ev}{2\sqrt{2}} \frac{1}{\tilde{m}_a m_d} (\Delta)_{jd} (Y_R^*)_{dc} (Y_R^*)_{ba} (\tilde{\Delta}^\dagger)_{ai}\, \varepsilon_\alpha \times
$$

$$
\times \bar{e}_{Lj} \Bigg\{ \int \frac{\mathrm{d}^4 k}{(2\pi)^4} \frac{1}{[k^2 - \tilde{m}_c^2][k^2 - m_b^2][(k+q)^2 - m_b^2][(k-p')^2 - M_h^2]} \times
$$

$$
\times (\slashed{k} + \tilde{m}_c) \left((Y_L^{*\dagger})_{cb} P_R + (Y_R^{*\dagger})_{cb} P_L \right) (\slashed{k} + m_b) \gamma^\alpha (\slashed{k} + \slashed{q} + m_b) \Bigg\} \tilde{e}_{Ri}
$$

$$
= \frac{ev}{2\sqrt{2}} \frac{1}{\tilde{m}_a m_d} (\Delta)_{jd} (Y_R^*)_{dc} (Y_R^*)_{ba} (\tilde{\Delta}^\dagger)_{ai}\, \varepsilon_\alpha \times
$$

$$
\times \bar{e}_{Lj} \Bigg\{ \int \frac{\mathrm{d}^4 k}{(2\pi)^4} \frac{1}{[k^2 - \tilde{m}_c^2][k^2 - m_b^2][(k+q)^2 - m_b^2][(k-p')^2 - M_h^2]} \times
$$

$$
\times \left(\tilde{m}_c (Y_L^{*\dagger})_{cb} P_R + \slashed{k} (Y_R^{*\dagger})_{cb} P_L \right) (\slashed{k} + m_b) \gamma^\alpha (\slashed{k} + \slashed{q} + m_b) \Bigg\} \tilde{e}_{Ri}
$$

$$
= \frac{ev}{2\sqrt{2}} \frac{1}{\tilde{m}_a m_d} (\Delta)_{jd} (Y_R^*)_{dc} (Y_R^*)_{ba} (\tilde{\Delta}^\dagger)_{ai}\, \varepsilon_\alpha \times
$$

$$
\times \bar{e}_{Lj} \Bigg\{ \int \frac{\mathrm{d}^4 k}{(2\pi)^4} \frac{1}{[k^2 - \tilde{m}_c^2][k^2 - m_b^2][(k+q)^2 - m_b^2][(k-p')^2 - M_h^2]} \times
$$

$$
\times \left[m_b \tilde{m}_c (Y_L^{*\dagger})_{cb} (2k^\alpha + \gamma^\alpha \slashed{q}) + (Y_R^{*\dagger})_{cb} (m_b^2 \slashed{k} \gamma^\alpha + k^2 \gamma^\alpha (\slashed{k} + \slashed{q})) \right] \Bigg\} \tilde{e}_{Ri} \,. \quad (4.69)
$$

To deal with the denominator inside the loop integral we will use the method of the Feynman parametrization. But before it we exploit a straightforward but useful relation to simplify the computations. It is easy to verify that:

$$
\frac{1}{[k^2 - \tilde{m}_c^2][k^2 - m_b^2]} = \frac{-1}{m_b^2 - \tilde{m}_c^2} \left(\frac{1}{k^2 - \tilde{m}_c^2} - \frac{1}{k^2 - m_b^2} \right) \,, \qquad (4.70)
$$

this trick allow us to reduce the order of the denominator. We have:

$$
\frac{1}{[k^2 - \tilde{m}_c^2][k^2 - m_b^2][(k+q)^2 - m_b^2][(k-p')^2 - M_h^2]}
$$

$$
= \frac{-1}{m_b^2 - \tilde{m}_c^2} \Bigg[\frac{1}{[k^2 - \tilde{m}_c^2][(k+q)^2 - m_b^2][(k-p')^2 - M_h^2]}
$$

$$
- \frac{1}{[k^2 - m_b^2][(k+q)^2 - m_b^2][(k-p')^2 - M_h^2]} \Bigg] \,. \qquad (4.71)
$$

We are now ready to recast the denominator using the Feynman parametrization:

$$\frac{1}{ABC} = 2 \int_0^1 dx \int_0^{1-x} dy \frac{1}{[xA + yB + (1-x-y)C]^3} \,. \tag{4.72}$$

Starting from the first part in the brackets in Eq. (4.71):

$$\frac{1}{[k^2 - \tilde{m}_c^2][(k+q)^2 - m_b^2][(k-p')^2 - M_h^2]}$$
$$= 2 \int_0^1 dx \int_0^{1-x} dy \frac{1}{\{x[k^2 - \tilde{m}_c^2] + y[(k+q)^2 - m_b^2] + (1-x-y)[(k-p')^2 - M_h^2]\}^3} \,, \tag{4.73}$$

where

$$x[k^2 - \tilde{m}_c^2] + y[(k+q)^2 - m_b^2] + (1-x-y)[(k-p')^2 - M_h^2]$$
$$= [k + yq - (1-x-y)p']^2 - [x\tilde{m}_c^2 + ym_b^2 + (1-x-y)M_h^2] \,, \tag{4.74}$$

and the computations for the second part of (4.71) is analogous, once replaced $\tilde{m}_c^2$ with m_b.

Then:

$$\frac{1}{[k^2 - \tilde{m}_c^2][k^2 - m_b^2][(k+q)^2 - m_b^2][(k-p')^2 - M_h^2]}$$
$$= \frac{-2}{m_b^2 - \tilde{m}_c^2} \int_0^1 dx \int_0^{1-x} dy \frac{1}{\{[k+Q]^2 - \Omega_1\}^3} - \frac{1}{\{[k+Q]^2 - \Omega_2\}^3} \,, \tag{4.75}$$

where:

$$\begin{cases} Q &\equiv yq - (1-x-y)p' \\ \Omega_1 &\equiv x\tilde{m}_c^2 + ym_b^2 + (1-x-y)M_h^2 \\ \Omega_2 &\equiv (x+y)m_b^2 + (1-x-y)M_h^2 \end{cases} \,. \tag{4.76}$$

We now perform in the expression (4.69) the change of variable

$$k \to k - Q \,. \tag{4.77}$$

We will start from the numerator inside the integral, namely:

$$\varepsilon_\alpha \bar{e}_{Lj} \left[m_b \tilde{m}_c (Y_L^{*\dagger})_{cb} (2k^\alpha + \gamma^\alpha \slashed{q}) + (Y_R^{*\dagger})_{cb} (m_b^2 \slashed{k} \gamma^\alpha + k^2 \gamma^\alpha (\slashed{k} + \slashed{q})) \right] \tilde{e}_{Ri} \,, \tag{4.78}$$

but it is useful to remind some equalities and allowed substitutions to be used in the calculations first:

- Since $q \cdot \varepsilon = 0$, we have:

$$\varepsilon_\alpha \bar{e}_{Lj} \slashed{q} \gamma^\alpha \tilde{e}_{Ri} = -\varepsilon_\alpha \bar{e}_{Lj} \gamma^\alpha \slashed{q} \tilde{e}_{Ri} = i\varepsilon_\alpha q_\beta \bar{e}_{Lj} \sigma^{\alpha\beta} e_{Ri} = Q_{\gamma L} \,,$$

and also $p \cdot \varepsilon = p' \cdot \varepsilon$.

- According to the general discussion made before, we are allowed to make the substitution

$$2\varepsilon \cdot p\, \bar{e}_{Lj} e_{Ri} \to i\varepsilon_\alpha q_\beta \bar{e}_{Lj} \sigma^{\alpha\beta} e_{Ri} = Q_{\gamma L} \,.$$

- After the chosen change of variables, the loop integral will become even in the variable k. Thus, every odd term with respect to k should be neglected since it gives rise to a vanishing contribution to the integral.

- The following relation holds:

$$\int \mathrm{d}^4k \; k^\alpha k^\beta f(k^2) = \frac{1}{4}\eta^{\alpha\beta} \int \mathrm{d}^4k \; k^2 f(k^2) \;,$$

and then the following substitution into the integral is allowed:

$$k^\alpha k^\beta \to \frac{1}{4}k^2 \;,$$

- Finally, we always have to keep in mind the Dirac equations (4.66).

We are now ready to compute the change of variable (4.77) into (4.78):

$$\varepsilon_\alpha \bar{e}_{Lj} \left[m_b \tilde{m}_c (Y_L^{*\dagger})_{cb}(2k^\alpha + \gamma^\alpha \slashed{q}) + (Y_R^{*\dagger})_{cb}(m_b^2 \slashed{k}\gamma^\alpha + k^2\gamma^\alpha(\slashed{k} + \slashed{q})) \right] \tilde{e}_{Ri}$$

$$\to \varepsilon_\alpha \bar{e}_{Lj} \Big\{ m_b \tilde{m}_c (Y_L^{*\dagger})_{cb} \left[2k^\alpha - 2yq^\alpha + 2(1 - x - y)p'^\alpha + \gamma^\alpha \slashed{q} \right]$$

$$+ (Y_R^{*\dagger})_{cb} \left[m_b^2 \slashed{k}\gamma^\alpha - m_b^2 y\slashed{q}\gamma^\alpha + m_b^2(1 - x - y)\slashed{p}'\gamma^\alpha \right.$$

$$\left. + (k^2 - 2yk \cdot q + 2(1 - x - y)k \cdot p')\gamma^\alpha(\slashed{k} + (1 - y)\slashed{q} + (1 - x - y)\slashed{p}') \right] \Big\} \tilde{e}_{Ri}$$

$$= \varepsilon_\alpha \bar{e}_{Lj} \Big\{ m_b \tilde{m}_c (Y_L^{*\dagger})_{cb} \left[2(1 - x - y)p^\alpha + \gamma^\alpha \slashed{q} \right] - (Y_R^{*\dagger})_{cb} \left[m_b^2 y\slashed{q}\gamma^\alpha \right.$$

$$\left. + k^2\gamma^\alpha((1 - y)\slashed{q} + (1 - x - y)\slashed{p}') + 2k \cdot (-yq + (1 - x - y)p')\gamma^\alpha\slashed{k} \right] \Big\} \tilde{e}_{Ri}$$

$$= - \left[m_b \tilde{m}_c (Y_L^{*\dagger})_{cb}(x + y) + (Y_R^{*\dagger})_{cb} m_b^2 y - (Y_R^{*\dagger})_{cb}\frac{1}{2}k^2(1 - 3x) \right] Q_{\gamma L} \;. \qquad (4.79)$$

Plugging this result into (4.69), using also (4.75), we get

$$A_1 = \frac{ev}{2\sqrt{2}} \frac{1}{\tilde{m}_a m_d}(\Delta)_{jd}(Y_R^*)_{dc}(Y_R^*)_{ba}(\tilde{\Delta}^\dagger)_{ai}\frac{2}{m_b^2 - \tilde{m}_c^2} \times$$

$$\times \left\{ \int_0^1 \mathrm{d}x \int_0^{1-x} \mathrm{d}y \left[m_b \tilde{m}_c (Y_L^{*\dagger})_{cb}(x + y) + (Y_R^{*\dagger})_{cb} m_b^2 y \right] F_1(\Omega_1, \Omega_2) \right.$$

$$\left. - \left[(Y_R^{*\dagger})_{cb}\frac{1}{2}(1 - 3x) \right] F_2(\Omega_1, \Omega_2) \right\} Q_{\gamma L} \;, \qquad (4.80)$$

where F_1 and F_2 are integral over the loop momentum k that can now be evaluated using standard techniques:

$$F_1(\Omega_1, \Omega_2) \equiv \int \frac{\mathrm{d}^4k}{(2\pi)^4} \left[\frac{1}{\{k^2 - \Omega_1\}^3} - \frac{1}{\{k^2 - \Omega_2\}^3} \right] = \frac{-i}{32\pi^2} \left[\frac{1}{\Omega_1} - \frac{1}{\Omega_2} \right] \;, \qquad (4.81)$$

$$F_2(\Omega_1, \Omega_2) \equiv \int \frac{\mathrm{d}^4k}{(2\pi)^4} \left[\frac{k^2}{\{k^2 - \Omega_1\}^3} - \frac{k^2}{\{k^2 - \Omega_2\}^3} \right] = \frac{i}{16\pi^2} \log\frac{\Omega_2}{\Omega_1} + o(\varepsilon) \;. \qquad (4.82)$$

Then:

$$A_1 = \frac{-iev}{32\sqrt{2}\pi^2} \frac{1}{\tilde{m}_a m_d} (\Delta)_{jd} (Y_R^*)_{dc} (Y_R^*)_{ba} (\tilde{\Delta}^\dagger)_{ai} \frac{1}{m_b^2 - \tilde{m}_c^2} \times$$

$$\left\{ \int \mathrm{d}x \int \mathrm{d}y \left[\frac{1}{\Omega_1} - \frac{1}{\Omega_2} \right] \left[m_b \tilde{m}_c (Y_L^{*\dagger})_{cb}(x+y) + m_b^2 (Y_R^{*\dagger})_{cb} y \right] \right.$$

$$\left. - \log \frac{\Omega_1}{\Omega_2} \left[(Y_R^{*\dagger})_{cb}(1-3x) \right] \right\} Q_{\gamma L} \ . \tag{4.83}$$

We are now left only with the evaluation of some simple integrals over the Feynman variables. They are:

$$\int_0^1 \mathrm{d}x \int_0^{1-x} \mathrm{d}y \, \frac{x}{\Omega_1(x,y)} =$$

$$= \frac{1}{2(m_b^2 - M_h^2)} \left[-\frac{m_b^2}{m_b^2 - \tilde{m}_c^2} + \frac{m_b^4}{(m_b^2 - \tilde{m}_c^2)^2} \log \frac{m_b^2}{\tilde{m}_c^2} - \frac{M_h^2}{\tilde{m}_c^2 - M_h^2} - \frac{M_h^4}{(\tilde{m}_c^2 - M_h^2)^2} \log \frac{M_h^2}{\tilde{m}_c^2} \right]$$

$$\simeq -\frac{1}{2(m_b^2 - \tilde{m}_c^2)} + \frac{m_b^2}{2(m_b^2 - \tilde{m}_c^2)^2} \log \frac{m_b^2}{\tilde{m}_c^2} \ , \tag{4.84a}$$

$$\int_0^1 \mathrm{d}x \int_0^{1-x} \mathrm{d}y \, \frac{y}{\Omega_1(x,y)} =$$

$$= \frac{1}{2(\tilde{m}_c^2 - M_h^2)} \left[-\frac{\tilde{m}_c^2}{\tilde{m}_c^2 - m_b^2} - \frac{\tilde{m}_c^4}{(m_b^2 - \tilde{m}_c^2)^2} \log \frac{m_b^2}{\tilde{m}_c^2} - \frac{M_h^2}{m_b^2 - M_h^2} - \frac{M_h^4}{(m_b^2 - M_h^2)^2} \log \frac{M_h^2}{m_b^2} \right]$$

$$\simeq \frac{1}{2(m_b^2 - \tilde{m}_c^2)} - \frac{\tilde{m}_c^2}{2(m_b^2 - \tilde{m}_c^2)^2} \log \frac{m_b^2}{\tilde{m}_c^2} \ , \tag{4.84b}$$

$$\int_0^1 \mathrm{d}x \int_0^{1-x} \mathrm{d}y \, \frac{x}{\Omega_2(x,y)} = \int_0^1 \mathrm{d}x \int_0^{1-x} \mathrm{d}y \, \frac{y}{\Omega_2(x,y)} =$$

$$= \frac{1}{2(m_b^2 - M_h^2)} \left[\frac{1}{2} - \frac{M_h^2}{\tilde{m}_c^2 - M_h^2} - \frac{M_h^4}{(\tilde{m}_c^2 - M_h^2)^2} \log \frac{M_h^2}{\tilde{m}_c^2} \right] \simeq \frac{1}{4m_b^2} \ , \tag{4.84c}$$

$$\int_0^1 \mathrm{d}x \int_0^{1-x} \mathrm{d}y \, (1-3x) \log \frac{\Omega_1}{\Omega_2} =$$

$$= \frac{1}{12m_b^2} \left[\frac{2m_b^4 + 5\tilde{m}_c^2 m_b^2 - \tilde{m}_c^4}{m_b^2 - \tilde{m}_c^2} + \frac{2M_h^4 + 5\tilde{m}_c^2 M_h^2 - \tilde{m}_c^4}{\tilde{m}_c^2 - M_h^2} + \frac{2m_b^4 + 5M_h^2 m_b^2 - M_h^4}{m_b^2 - M_h^2} \right]$$

$$- \frac{m_b^2 \tilde{m}_c^2}{2(m_b^2 - \tilde{m}_c^2)^2} \log \frac{m_b^2}{\tilde{m}_c^2} + \frac{M_h^4 \tilde{m}_c^2}{2m_b^2(M_h^2 - \tilde{m}_c^2)^2} \log \frac{\tilde{m}_c^2}{M_h^2} + \frac{M_h^4}{2(M_h^2 - m_b^2)^2} \log \frac{m_b^2}{M_h^2}$$

$$\simeq \frac{m_b^2 + \tilde{m}_c^2}{4(m_b^2 - \tilde{m}_c^2)} - \frac{m_b^2 \tilde{m}_c^2}{2(m_b^2 - \tilde{m}_c^2)^2} \log \frac{m_b^2}{\tilde{m}_c^2} \ , \tag{4.84d}$$

where, since $M_h \ll m, \tilde{m}$, the limit $M_h \to 0$ has been eventually taken. Indeed, no large logarithms nor infrared divergences prevent this to be a fair procedure.

Substituting the expressions (4.84) into (4.83) we finally find the amplitude for

the A_1 diagram:

$$A_1 = -\frac{iev}{32\sqrt{2}\pi^2}\frac{1}{\tilde{m}_a m_d}(\Delta)_{jd}(Y_R^*)_{dc}(Y_R^*)_{ba}(\tilde{\Delta}^\dagger)_{ai}\frac{1}{m_b^2 - \tilde{m}_c^2}\times$$

$$\times\frac{1}{2}\left[(Y_L^{*\dagger})_{cb}\left(-\frac{\tilde{m}_c}{m_b} + \frac{m_b\tilde{m}_c}{m_b^2 - \tilde{m}_c^2}\log\frac{m_b^2}{\tilde{m}_c^2}\right)\right]Q_{\gamma L}$$

$$= -\frac{iev}{64\sqrt{2}\pi^2}\frac{1}{\tilde{m}_a m_d}(\Delta)_{jd}(Y_R^*)_{dc}(Y_L^{*\dagger})_{cb}(Y_R^*)_{ba}(\tilde{\Delta}^\dagger)_{ai}\frac{1}{m_b^2 - \tilde{m}_c^2}\times$$

$$\times\left[\left(-\frac{\tilde{m}_c}{m_b} + \frac{m_b\tilde{m}_c}{m_b^2 - \tilde{m}_c^2}\log\frac{m_b^2}{\tilde{m}_c^2}\right)\right]Q_{\gamma L}\ . \tag{4.85}$$

The computations regarding the other three amplitudes in Fig. 4.2 involve the same techniques and tricks used for the evaluation of A_1. Here we will state just the final results, while in appendix A.4 can be found more detailed calculations.

The resulting amplitudes are:

$$A_2 = \frac{iev}{64\sqrt{2}\pi^2}\frac{1}{\tilde{m}_a m_d}(\Delta)_{jd}(Y_R^*)_{dc}(Y_L^{*\dagger})_{cb}(Y_R^*)_{ba}(\tilde{\Delta}^\dagger)_{ai}\frac{1}{m_b^2 - \tilde{m}_c^2}\times$$

$$\times\left[\left(-\frac{m_b}{\tilde{m}_c} + \frac{m_b\tilde{m}_c}{m_b^2 - \tilde{m}_c^2}\log\frac{m_b^2}{\tilde{m}_c^2}\right)\right]Q_{\gamma L}\ , \tag{4.86}$$

$$B_1 = -\frac{iev}{64\sqrt{2}\pi^2}\frac{1}{\tilde{m}_a m_b \tilde{m}_c m_d}(\Delta)_{jd}(Y_R^*)_{dc}(Y_L^{*\dagger})_{cb}(Y_R^*)_{ba}(\tilde{\Delta}^\dagger)_{ai}Q_{\gamma L}\ , \tag{4.87}$$

$$B_2 = -\frac{iev}{64\sqrt{2}\pi^2}\frac{1}{\tilde{m}_a m_b \tilde{m}_c m_d}(\Delta)_{jd}(Y_R^*)_{dc}(Y_L^{*\dagger})_{cb}(Y_R^*)_{ba}(\tilde{\Delta}^\dagger)_{ai}Q_{\gamma L}.\ . \tag{4.88}$$

After having evaluated all the diagrams of Fig. 4.2, we can derive the full one-loop expression of the Higgs-mediated contribution to the amplitude $\mathcal{M}_L$ of Eq. (4.53a). Summing the amplitudes (4.85), (4.86), (4.87) and (4.88), we get:

$$\mathcal{M}_{L,h} = -\frac{3iev}{64\sqrt{2}\pi^2}\sum_{a,b,c,d}\frac{1}{\tilde{m}_a m_b \tilde{m}_c m_d}(\Delta)_{jd}(Y_R^*)_{dc}(Y_L^{*\dagger})_{cb}(Y_R^*)_{ba}(\tilde{\Delta}^\dagger)_{ai}\ Q_{\gamma L}\ . \tag{4.89}$$

The $\mathcal{M}_R$ amplitude

To evaluate also $\mathcal{M}_R$, one should in principle start again from building up all the possible Feynman diagrams and then compute them. However it is very easy to see that, for the process (4.53b), the possible Feynman diagrams can be straightforwardly obtained "reading backwards" the ones of Fig. 4.2. Furthermore, it can be seen that also the computations of the resulting amplitudes are absolutely analogous to the ones just performed, in particular they involve the same loop integrals already evaluated.

Using the above considerations, we can easily arrive to the conclusion that $c_L = c_R$, where $c_{L,R}$ have been defined in Eqs. (4.62) and (4.64). Thus, the final result for the Higgs contribution is:

$$\mathcal{M}_{R,h} = -\frac{3iev}{64\sqrt{2}\pi^2}\sum_{a,b,c,d}\frac{1}{m_a \tilde{m}_b m_c \tilde{m}_d}(\tilde{\Delta})_{jd}(Y_R^{*\dagger})_{dc}(Y_L^*)_{cb}(Y_R^{*\dagger})_{ba}(\Delta^\dagger)_{ai}\ Q_{\gamma R}\ , \tag{4.90}$$
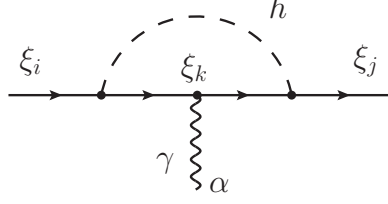
Figure 4.4: The only diagram representing the Higgs contribution to the dipole operator using the mass basis. To reproduce the $\mu \to e\gamma$ process, it is sufficient to set $i = 2$ and $j = 1$.

with

$$\mathcal{M}_h = \mathcal{M}_{L,h} + \mathcal{M}_{R,h} \ . \tag{4.91}$$

Alternative procedure

Before having introduced the mass insertion approximation, we have developed a different formalism to account for the Higgs interaction with the leptonic sector. Rotating the fermion fields to the mass basis for the SM leptons, we have found the Lagrangian (4.28):

$$\mathcal{L}_{\text{fermion}} = \bar{\xi}_L i\slashed{D}\xi_R - \bar{\xi}_L M_E^{\text{diag}}\xi_R - \frac{1}{\sqrt{2}}\, h\, \bar{\xi}_L \Upsilon \xi_R + \text{h.c.} + \text{other terms} \ ,$$

where now we have dropped the 'm' index and Υ is defined in (4.29). Here "other terms" stands for the remaining terms in (4.28), that does not influence the Higgs boson contribution. From this Lagrangian, the Feynman rule for the trilinear lepton-Higgs interaction is easy derivable:

$$= \frac{-i}{\sqrt{2}}\left(\Upsilon_{ji}P_R + (\Upsilon^\dagger)_{ji}P_L\right) \ . \tag{4.92}$$

In addiction, now there is only one diagram that encloses the Higgs contribution to the $\xi_i \to \xi_j\gamma$ process (and thus to the dipole operator) at the one-loop order, represented in Fig. 4.4. According to Eq. (4.26), to reproduce the $\mu \to e\gamma$ process, one have to set $i = 2$ and $j = 1$.

Evaluating the diagram of Fig. 4.4 using the Feynman rule (4.92) one finds:

$$\begin{aligned}
\mathcal{M}_h = \frac{ie}{32\pi^2} \sum_{k=1}^{9} \int_0^1 \mathrm{d}x \int_0^x \mathrm{d}y\, \frac{1}{\Omega_k(x,y)} &\Big[m_k\, x \left(\Upsilon_{1k}\Upsilon_{k1}Q_{\gamma L} + \Upsilon_{1k}^\dagger\Upsilon_{k1}^\dagger Q_{\gamma R}\right) \\
&- m_\mu\,(x-y)(1-x)\left(\Upsilon_{1k}\Upsilon_{k1}^\dagger Q_{\gamma L} + \Upsilon_{1k}^\dagger\Upsilon_{k1}Q_{\gamma R}\right) \\
&+ m_e\, y(1+x-2y)\left(\Upsilon_{1k}^\dagger\Upsilon_{k1}Q_{\gamma L} + \Upsilon_{1k}\Upsilon_{k1}^\dagger Q_{\gamma R}\right) \Big] \ ,
\end{aligned} \tag{4.93}$$

where

$$\Omega_k(x, y) = x m_k^2 + (1 - x) M_h^2 - (x - y)(1 - x) m_\mu^2 - y(1 - x) m_e^2 \,. \qquad (4.94)$$

To evaluate Eq. (4.93) consistently in a perturbative fashion, one should make use of Eqs. (4.19), (4.20) and (4.29) to find an approximate expression for the Υ matrix elements. Further, one should recall that the SM lepton masses are third order quantities. Using these notions, one can find that the leading order contribution of Eq. (4.93) arises at the third order and it is:

$$\mathcal{M}_h \simeq \frac{ie}{32\pi^2} \sum_{k=4}^{9} \left(\Upsilon_{1k} \Upsilon_{k1} Q_{\gamma L} + \Upsilon_{1k}^\dagger \Upsilon_{k1}^\dagger Q_{\gamma R} \right) \int_0^1 \mathrm{d}x \int_0^x \mathrm{d}y \, \frac{x \, m_k}{\Omega_k(x, y)}$$

$$\simeq \frac{ie}{64\pi^2} \sum_{k=4}^{9} \frac{1}{m_k} \left(\Upsilon_{1k} \Upsilon_{k1} Q_{\gamma L} + \Upsilon_{1k}^\dagger \Upsilon_{k1}^\dagger Q_{\gamma R} \right) \,. \qquad (4.95)$$

Since, at the leading order, one finds:

$$\sum_{k=4}^{9} \frac{1}{m_k} \Upsilon_{1k} \Upsilon_{k1} = -\frac{3v}{\sqrt{2}} \Delta m^{-1} Y_R^* \tilde{m}^{-1} Y_L^{*\dagger} m^{-1} Y_R^* \tilde{m}^{-1} \tilde{\Delta}^\dagger \,, \qquad (4.96a)$$

$$\sum_{k=4}^{9} \frac{1}{m_k} \Upsilon_{1k}^\dagger \Upsilon_{k1}^\dagger = -\frac{3v}{\sqrt{2}} \tilde{\Delta} \tilde{m}^{-1} Y_R^{*\dagger} m^{-1} Y_L^* \tilde{m}^{-1} Y_R^{*\dagger} m^{-1} \Delta^\dagger \,, \qquad (4.96b)$$

it is easy to verify that one obtains the same result as in Eq. (4.91).

4.3.2 W and Z bosons contribution

It is well-known that, in a generic gauge, to compute the exact contribution from the $W^\pm$ and Z bosons one should consider also diagrams build up using the associated would-be Goldstone bosons $\varphi^\pm$ and φ_Z. This is necessary in order to evaluate correctly the contribution from the longitudinal polarization of the weak gauge bosons. In particular, there are two notable gauge choices:

- Unitary gauge. In this gauge the would-be Goldstone bosons are "rotated out" and only the W and Z bosons should be considered. Their propagator becomes:

$$D_{\mu\nu}^{W_{tr}, Z_{tr}}(k) = \frac{-i}{k^2 - M_{W,Z}^2} \left(\eta_{\mu\nu} - \frac{k_\mu k_\nu}{k^2} \right) \,, \qquad (4.97a)$$

$$D_{\mu\nu}^{W_l, Z_l}(k) = \frac{-i}{k^2 - M_{W,Z}^2} \left(\frac{k_\mu k_\nu}{k^2} - \frac{k_\mu k_\nu}{M_{W,Z}^2} \right) \,, \qquad (4.97b)$$

  where we have separated the transverse ('tr') and longitudinal ('l') components of the propagators.

- Feynman–'t Hooft gauge. In this other gauge, as we will see, the would-be Goldstone bosons account for the leading contribution from the longitudinal
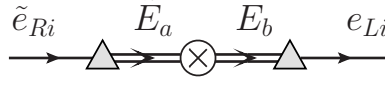
Figure 4.5: Allowed fermionic line with only one Yukawa insertion. A licit dipole diagram can be obtained by inserting a Z loop and an outgoing photon anyhow through this line. This diagram gives also the leading order contribution to the SM fermion masses.

polarization of the weak gauge bosons. Indeed, in this gauge, the longitudinal component of the W and Z propagators now becomes

$$D_{\mu\nu}^{W_l, Z_l}(k) = \frac{-i}{k^2 - M_{W,Z}^2} \frac{k_\mu k_\nu}{k^2} \, , \qquad (4.98)$$

the terms proportional to $\frac{k_\mu k_\nu}{M_{W,Z}^2}$ being now provided by the would-be Goldstone bosons contribution.

We will use the unitary gauge to show how the leading contribution to the dipole operator arises from the longitudinal polarizations of the weak gauge bosons. Then, we will use the Feynman–'t Hooft gauge to isolate and compute only such contribution; this can be done, as we will show, considering only the would-be Goldstone bosons exchange in the loop.

Let us put ourselves in the unitary gauge, where only the W and Z bosons should be considered. We now show that the leading contribution of the Z boson is due to its longitudinal polarization and that such contribution has the same order of magnitude as the Higgs one evaluated above. Of course this should be a gauge-independent conclusion and we are using the unitary gauge only for convenience. Further, our argument can be straightforwardly extended to the W contribution.

The first observation that can be made is that the lepton-lepton-Z vertex is flavor diagonal. Consequently, the argument used to derive the fermionic structure of Fig. 4.1 (in particular the needs for three Yukawa insertions) apparently ceases to hold and a new fermionic line is allowed at the leading order, namely the one of Fig. 4.5. However, diagrams arising from that fermionic line cannot contribute to LFV processes. This happens because the diagram of Fig. 4.5, taken alone without other insertions, contribute at the leading order to the SM lepton masses, and thus is flavor diagonal in the mass basis by definition[3] (see also Eq. (4.107)). Nevertheless, such fermionic line can be used to generate diagrams which give NP contributions to flavor conserving observables, such as anomalous magnetic moments and the EDMs for leptons.

As a consequence of the above considerations, we are then back to consider the fermionic line of Fig. 4.1 as the source of the leading contributions. However, now all the three Yukawa insertions should be mass mixing terms, giving a v^3 overall coefficient; further, an additional $(g_1^{SM}/\cos\theta_W)^2$ factor arises from the two Z interaction vertices. Thus, apparently, these kind of diagrams has an extra suppression

---

[3]This argument is not completely correct. Indeed, the insertion of a Z loop in the fermionic line could in principle modify its spurionic structure, thus resulting in a partial misalignment with the mass matrix (i.e. the object that one diagonalizes). Thus a residual flavor violating contribution can still survive, but it can be shown that it is subleading, thus we can safely neglect it.

factor $\sim (M_Z/\Lambda)^2$ (with $\Lambda \sim m, \tilde{m}$) with respect to their counterpart with the exchange of an Higgs boson. This is actually true only for the contribution from the transversal polarizations of Z, while it is not for the longitudinal one. This can be at least qualitatively understood analysing separately the two pieces of the Z propagator (Eq. (4.97)):

$$D_{\mu\nu}^{Z_{tr}}(k) = \frac{-i}{k^2 - M_Z^2} \left(\eta_{\mu\nu} - \frac{k_\mu k_\nu}{k^2} \right) \sim \eta_{\mu\nu} \frac{1}{k^2} \sim \eta_{\mu\nu} \frac{1}{\Lambda^2} \; , \tag{4.99}$$

$$D_{\mu\nu}^{Z_l}(k) = \frac{-i}{k^2 - M_{W,Z}^2} \left(\frac{k_\mu k_\nu}{k^2} - \frac{k_\mu k_\nu}{M_{W,Z}^2} \right) \sim \frac{1}{k^2} \eta_{\mu\nu} \frac{k^2}{M_Z^2} \sim \eta_{\mu\nu} \frac{1}{M_Z^2} \; , \tag{4.100}$$

where we have taken k^2 to approximately assume the value of the NP scale Λ. Now we can appreciate that, while the transversal polarizations effectively decouples as $\sim (M_Z/\Lambda)^2$, part of the longitudinal contribution has the same magnitude as the Higgs contribution.

A completely analogous argument can be adduced for the case of the W contribution. The final result, as anticipated, is that the leading contribution comes from the longitudinal polarizations for the weak gauge bosons. Further, the Feynman–'t Hooft gauge furnishes the perfect framework to compute only such leading contribution, since it is easy to see from Eqs. (4.98) that it is enclosed only in the would-be Goldstone bosons contributions. This conclusion can be seen as a result of the equivalence theorem [62], that states the equivalence in the high energy limit (or, equivalently, in the gaugeless limit $g_{1,2}^{SM} \to 0$) of the contribution of the W and Z and of the would-be Goldstone bosons.

We then switch to the Feynman–'t Hooft gauge. Now that the computational technicalities have been introduced and described while calculating the Higgs contribution, we can easily derive the Feynman diagrams and the corresponding amplitudes for the contributions to the dipole operator of the would-be Goldstone bosons.

Regarding the pseudoscalar φ_Z, it is straightforward to verify that the Feynman diagrams to be considered are the same of Fig. 4.2, once substituted h with φ_Z. Further, also the calculations are completely analogous, the only difference being the substitutions of the Feynman rules (A.86) and (A.87) with (A.88) and (A.89). One then finds:

$$\mathcal{M}_{\varphi_Z} = \mathcal{M}_{L,\varphi_Z} + \mathcal{M}_{R,\varphi_Z} \; , \tag{4.101a}$$

$$\mathcal{M}_{L,\varphi_Z} = \frac{-iev}{64\sqrt{2}\pi^2} \sum_{a,b,c,d} \frac{1}{\tilde{m}_a m_b \tilde{m}_c m_d} (\Delta)_{jd} (Y_R^*)_{dc} (Y_L^{*\dagger})_{cb} (Y_R^*)_{ba} (\tilde{\Delta}^\dagger)_{ai} \, Q_{\gamma L} \; , \tag{4.101b}$$

$$\mathcal{M}_{R,\varphi_Z} = \frac{-iev}{64\sqrt{2}\pi^2} \sum_{a,b,c,d} \frac{1}{m_a \tilde{m}_b m_c \tilde{m}_d} (\tilde{\Delta})_{jd} (Y_R^{*\dagger})_{dc} (Y_L^*)_{cb} (Y_R^{*\dagger})_{ba} (\Delta^\dagger)_{ai} \, Q_{\gamma R} \; . \tag{4.101c}$$

Concerning the charged would-be Goldstone boson φ^+, in principle one should again consider the four diagrams of Fig. 4.2, once substituted h with φ^+ and the charged leptons in the loop with neutral leptons. However, noticing that no mass
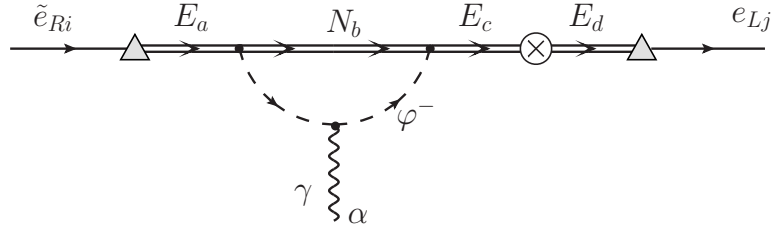
Figure 4.6: The only leading order diagram representing the contribution of the φ^+ boson to the dipole operator.

insertions in the neutral sector are presents (in other words, no neutral lepton singlets are considered) and that only the charged singlets $\tilde{E}$ interact through $\varphi^\pm$ with the neutral sector, the only valid diagram left is the one corresponding to B_2 (and, of course, its chirality-flipped counterpart), represented in Fig. 4.6.

Evaluating the contribution of the diagram in Fig. 4.6 using the same techniques already developed, one can easily find:

$$\mathcal{M}_{L,\varphi^+} = \frac{iev}{32\sqrt{2}\pi^2} \sum_{a,b,c,d} \frac{1}{\tilde{m}_a m_b \tilde{m}_c m_d} (\Delta)_{jd}(Y_R^*)_{dc}(Y_L^{*\dagger})_{cb}(Y_R^*)_{ba}(\tilde{\Delta}^\dagger)_{ai} \, Q_{\gamma L} \; , \quad (4.102)$$

and, considering the process of opposite chirality:

$$\mathcal{M}_{R,\varphi^+} = \frac{iev}{32\sqrt{2}\pi^2} \sum_{a,b,c,d} \frac{1}{m_a \tilde{m}_b m_c \tilde{m}_d} (\tilde{\Delta})_{jd}(Y_R^{*\dagger})_{dc}(Y_L^*)_{cb}(Y_R^{*\dagger})_{ba}(\Delta^\dagger)_{ai} \, Q_{\gamma R} \; ,$$

$$(4.103)$$

$$\mathcal{M}_{\varphi^+} = \mathcal{M}_{L,\varphi^+} + \mathcal{M}_{R,\varphi^+} \; . \tag{4.104}$$

We are now able to write down the complete leading order contribution of the Higgs doublet ϕ to the amplitude for the process $e_i \rightarrow e_j\gamma$:

$$\mathcal{M}_\phi = \mathcal{M}_{L,\phi} + \mathcal{M}_{R,\phi} \tag{4.105a}$$

$$\mathcal{M}_{L,\phi} = -\frac{iev}{32\sqrt{2}\pi^2} \sum_{a,b,c,d} \frac{1}{\tilde{m}_a m_b \tilde{m}_c m_d} (\Delta)_{jd}(Y_R^*)_{dc}(Y_L^{*\dagger})_{cb}(Y_R^*)_{ba}(\tilde{\Delta}^\dagger)_{ai} \, Q_{\gamma L} \; ,$$

$$(4.105b)$$

$$\mathcal{M}_{R,\phi} = -\frac{iev}{32\sqrt{2}\pi^2} \sum_{a,b,c,d} \frac{1}{m_a \tilde{m}_b m_c \tilde{m}_d} (\tilde{\Delta})_{jd}(Y_R^{*\dagger})_{dc}(Y_L^*)_{cb}(Y_R^{*\dagger})_{ba}(\Delta^\dagger)_{ai} \, Q_{\gamma R} \; .$$

$$(4.105c)$$

We can straightforwardly translate the above result in terms of the effective Lagrangian (4.43), resulting in:

$$C_{\ell\ell'} = \frac{v}{16\sqrt{2}\pi^2 m_\ell} \sum_{a,b,c,d} \frac{1}{\tilde{m}_a m_b \tilde{m}_c m_d} (\Delta)_{\ell'd}(Y_R^*)_{dc}(Y_L^{*\dagger})_{cb}(Y_R^*)_{ba}(\tilde{\Delta}^\dagger)_{a\ell} \; . \tag{4.106}$$

4.3.3 Phenomenological bounds

In section 4.2, we have discussed how NP contributions to the Wilson coefficients of the dipole operator are constrained by present experimental measurements. We have in particular focused our attention on the search for the cLFV process $\mu \to e\gamma$ and on the measurement of the flavor conserving parameters Δa_ℓ and d_ℓ (the anomalous magnetic moments and the electric dipole moments of the leptons respectively). Then, in this section, we have computed the leading order NP contribution of the SM bosons to the dipole operator, within the two-site model we are considering. We are now ready to put the two discussions together in order to extrapolate some quantitative informations about our two-site model.

Our final aim will be to derive a lower bound for the NP scale Λ for this class of models, using the present experimental results. Thus, we should reduce the great number of free parameters appearing in our NP Lagrangian ($Y^*_{L,R}$, m, $\tilde{m}$, Δ, $\tilde{\Delta}$, ...) to a limited number of significant parameters, possibly only Λ itself. For this purpose, we can make the following considerations:

- We can safely assume $m, \tilde{m} \sim \Lambda$.

- Recalling the partial compositeness discussion of section 3.2, we can assume the hierarchical structure of the SM Yukawas to arise completely because of the hierarchy in the mixing parameters Δ, $\tilde{\Delta}$. In this scenario, the Yukawa interactions in the composite sector are completely anarchic[4] and then $|(Y^*_{L,R})_{ij}| \sim \hat{Y}^*$ $\forall \, i,j$. Here $\hat{Y}^*$ is a flavor-blind parameter that encloses the strong dynamics of the Higg-composite interaction, thus $\hat{Y}^* > 1$. Nevertheless, we have assumed through the discussion that a perturbative expansion is meaningful, i.e. $v\hat{Y}^* \ll \Lambda$.

- Using the mass insertion approximation, one can easily see that the third order diagram giving the leading contribution to the SM fermion mass terms is the one of Fig. 4.5:

$$\underset{\tilde{e}_{Ri} \quad \tilde{E}_a \quad E_b \quad e_{Li}}{\underbrace{\triangleright\!\!\blacktriangleright\!\!\otimes\!\!\blacktriangleright\!\!\triangleright}} \quad = \quad \frac{v}{\sqrt{2}} \sum_{a,b} \frac{\Delta_{ia}}{m_a}(Y^*_R)_{ab}\frac{\tilde{\Delta}^\dagger_{bi}}{\tilde{m}_b}\, \bar{e}_{Li}\tilde{e}_{Ri} \;, \qquad (4.107)$$

and then we have[5]:

$$m_\ell = \frac{v}{\sqrt{2}} \sum_{a,b} \frac{\Delta_{\ell a}}{m_a}(Y^*_R)_{ab}\frac{\tilde{\Delta}^\dagger_{b\ell}}{\tilde{m}_b} \simeq \frac{v}{\sqrt{2}} \left[\sum_a \frac{\Delta_{\ell a}}{m_a}\right]\left[\sum_b \frac{\tilde{\Delta}^\dagger_{b\ell}}{\tilde{m}_b}\right]\hat{Y}^* \;, \qquad (4.108)$$

where the analogy with Eqs. (3.26) and (3.29) of section 3.2 can be appreciated. In the following we will assume the last equality to hold exactly.

---

[4]It should be clear that this is not the only possibility, i.e. also the strong sector (and then the $Y^*_{L,R}$ matrices) can be provided of additional flavor symmetries. We are considering the anarchical case since it is the most conservative one, resulting in the most stringent experimental constraints.

[5]We have assumed to have switched to the basis where the SM leptons are diagonal at the third order. In practice, this can always be seen as a redefinition of the matrices Δ, $\tilde{\Delta}$ and then the calculations made above in this section are not affected by this basis rotation. In such basis, of course the quantity (4.108) is real.

Through these approximations, we can rewrite the $C_{\ell\ell'}$ coefficients of Eq. (4.106) using fewer parameters:

$$C_{\ell\ell'} = \frac{c_{\ell\ell'}}{\Lambda^2} \simeq \frac{v}{16\sqrt{2}\pi^2 m_\ell} \sum_{a,b,c,d} \frac{1}{\tilde{m}_a m_b \tilde{m}_c m_d} (\Delta)_{\ell'd} (\tilde{\Delta}^\dagger)_{a\ell} (\hat{Y}^*)^3$$

$$\simeq \frac{v}{16\sqrt{2}\pi^2 m_\ell} \frac{1}{\Lambda^2} \left[\sum_d \frac{\Delta_{\ell'd}}{m_d} \right] \left[\sum_a \frac{\tilde{\Delta}^\dagger_{a\ell}}{\tilde{m}_a} \right] (\hat{Y}^*)^3 , \qquad (4.109)$$

$$C_{\ell\ell} = \frac{c_{\ell\ell}}{\Lambda^2} \simeq \frac{1}{16\pi^2} \frac{1}{\Lambda^2} (\hat{Y}^*)^2 . \qquad (4.110)$$

notice that, summing over the b and c indices, we have considered an incoherent contribution from the phases of the $Y^*_{L,R}$ matrix elements, that then sum up to approximately ~ 1. In the best case, where all such contributions would sum up coherently, one would find a further factor 9.

We also define the following mixing angles:

$$\theta_{\ell\ell'} = \frac{\sqrt{|c_{\ell\ell'}|^2 + |c_{\ell'\ell}|^2}}{|c_{\ell\ell}|} , \qquad (4.111)$$

that somehow parametrize the fine tuning of the flavor structure in the composite sector. They have a minimum value due to the constraint of Eq. (4.108), that is[6]:

$$\theta_{\ell\ell',\min} = \sqrt{\frac{2m_{\ell'}}{m_\ell}} . \qquad (4.112)$$

Now we are able to recast $\mathrm{BR}(\ell \to \ell'\gamma)$ using only the NP scale Λ, the strong interaction parameter $\hat{Y}^*$ and the mixing angles $\theta_{\ell\ell'}$. Starting from Eq. (4.44), one finds:

$$\frac{\mathrm{BR}(\ell \to \ell'\gamma)}{\mathrm{BR}(\ell \to \ell'\nu_\ell\bar{\nu}_{\ell'})} = \frac{48\pi^3\alpha}{G_F^2} \theta_{\ell\ell'}^2 |C_{\ell\ell}|^2 = \frac{3\alpha}{16\pi} \theta_{\ell\ell'}^2 (\hat{Y}^*)^4 \frac{1}{G_F^2 \Lambda^4} . \qquad (4.113)$$

In particular, focusing on the $\mu \to e\gamma$ decay, we get:

$$\mathrm{BR}(\mu \to e\gamma) \simeq 2 \cdot 10^{-13} \left(\frac{\theta_{e\mu}}{\theta_{e\mu,\min}} \right)^2 \left(\frac{20 \text{ TeV}}{\Lambda} \right)^4 (\hat{Y}^*)^4 . \qquad (4.114)$$

We can see that, within our approximations, the current experimental bound imposes a severe constraint on the NP scale. It is worthwhile to notice that the suppression factor goes as $\sim 1/\Lambda^4$, then increasing by a factor of two the NP scale already lowers of more than an order of magnitude the predicted branching ratio.

Analogous considerations can be made taking into account the flavor conserving observables Δa_ℓ and d_ℓ discussed in section 4.2. However, now one should be aware of the fact that, since we are considering flavor conserving processes, other leading contributions arising from different diagrams with different spurionic structures can exist, as already mentioned while analysing Fig. 4.5. Nevertheless, we can assume

---

[6]It can be found e.g. using the method of the Lagrange multipliers.

our result to be representative of the correct order of magnitude of the overall contribution.

Using Eq. (4.46), one finds:

$$\Delta a_\ell = \frac{1}{8\pi^2}\frac{m_\ell^2}{\Lambda^2}(\hat{Y}^*)^2 \cos\phi_\ell \, , \qquad \frac{d_\ell}{e} = -\frac{1}{16\pi^2}\frac{m_\ell}{\Lambda^2}(\hat{Y}^*)^2 \sin\phi_\ell \, , \qquad (4.115)$$

where ϕ_ℓ is the phase of $c_{\ell\ell}$, that cannot be predicted through our approximations and that remains a free parameter. Again focusing on the most promising observables (discussed in section 4.2):

$$\Delta a_\mu \simeq 3.5 \cdot 10^{-9} \left(\frac{200 \text{ GeV}}{\Lambda}\right)^2 (\hat{Y}^*)^2 \cos\phi_\mu \, , \qquad (4.116)$$

$$\frac{d_\ell}{e} \simeq -7 \cdot 10^{-29} \left(\frac{30 \text{ TeV}}{\Lambda}\right)^2 (\hat{Y}^*)^2 \sin\phi_e \text{ cm} \, . \qquad (4.117)$$

The complete picture arising from the above analysis can be summarized as follows. If we compare our model predictions for $\text{BR}(\mu \to e\gamma)$ and d_e with the present experimental constraints, Eqs. (4.114) and (4.117), we essentially find that the existence of a TeV scale composite sector can still be accommodated only assuming $\Lambda \gtrsim 30$ TeV. However, this estimation refers to the optimistic situation in which the free parameters (especially $\theta_{e\mu}$ and $\hat{Y}^*$) take their most advantageous values.

The claimed Δa_μ anomaly could hardly be explained within our model, if one pretend simultaneously to satisfy the present constrains on $\text{BR}(\mu \to e\gamma)$ and d_e. Indeed, for $\Lambda \sim 20$ TeV, one obtains an exceedingly small value for the anomaly (four orders of magnitude).

In this thesis, we have performed an explicit analysis limiting ourselves to the dipole operator and in particular to the dipole-mediated processes $\ell \to \ell'\gamma$. We have already argued in section 4.2 that the dipole operator is the most sensitive one in PC scenarios and also that, among the dipole-mediated processes, the most enhanced are exactly the one we have considered. Thus, also taking into account the present experimental sensitivity for other cLFV processes, it turns out that the constraints derived through our analysis using the dipole operator and the $\mu \to e\gamma$ decay are the most stringent that can be inferred using flavor physics in the leptonic sector.

In conclusion, the current experimental bounds (or at least the ones we have considered in this work) are becoming a serious issue for CH models, as can be appreciated with the above analysis. The most important question is then how much the strong sector energy scale Λ can be raised with respect to the Higgs mass, before the hierarchy problem is basically restored. We have seen that, presently, already two orders of magnitude between the two energies are needed in order to satisfy the experimental constraints. Thus we are clearly reaching a turning point for these class of models and in the near future we will hopefully be able to give a definitive answer to the question whether nature has chosen or not to give a natural mass to the Higgs boson through a TeV scale strong interacting sector.

Conclusion

Whether new physics (NP) at the TeV scale exists or not is one major question in modern particle physics, the hierarchy problem being the primary (if not the only) reason to assume its existence. With nowadays and next-generation experimental facilities at the LHC, we will be finally able to test experimentally the TeV scale; thus, hopefully, an answer to the above question is about to be found.

In this context, flavor physics provides a unique framework for testing the SM. It furnishes a great variety of suppressed processes, through which one can look for deviations of the experimental results from the SM predictions. Unfortunately, so far no NP signals have been found in flavor physics and, as a consequence, TeV scale NP models with generic (anarchical) flavor structures are definitely ruled out [29]. Insisting on TeV scale NP for naturalness arguments, highly non generic flavor structures should be imposed to the NP models, such as the Minimal Flavor Violation (MFV) [6] or the Partial Compositeness (PC) paradigms [7].

An important technique that has been used in this work, originally developed to implement the MFV concept but that can be extended to more general situations, is the spurionic analysis [6]. The basic idea of this method is to formally restore the flavor symmetry group of the theory by defining suitable transformation properties for the symmetry breaking terms, that are now called spurions. This technique is very useful since it allows to immediately associate with a definite operator its suppression factor in the theory one is considering.

Switching to a model-dependent analysis, Composite Higgs (CH) models [8] are an interesting alternative to supersymmetry as TeV scale NP candidates. Assuming a new strong interacting sector near the Fermi scale, one can imagine the Higgs boson to be a composite particle, arising as a bound state of such new sector. Its lightness can thus be explained assuming it to be a pseudo Nambu–Goldstone boson, solving also the little hierarchy problem (that is the presence of a hierarchy between the Higgs mass and the remaining mass spectrum of the NP sector) without any significant fine tuning [9].

Further, CH models provide the intriguing mechanism of partial compositeness, that is the idea that the SM particles are an admixture of elementary and composite particles. Assuming that only the latter component can interact with the Higgs boson

(and thus feel the EWSB), the PC paradigm can provide both a fascinating explanation of the hierarchies in the fermionic mass spectrum and an effective suppression mechanism for NP contributions to flavor observables [63]. It is important to stress that MFV and PC outline two different scenarios, with different patterns of flavor violation, thus potentially distinguishable experimentally.

However, unlike supersymmetry, the CH models are strong interacting models and thus precise phenomenological predictions are far more difficult to be extracted. For this purpose, in recent years simplified CH models have been proposed, that still retain the important features of the CH phenomenology (such as PC), but at the same time provide a framework to perform simpler (and still reliable) explicit computations [10, 64]. The two-site model we have considered in this work has exactly this aim: only the lowest-lying set of composite states has been retained, resulting in a model which still presents a PC scenario but that allows simpler, perturbative computations.

Regarding the perturbative approach, another important technique that has been exploited in this thesis is the mass insertion approximation. Instead of working in the mass basis (something requiring a computationally involved rotation of the fermion fields), this approximation allows to work in a more suitable basis and to consider the off-diagonal elements of the fermion mass matrix as new interaction terms, to be described with their own Feynman rules. It furnishes also a different point of view to appreciate the mechanism behind the PC paradigm.

In this work we have considered a popular two-site model, that fully recreates a PC scenario both for the fermions and for the bosons (indeed also the massless SM gauge bosons can be nevertheless thought of as partially composite particles). After having characterized in detail the leptonic sector of such model, we have settled both a complete spurionic analysis and a coherent perturbative computation through the mass insertion approximation.

Thus we have focused on the dipole operator, since it benefits of a significant enhancement in this kind of models. First, by means of the spurionic analysis we have successfully predicted the structure of the Wilson coefficient of the dipole operator. Then, using the mass insertion approximation, we have explicitly computed through one-loop calculations the leading order expression of such Wilson coefficient. Remarkably, we also managed to partially perform such computations in the mass basis, correctly reproducing the corresponding results obtained with the mass insertion approximation.

We have argued that the leading contribution arises from the exchange of SM bosons and heavy fermions and in particular, in the Feynman–'t Hooft gauge, only by the Higgs doublet exchange (i.e. when the Higgs boson or a would-be Goldstone boson circulate in the loop). Expressing this result in a gauge-independent form, we can say that the W and Z bosons contribute at the leading order only through their longitudinal polarization: this can be seen as a non-trivial consequence of the equivalence theorem.

Knowing the expression of the Wilson coefficient associated with the dipole operator, we have easily derived the predictions of our two-site model for some phenomenologically relevant observables, in particular the branching ratio for the muon decay mode $\mu \to e\gamma$, the electron EDM d_e (which are both overwhelmingly small within a SM framework) and the anomalous magnetic moment of the muon a_μ. Through

these results, we have been able to make comparisons with the current experimental bounds in order to establish if there is compatibility with the assumption that the NP scale is not far above the Fermi scale. We have found that the present experimental results regarding flavor violating and flavor conserving observables in the leptonic sector, mainly $\mathrm{BR}(\mu \to e\gamma)$ and d_e, put some stringent constraints on the NP scale Λ, imposing $\Lambda \gtrsim 30$ TeV assuming a flavor-anarchical strong sector, see Eqs. (4.114) and (4.117).

An even more drastic conclusion is drawn if one consider the claimed discrepancy between SM prediction and experimental value for Δa_μ, the anomalous magnetic moment of the muon. Even though this result is still ambiguous, one can decide to trust it and try to predict its value using our two-site model. The conclusion in this case is that the numerical value of such anomaly cannot be satisfactorily reproduced (in a flavor-anarchic scenario for the strong sector) while accommodating also the bounds on $\mathrm{BR}(\mu \to e\gamma)$ and d_e.

In conclusion, here we have studied a very general scenario related to the CH models with PC. Exploiting the fundamental tools of spurionic analysis and mass insertion approximation, we managed to compute phenomenological predictions for this class of models. Comparing our predictions with experimental results, we have found that flavor physics observables are becoming a severe issue for CH models and the PC paradigm in an anarchical scenario is seriously challenged.

Appendix

A.1   Flavor violating observables

In section 2.2, we have seen how EFTs can be used to describe and parametrize NP contributions to physical observables in a very economical way; also, we have discussed how dimension six operators are particularly important in this context, since they often furnish the leading contribution to the observables under study. We have further seen how flavor physics, especially flavor violating processes, provides an important framework where severe tests to the SM predictions and searches for NP signals can be carried out.

For these reasons, when dealing with flavor physics, it is compulsory to perform a thorough analysis of all the possible flavor violating dimension six operators and of their contributions to physical observables. This is what will be done here. We will divide the discussion in two pieces: first $\Delta F = 2$ processes will be discussed, then we will switch to $\Delta F = 1$ processes.

A.1.1 $\Delta F = 2$ processes

The $\Delta F = 2$ sector concerns the neutral meson systems, i.e. the $K^0 - \bar{K}^0$, $D^0 - \bar{D}^0$, $B_d^0 - \bar{B}_d^0$ and $B_s^0 - \bar{B}_s^0$ mixing. Before discussing in detail the observables accessible in these systems, we briefly make some general comments about the basics of meson mixing and the $\Delta F = 2$ effective Hamiltonian.

The amplitude for the transition of a neutral meson $\bar{M}^0$ into its antiparticle M^0 can be written as follows

$$\langle M^0 | H_{eff} | \bar{M}^0 \rangle = M_{12} - \frac{i}{2}\Gamma_{12} \, , \tag{A.1}$$

where M_{12} and Γ_{12} are called dispersive part and absorptive part of the amplitude, respectively. The phases of M_{12} and Γ_{12} are convention dependent, but their relative phase is instead a physical observable. Then, the three fundamental parameters describing meson–antimeson mixing are

$$|M_{12}|, \quad |\Gamma_{12}|, \quad \phi_{12} = \mathrm{Arg}\left(\frac{M_{12}}{\Gamma_{12}}\right) \, . \tag{A.2}$$

While in most BSM models the SM absorptive part Γ_{12} is hardly affected by NP, the dispersive part M_{12} is sensitive to new short distance dynamics that can be encoded in the Wilson coefficients of the $\Delta F = 2$ effective Hamiltonian

$$H_{eff} = -\sum_{i=1}^{5} C_i Q_i - \sum_{i=1}^{3} \tilde{C}_i \tilde{Q}_i + \text{h.c.} , \qquad (A.3)$$

where the Q_i and $\tilde{Q}_i$ operators form a complete basis of $\Delta F = 2$ dimension six operators. They are:

$$
\begin{aligned}
Q_1 &= (\bar{u}_\alpha \gamma_\mu P_L c_\alpha)(\bar{u}_\beta \gamma^\mu P_L c_\beta) , & \tilde{Q}_1 &= (\bar{u}_\alpha \gamma_\mu P_R c_\alpha)(\bar{u}_\beta \gamma^\mu P_R c_\beta) , \\
Q_2 &= (\bar{u}_\alpha P_L c_\beta)(\bar{u}_\beta P_L c_\beta) , & \tilde{Q}_2 &= (\bar{u}_\alpha P_R c_\beta)(\bar{u}_\beta P_R c_\beta) , \\
Q_3 &= (\bar{u}_\alpha P_L c_\beta)(\bar{u}_\beta P_L c_\alpha) , & \tilde{Q}_3 &= (\bar{u}_\alpha P_R c_\beta)(\bar{u}_\beta P_R c_\alpha) , \\
Q_4 &= (\bar{u}_\alpha P_L c_\alpha)(\bar{u}_\beta P_R c_\beta) , \\
Q_5 &= (\bar{u}_\alpha P_L c_\beta)(\bar{u}_\beta P_R c_\alpha) ,
\end{aligned}
\qquad (A.4)
$$

where α and β are color indices and $P_{R,L} = \frac{1}{2}(\mathbb{1} \pm \gamma_5)$. For definiteness we quoted here the operator basis for the $c\bar{u} \to \bar{c}u$ transition. Completely analogous expressions holds of course also in the case of the $s\bar{d} \to \bar{s}d$, $b\bar{d} \to \bar{b}d$ and $b\bar{s} \to \bar{b}s$ transitions.

As described in section 2.2, in the framework of specific UV completions of the SM the Wilson coefficients C_i and $\tilde{C}_i$ in (A.3) can be determined at a high matching scale μ_{NP} by integrating out the heavy degrees of freedom of the model. Then, one can perform a RG running of the coefficients from this high scale down to the low hadronic scale $\mu_l \simeq M_M$, where M_M is the mass of the meson under study. The NP contributions to the mixing amplitude is thus given by:

$$M_{12}^{NP} = \langle M^0 | H_{eff}^{NP} | \bar{M}^0 \rangle = -\sum_{i=1}^{5} C_i^{NP}(\mu_l) \langle Q_i(\mu_l) \rangle - \sum_{i=1}^{3} \tilde{C}_i^{NP}(\mu_l) \langle \tilde{Q}_i(\mu_l) \rangle . \quad (A.5)$$

While the Wilson coefficients encapsulate the high energy informations of the theory, the operator matrix elements $\langle Q_i \rangle$ and $\langle \tilde{Q}_i \rangle$ enclose the low energy physics and then they can be evaluated at the low scale with lattice QCD methods. They are commonly written in the following way:

$$
\begin{aligned}
\langle Q_1 \rangle = \langle \tilde{Q}_1 \rangle &= \frac{1}{3} M_D F_D^2 B_1^D , & \langle Q_4 \rangle &= \frac{1}{4} R_D^2 M_D F_D^2 B_4^D , \\
\langle Q_2 \rangle = \langle \tilde{Q}_1 \rangle &= -\frac{5}{24} R_D^2 M_D F_D^2 B_2^D , & \langle Q_5 \rangle &= \frac{1}{12} R_D^2 M_D F_D^2 B_5^D , \\
\langle Q_3 \rangle = \langle \tilde{Q}_1 \rangle &= \frac{1}{24} R_D^2 M_D F_D^2 B_3^D ,
\end{aligned}
\qquad (A.6)
$$

where again we have considered for definiteness the $c\bar{u} \to \bar{c}u$ transition. Here, M_D and F_D are the D^0 meson mass and decay constant respectively, R_D is a chiral factor given by $R_D = M_D/(m_c + m_u)$ and the so called Bag parameter B_i^D parametrizes the deviation of the matrix element from the vacuum insertion approximation. All these numerical inputs can be found in literature, see e.g. [22, 65].

With the description developed above, one is thus able to fully parametrize NP contributions to the mixing amplitude of the neutral meson systems; this enables to

translate the experimental results of observables quantities into constraints on the Wilson coefficients and thus on NP scenarios. Then, the only thing left to do is to discuss which observables are accessible in the different neutral meson systems in terms of the mixing amplitude (A.1).

$D^0 - \bar{D}^0$ mixing

The neutral D meson mass eigenstates D_1 and D_2 are linear combinations of the strong interaction eigenstates, D^0 and $\bar{D}^0$:

$$|D_{1,2}\rangle = p|D^0\rangle \pm q|\bar{D}^0\rangle \,, \quad \frac{q}{p} = \sqrt{\frac{M_{12}^{D*} - \frac{i}{2}\Gamma_{12}^{D*}}{M_{12}^{D} - \frac{i}{2}\Gamma_{12}^{D}}} \,. \tag{A.7}$$

Their normalized mass and width differences, x_D and y_D, are given by:

$$x_D = \frac{\Delta M_D}{\Gamma_D} = 2\tau_D \text{Re}\left[\frac{q}{p}\left(M_{12}^D - \frac{i}{2}\Gamma_{12}^D\right)\right] \,, \tag{A.8}$$

$$y_D = \frac{\Delta\Gamma_D}{2\Gamma_D} = -2\tau_D \text{Im}\left[\frac{q}{p}\left(M_{12}^D - \frac{i}{2}\Gamma_{12}^D\right)\right] \,. \tag{A.9}$$

Experimentally, $D^0 - \bar{D}^0$ mixing is now firmly established, whereas there is still no evidence for CP violation [66]. Anyway, both mixing and CP violating observables are until now compatibles with the SM predictions and therefore the mass and width difference in $D^0 - \bar{D}^0$ mixing can only be used to bound possible NP contributions.

The CP violating observables are of particular interest in this system, since any experimental signal for CP violation above the per mill level would be an unambiguous NP effect as in the SM CP violation is predicted to be of order 10^{-3}. For this reason, we now briefly focus on two of such observables.

The first one is the time dependent CP asymmetry S_f^D in decays of D^0 and $\bar{D}^0$ to CP eigenstates f. These decay rates are to a good approximation given by [67]:

$$\Gamma(D^0(t) \to f) \propto \exp\left[-\hat{\Gamma}_{D^0(t)\to f}t\right] \,, \quad \Gamma(\bar{D}^0(t) \to f) \propto \exp\left[-\hat{\Gamma}_{\bar{D}^0(t)\to f}t\right] \,, \tag{A.10}$$

with effective decay widths:

$$\hat{\Gamma}_{D^0(t)\to f} = \Gamma_D\left[1 + \eta_f^{CP}\left|\frac{q}{p}\right|(y_D\cos\phi_D - x_D\sin\phi_D)\right] \,, \tag{A.11a}$$

$$\hat{\Gamma}_{\bar{D}^0(t)\to f} = \Gamma_D\left[1 + \eta_f^{CP}\left|\frac{p}{q}\right|(y_D\cos\phi_D - x_D\sin\phi_D)\right] \,, \tag{A.11b}$$

where η_f^{CP} is the CP parity of the final state f. One then defines the following CP violating combination:

$$S_f^D = 2\Delta Y_f = \frac{1}{\Gamma_D}\left(\hat{\Gamma}_{D^0\to f} - \hat{\Gamma}_{\bar{D}^0\to f}\right) \,, \tag{A.12}$$

that, using Eqs. (A.11) becomes:

$$\eta_f^{CP}S_f^D = x_D\left(\left|\frac{q}{p}\right| + \left|\frac{p}{q}\right|\right)\sin\phi_D - y_D\left(\left|\frac{q}{p}\right| - \left|\frac{p}{q}\right|\right)\cos\phi_D \,. \tag{A.13}$$

As explained in [67], to an excellent approximation the above relations hold also in the presence of new weak phases in the decay, due to the nowadays experimental constraints on such phases. Thus, $\eta_f^{CP} S_f^D$ is universal for all final states and practically independent of direct CP violation in the decays. The present experimental value for this quantity is [68]:

$$\eta_f^{CP} S_f^D = (-0.20 \pm 0.22)\% \ , \tag{A.14}$$

and thus it is consistent with the SM estimation.

The second interesting CP violating observable is the semileptonic asymmetry in the decay to "wrong sign" leptons. It is defined as

$$a_{SL}^D = \frac{\Gamma(D^0 \to K^+ \ell^- \nu) - \Gamma(\bar{D}^0 \to K^- \ell^+ \nu)}{\Gamma(D^0 \to K^+ \ell^- \nu) + \Gamma(\bar{D}^0 \to K^- \ell^+ \nu)} = \frac{|q|^4 - |p|^4}{|q|^4 + |p|^4} \tag{A.15}$$

and it is a direct measure of CP violation in the mixing. It turns out that this observable is correlated to the universal time dependent CP asymmetry S_f^D [67]:

$$S_f^D = -\eta_f^{CP} \frac{x_D^2 + y_D^2}{|y_D|} a_{SL}^D \ . \tag{A.16}$$

$K^0 - \bar{K}^0$ mixing

The two main observables in $K^0 - \bar{K}^0$ mixing are the mass difference ΔM_K and the parameter ϵ_K that is a measure of CP violation in such mixing. In terms of the mixing amplitude M_{12}^K they can be written as:

$$\Delta M_K = 2\text{Re}(M_{12}^K) \ , \quad |\epsilon_K| = \frac{\kappa_\epsilon}{\sqrt{2}} \frac{\text{Im}(M_{12}^K)}{\Delta M_K} \ , \tag{A.17}$$

where $\kappa_\epsilon \simeq 0.94$ is a corrective factor that takes into account the long distance contributions to ϵ_K [69]. While the SM prediction for ΔM_K has a large uncertainty due to unknown long distance contributions, the ϵ_K parameter is dominated by short distance physics and can be predicted with good accuracy.

Using the SM expression for M_{12}^K one finds:

$$|\epsilon_K|^{SM} = \kappa_\epsilon C_\epsilon \hat{B}_K \lambda^2 |V_{cb}|^2 \sin\beta \Big(|V_{cb}|^2 R_t^2 \eta_{tt} S_0(x_t) \cos\beta + R_t(\eta_{ct} S_0(x_c, x_t) - \eta_{cc} x_c) \Big) \ , \tag{A.18}$$

where S_0 is a SM loop function that can be found e.g. in [3] and depends on the ratios $x_i = m_i^2/M_W^2$ (with $i = c, t$), η_{ij} (with $i, j = c, t$) are QCD correction factors known at the NLO [70], λ and R_t have been defined in section 2.1 and the factor C_ϵ is given by:

$$C_\epsilon = \frac{G_F^2 M_W^2 F_K^2 M_K}{6\sqrt{2}\pi^2 \Delta M_K} \simeq 3.655 \cdot 10^4 \ . \tag{A.19}$$

Also here, the experimental and the SM values are in agreement (at the 1σ level), leading to strong constraints on the flavor structure of NP models.

$B_d - \bar{B}_d$ mixing

The two most important observables in the B_d system are the mass difference ΔM_d and the time-dependent CP asymmetry in the tree level decay $B_d \to \psi K_S$

$$\frac{\Gamma(\bar{B}_d(t) \to \psi K_S) - \Gamma(B_d(t) \to \psi K_S)}{\Gamma(\bar{B}_d(t) \to \psi K_S) + \Gamma(B_d(t) \to \psi K_S)} = S_{\psi K_S} \sin(\Delta M_d t) \,, \qquad (A.20)$$

where we neglected CP violation in the $B_d \to \psi K_S$ decay amplitude.

Parametrizing the $B_d - \bar{B}_d$ mixing amplitude M_{12}^d in the following way:

$$M_{12}^d = (M_{12}^d)^{SM} + (M_{12}^d)^{NP} = |(M_{12}^d)^{SM}|e^{2i\beta_d} + |(M_{12}^d)^{NP}|e^{i\theta_d} = C_d e^{2i\phi_d}(M_{12}^d)^{SM} \,,$$
$$(A.21)$$

the mass difference ΔM_d and the coefficient $S_{\psi K_S}$ can be written as

$$\Delta M_d = 2|M_{12}^d| = C_d(\Delta M_d)^{SM} \,, \quad S_{\psi K_S} = -\sin\left(\mathrm{Arg}(M_{12}^d)\right) = \sin(2\beta + 2\phi_d) \,.$$
$$(A.22)$$

While ΔM_d measures the absolute value of the mixing amplitude, $S_{\psi K_S}$ measures its phase that, in the SM, is determined by the CKM angle β, i.e. the phase of the CKM element V_{td}. In fact in the SM one has

$$(M_{12}^d)^{SM} = \frac{G_F^2 M_W^2}{12\pi^2} \eta_B M_{B_d} F_{B_d}^2 \hat{B}_{B_d} S_0(x_t)(V_{tb}V_{td}^*)^2 \,, \qquad (A.23)$$

where again η_B is a QCD correction factor and S_0 a loop function depending on $x_t = m_t^2/M_W^2$, see the discussion of the $K^0 - \bar{K}^0$ for references.

Again, one finds a good agreement between SM predictions and experimental measurements, implying severe constraints on NP models.

$B_s - \bar{B}_s$ mixing

In analogy with the B_d system, also in the $B_s - \bar{B}_s$ mixing the important observables are the mass difference ΔM_s and the time dependent CP asymmetry in the tree level decay $B_s \to \psi\phi$:

$$\frac{\Gamma(\bar{B}_s(t) \to \psi\phi) - \Gamma(B_s(t) \to \psi\phi)}{\Gamma(\bar{B}_s(t) \to \psi\phi) + \Gamma(B_s(t) \to \psi\phi)} = S_{\psi\phi} \sin(\Delta M_s t) \,, \qquad (A.24)$$

where we set to zero CP violation in the decay amplitude. The $S_{\psi\phi}$ asymmetry is induced by $\beta_s \simeq -1°$, the tiny phase of the CKM element V_{ts}, and therefore is very small. Consequently, $S_{\psi\phi}$ represents a very promising probe for NP effects.

Again, to parametrize NP contributions to the mixing amplitude M_{12}^s, we make use of the following decomposition (see Eq. (A.21)):

$$M_{12}^s = (M_{12}^s)^{SM} + (M_{12}^s)^{NP} = |(M_{12}^s)^{SM}|e^{2i\beta_s} + |(M_{12}^s)^{NP}|e^{i\theta_s} = C_s e^{2i\phi_s}(M_{12}^s)^{SM} \,.$$
$$(A.25)$$

As in the case of the $B_d - \bar{B}_d$ mixing, the mass difference measures the absolute value of the mixing amplitude, while the coefficient $S_{\psi\phi}$ measures its phase:

$$\Delta M_s = 2|M_{12}^s| = C_s(\Delta M_s)^{SM} \,, \quad S_{\psi\phi} = -\sin\left(\mathrm{Arg}(M_{12}^s)\right) = \sin(2|\beta_s| - 2\phi_s) \,.$$
$$(A.26)$$

The mixing amplitude in the SM is given by:

$$(M_{12}^s)^{SM} = \frac{G_F^2 M_W^2}{12\pi^2} \eta_B M_{B_s} F_{B_s}^2 \hat{B}_{B_s} S_0(x_t)(V_{tb}V_{ts}^*)^2 \ , \tag{A.27}$$

and again no tensions with the experimental value arise.

A.1.2 $\Delta F = 1$ processes

The $\Delta F = 1$ sector spans a wide range of weak decays. In this context, a systematic description of the most general effective Hamiltonian, made up of all the possible $\Delta F = 1$ dimension six operators, is far more complicate than in the $\Delta F = 2$ case, since now there are 35 such operators in all [28]. Typically, only some of them give a contribution to the specific process under study and only few of them are relevant for phenomenological computations.

For all these reasons, when dealing with $\Delta F = 1$ processes it is more advantageous to consider and characterize the relevant operators case by case. Again, such analyses allow to translate experimental results directly into bounds on the Wilson coefficients and then on NP contributions.

Here we will briefly review only some representative weak decays, introducing for each of them the important operators that describe the effective Hamiltonian for that process. A systematic description of the effective Hamiltonian for a broad variety of weak decays can be found in [3].

The radiative $b \to s\gamma$ decay

The suitable framework for the theoretical description of the $b \to s\gamma$ decay is given by the effective Hamiltonian [71]

$$H_{eff} = -\frac{4G_F}{\sqrt{2}} V_{tb}V_{ts}^* \sum_i \left(C_i Q_i + C_i' Q_i' \right) \ , \tag{A.28}$$

where

$$Q_{7\gamma} = \frac{e}{16\pi^2} m_b F_{\mu\nu} \, \bar{s}\sigma^{\mu\nu} P_R b \ , \qquad\qquad Q_{7\gamma}' = \frac{e}{16\pi^2} m_b F_{\mu\nu} \, \bar{s}\sigma^{\mu\nu} P_L b \ , \tag{A.29}$$

$$Q_{8G} = \frac{g_s}{16\pi^2} m_b G_{\mu\nu}^a \, \bar{s}\sigma^{\mu\nu} T^a P_R b \ , \qquad Q_{8G}' = \frac{g_s}{16\pi^2} m_b G_{\mu\nu}^a \, \bar{s}\sigma^{\mu\nu} T^a P_L b \ . \tag{A.30}$$

The operators (A.29) and (A.30) are the most sensitive to NP effects, they are called electromagnetic and cromomagnetic dipole operators respectively. As explained in section 2.3, in the SM and more generally in models with MFV the unprimed operators are necessarily proportional to the bottom quark mass m_b (a dependence that has been made explicit in their definition), whereas the primed operators are proportional to the strange quark mass m_s. Therefore, in such models, the contributions of $Q_{7\gamma}'$ and Q_{8G}' are suppressed by a factor $m_s/m_b \simeq 0.024$ and thus they are completely negligible. As discussed in section 3.2, instead, in other NP models this suppression could be lifted and in these cases large contributions to the corresponding Wilson coefficients $C_{7\gamma}'$ and C_{8G}' are expected.

The prediction for the inclusive $b \to X_s \gamma$ branching ratio in the presence of arbitrary NP contributions to the Wilson coefficients $C_{7\gamma}^{(\prime)}$ and $C_{8G}^{(\prime)}$ can be well approximated by the following expression [72]:

$$
\begin{aligned}
\frac{\mathrm{BR}(\mathrm{B} \to \mathrm{X_s}\gamma)}{\mathrm{BR}(\mathrm{B} \to \mathrm{X_s}\gamma)_{SM}} &= 1 + \hat{a}_{77} \left(|C_{7\gamma}^{NP}|^2 + |C_{7\gamma}^{\prime NP}|^2 \right) + \hat{a}_{88} \left(|C_{8G}^{NP}|^2 + |C_{8G}^{\prime NP}|^2 \right) \\
&\quad + \mathrm{Re}\left(\hat{a}_7 C_{7\gamma}^{NP} \right) + \mathrm{Re}\left(\hat{a}_8 C_{8G}^{NP} \right) \\
&\quad + \mathrm{Re}\left(\hat{a}_{78} \left[C_{7\gamma}^{NP} C_{8G}^{*NP} + C_{7\gamma}^{\prime NP} C_{8G}^{\prime *NP} \right] \right) ,
\end{aligned}
\tag{A.31}
$$

where $\hat{a}_i$ are $\mathcal{O}(1)$ numerical coefficients. Since the experimental data on the above branching ratio and the corresponding NNLO SM prediction are in good agreement with each other, the expression (A.31) can be used to derive severe contraints on the flavor sectors of many NP models [73].

The semileptonic $b \to s\ell^+\ell^-$ decay

Also semileptonic decays based on the $b \to s\ell^+\ell^-$ transition are sensitive probes of NP contributions to the electromagnetic dipole operators $C_{7\gamma}^{(\prime)}$ given in (A.29). In addition, such decays are also very sensitive to semileptonic four fermion operators in the effective Hamiltonian:

$$
Q_{7V} = \frac{e^2}{16\pi^2} (\bar{s}\gamma_\mu P_L b)(\bar{\ell}\gamma^\mu \ell) , \qquad Q_{7A} = \frac{e^2}{16\pi^2} (\bar{s}\gamma_\mu P_R b)(\bar{\ell}\gamma^\mu \ell) ,
\tag{A.32}
$$

$$
Q_{9V} = \frac{e^2}{16\pi^2} (\bar{s}\gamma_\mu P_L b)(\bar{\ell}\gamma^\mu \gamma_5 \ell) , \quad Q_{10A} = \frac{e^2}{16\pi^2} (\bar{s}\gamma_\mu P_R b)(\bar{\ell}\gamma^\mu \gamma_5 \ell) .
\tag{A.33}
$$

There are several meson decays that are based on the $b \to s\ell^+\ell^-$ transition at the parton level. They cover the inclusive $B \to X_s \ell^+\ell^-$ decay as well as the exclusive $B \to K\ell^+\ell^-$, $B \to K^*\ell^+\ell^-$ and $B_s \to \phi\ell^+\ell^-$ decays. The NP sensitivity of these decay modes has been extensively studied in literature (see e.g. [74]); we will restrict our discussion to a brief description of the $B \to K^*\ell^+\ell^-$ mode, referring to [75] for further details and references.

The exclusive $B \to K^*(\to K\pi)\ell^+\ell^-$ decay is regarded as a very important channel for B physics since its angular distribution gives access to a multitude of observables that offer new important tests of the SM and its extensions. With an on-shell K^*, the decay is completely described by four independent kinematic variables: the dilepton invariant mass squared q^2 and three angles, θ_{K^*}, θ_ℓ and ϕ as defined e.g. in [75]. The corresponding full angular decay distribution of $\bar{B}^0 \to \bar{K}^{*0}(\to K^-\pi^+)\mu^+\mu^-$ can be written as

$$
\frac{\mathrm{d}^4\Gamma}{\mathrm{d}q^2 \, \mathrm{d}\cos\theta_{K^*} \, \mathrm{d}\cos\theta_\ell \, \mathrm{d}\phi} = \frac{9}{32\pi} I(q^2, \theta_{K^*}, \theta_\ell, \phi) ,
\tag{A.34}
$$

where the q^2 dependence in $I(q^2, \theta_{K^*}, \theta_\ell, \phi)$ can be encapsulated in 12 angular coefficients $I_i^{(a)} = \{I_1^s, I_1^c, I_2^s, I_2^c, I_3, I_4, I_5, I_6^s, I_6^c, I_7, I_8, I_9\}$.

The corresponding expression for the CP conjugated mode, that is the process $\bar{B}^0 \to K^{*0}(\to K^+\pi^-)\mu^+\mu^-$, is

$$
\frac{\mathrm{d}^4\bar{\Gamma}}{\mathrm{d}q^2 \, \mathrm{d}\cos\theta_{K^*} \, \mathrm{d}\cos\theta_\ell \, \mathrm{d}\phi} = \frac{9}{32\pi} \bar{I}(q^2, \theta_{K^*}, \theta_\ell, \phi) ,
\tag{A.35}
$$

where again the q^2 dependence in $I(q^2, \theta_{K^*}, \theta_\ell, \phi)$ is enclosed in 12 angular coefficients $\bar{I}_i^{(a)}$.

All the 24 angular coefficient functions $I_i^{(a)}(q^2)$ and $\bar{I}_i^{(a)}(q^2)$ are independent and physical observables. They can be expressed in terms of the Wilson coefficients of the effective Hamiltonian and then they all can be used to bound NP contributions. They are often recast as 12 CP averaged angular coefficients $S_i^{(a)}$ and 12 CP asymmetries $A_i^{(a)}$, in order to separate CP conserving and CP violating NP effects:

$$S_i^{(a)} = \frac{I_i^{(a)} + \bar{I}_i^{(a)}}{\mathrm{d}(\Gamma + \bar{\Gamma})/\mathrm{d}q^2} \,, \qquad A_i^{(a)} = \frac{I_i^{(a)} - \bar{I}_i^{(a)}}{\mathrm{d}(\Gamma + \bar{\Gamma})/\mathrm{d}q^2} \,, \tag{A.36}$$

where the normalization to the CP averaged dilepton mass distribution reduces both experimental and theoretical uncertainties in these observables.

This discussion offers a clean and comprehensive way to appreciate and analyse the richness of angular distributions in $\bar{B}^0 \to \bar{K}^{*0}(\to K^-\pi^+)\mu^+\mu^-$ decays, as probes of NP signals.

The $B_s \to \mu^+\mu^-$ and $B_d \to \mu^+\mu^-$ decays

The purely leptonic $B_s \to \mu^+\mu^-$ and $B_d \to \mu^+\mu^-$ decays are strongly helicity suppressed in the SM by the small muon mass, leading to tiny SM predictions for their branching ratios.

The strong suppression of these decays make them ideal probes to investigate the quark flavor structure of BSM physics. Indeed, their helicity suppression can be lifted in the presence of scalar currents and even order of magnitude enhancements of the branching ratios are possible for example in some supersymmetric models.

The operator that is responsible for the $B_s \to \mu^+\mu^-$ decay in the SM is the semileptonic operator Q_{9V} defined in (A.33). Possible scalar currents in NP models give rise to scalar and pseudoscalar operators:

$$Q_S = \frac{e^2}{16\pi^2} m_b (\bar{s}P_R b)(\bar{\ell}\ell) \,, \qquad Q_S' = \frac{e^2}{16\pi^2} m_b (\bar{s}P_L b)(\bar{\ell}\ell) \,, \tag{A.37}$$

$$Q_P = \frac{e^2}{16\pi^2} m_b (\bar{s}P_R b)(\bar{\ell}\gamma_5\ell) \,, \qquad Q_P' = \frac{e^2}{16\pi^2} m_b (\bar{s}P_L b)(\bar{\ell}\gamma_5\ell) \,. \tag{A.38}$$

In terms of the Wilson coefficients of these operators, the branching ratio for the $B_s \to \mu^+\mu^-$ decay can be expressed in the following way:

$$\mathrm{BR}(B_s \to \mu^+\mu^-) = \tau_{B_s} \frac{G_F^2 \alpha^2}{64\pi^3} F_{B_s}^2 M_{B_s}^3 |V_{tb}V_{ts}^*|^2 \sqrt{1 - \frac{4m_\mu^2}{M_{B_s}^2}} \left(|B|^2 \left(1 - \frac{4m_\mu^2}{M_{B_s}^2}\right) + |A|^2 \right), \tag{A.39}$$

with A and B given by

$$A = 2\frac{m_\mu}{M_{B_s}} C_{9V}^{SM} + M_{B_s}(C_P - C_P') \,, \qquad B = M_{B_s}(C_S - C_S'), \tag{A.40}$$

and $C_{9V}^{SM} \simeq -4.1$ [75]. A totally analogous expression of course holds for the $B_d \to \mu^+\mu^-$ decay. The factor m_μ/M_{B_s} in front of C_{9V}^{SM} clearly shows the above mentioned

helicity suppression, that is lifted in the presence of the scalar and pseudoscalar operators.

Recently, these processes has been observed at LHCb [76], again resulting in a substantial agreement with the SM predictions and then to constraints on NP contributions.

The $K \to \pi\nu\bar{\nu}$ decays

The $K_L \to \pi^0\nu\bar{\nu}$ and $K^+ \to \pi^+\nu\bar{\nu}$ decays (see [77] for a review) are the theoretically cleanest processes among the many rare K and B decays. Their branching ratios have been calculated in the SM to an exceptionally high precision. On the contrary, on the experimental side, a precise measurement of such branching ratios is still missing. Both decays, in particular the neutral $K_L \to \pi^0\nu\bar{\nu}$ mode that in the SM is purely induced by direct CP violation, are known to offer unique possibilities in testing the structure of flavor and CP violation in extensions of the SM [78].

The operators sensitive to short distance dynamics for these decays are

$$Q_L^K = \frac{e^2}{16\pi^2}(\bar{s}\gamma_\mu P_L d)(\bar{\nu}\gamma^\mu P_L \nu) \,, \qquad Q_R^K = \frac{e^2}{16\pi^2}(\bar{s}\gamma_\mu P_R d)(\bar{\nu}\gamma^\mu P_L \nu) \,, \qquad (A.41)$$

with which one can build up the effective Hamiltonian relevant for these processes:

$$H_{eff} = -\frac{4G_F}{\sqrt{2}} \left[H_{eff}^{(c)} + V_{ts}^* V_{td}(C_L^K Q_L^K + C_R^K Q_R^K) \right] + \text{h.c.} \,, \qquad (A.42)$$

where $H_{eff}^{(c)}$ denotes the operators which encoded physics below the electroweak scale (i.e. not affected by possible NP contributions).

The dependence on the Wilson coefficients of the branching ratios for these decays, $K_L \to \pi^0\nu\bar{\nu}$ and $K^+ \to \pi^+\nu\bar{\nu}$, can then be computed using the Hamiltonian (A.42), in order to estimate the magnitude of possible NP contributions.

A.2 Extra dimensions theories

A.2.1 Generalities

Higher-dimensional theories have always had the principal aim of describing gravity at a deeper level, trying to explain its peculiarities with respect to the other interactions. One of the first to postulate the existence of extra dimensions was Kaluza in 1921 [79]. He wanted to unify gravity with electromagnetism (within a classical framework) an for this purpose he considered a 5D theory with only gravity.

Several years later, higher-dimensional theories were revitalized by string theory [17]. Strings were found to give a consistent description of quantum gravity, but this could only happen if strings were living in more than 4 dimensions. Therefore, as sentenced at the beginning, extra dimensions might be the correct answer to describe gravity at the quantum level.

In more recent years, QFT models with one warped extra dimension have been proposed [38]. In these models, the curved geometry of the fifth dimension can explain the huge hierarchy between gravity and the other interactions, using exponential suppression/enhancement factors arising from the warped metric.

We will not discuss here the different proposals of these models concerning the gravity interaction. A review of this subject can be found in [80]. Instead, we will for now on focus on theories with one flat extra dimension, describing how such models can furnish an alternative framework for the implementation of the CH ideas.

As we said before, Kaluza was one of the first to consider theories with more than four dimensions. Even though his initial motivation and ideas do not seem to be viable anymore, the formalism he and others developed is still useful nowadays. One of these tools, fundamental when dealing with compactified extra dimensions, is the so-called Kaluza-Klein (KK) reduction [81]. We now work out an explicit example of this method using a simple 5D field theory of a scalar Φ. This will also give us the opportunity to discuss some peculiarities of 5D field theories.

Let us consider a 5D action given by[1]:

$$S_5 = \int \mathrm{d}^4x \, \mathrm{d}y \left[|\partial_\mu \Phi|^2 + |\partial_y \Phi|^2 - g_5^2 |\Phi|^4 \right] , \tag{A.43}$$

where by y we refer to the extra fifth dimension.

In order to keep the action (A.43) dimensionless, we should have the following dimensions in mass unit: $[\Phi] = \frac{3}{2}$ and $[g_5^2] = -\frac{1}{2}$. This dimensional analysis allows us to recognize one feature of higher-dimensional theories: since the field self-coupling g_5^2 is dimensionful, the theory is non-renormalizable. This is true in general, thus every QFT in more than four dimensions necessarily requires an UV completion. Despite this fact, extra dimensions QFT can be thought of as EFT and thus can be safely used to make predictions, with the precautions discussed in section 2.2.

Let us now consider the fifth dimension compact and flat. Further, we will assume that its topology is that of a circle S^1, that corresponds to the identification of y with $y+2\pi R$, where R becomes a free parameter of the theory. Even though some proposed models can elude this conclusion [82], typically the compactification scale is found to

---

[1]Our convention here for the signature is $\eta_{MN} = \mathrm{diag}(1, -1, -1, -1, -1)$.

be of the order of the Planck length $R \sim \ell_P \simeq 10^{-34}$ m, when trying to describe gravity in a consistent way.

The basic idea of the KK reduction is to expand the 5D complex scalar field in Fourier series:

$$\Phi(x, y) = \sum_{n=-\infty}^{\infty} \frac{e^{iny/R}}{\sqrt{2\pi R}} \phi^{(n)}(x) = \frac{1}{\sqrt{2\pi R}} \phi^{(0)}(x) + \sum_{n\neq 0} \frac{e^{iny/R}}{\sqrt{2\pi R}} \phi^{(n)}(x) , \qquad \text{(A.44)}$$

that inserted in Eq. (A.43) and integrated over y gives

$$S_5 = S_4^{(0)} + S_4^{(n)} , \tag{A.45a}$$

$$S_4^{(0)} = \int \mathrm{d}^4x \left[|\partial_\mu \phi^{(0)}|^2 - \frac{g_5^2}{2\pi R} |\phi^{(0)}|^4 \right] , \tag{A.45b}$$

$$S_4^{(n)} = \int d^4x \sum_{n\neq 0} \left[|\partial_\mu \phi^{(n)}|^2 - \left(\frac{n}{R}\right)^2 |\phi^{(n)}|^2 \right] + \text{quartic} - \text{couplings} . \tag{A.45c}$$

We have reduced the initial 5D action to a more customary 4D action. This is very useful since we know much more about 4D theories that 5D theories. From Eqs. (A.45) we can see that the corresponding 4D theory in this case consists of a massless scalar field $\phi^{(0)}$ and a tower of massive modes $\phi^{(n)}$. The former will be referred to as the zero-mode, the latter will be referred to as the KK modes.

As a consequence, at energies far below $1/R$ the effective theory can be described using only the action (A.45b). Indeed, it is well-know that heavy fields effectively decouples in a low energy description and thus only the zero-mode remains as a dynamical degree of freedom. This is actually a very good approximation in models where $R \sim \ell_P$, since the suppression factor of planckian physics at the TeV scale or below is overwhelming. However, in models with a different compactification of the extra dimension ,value of $1/R$ around the TeV scale can naturally arise. In this case, it could be necessary to include in the effective description also the first KK modes. Below we will discuss in detail this second possibility.

A.2.2 Orbifold extra dimension

In the discussion above we have used a simple S^1 compactification. Of course this is not the only possibility, and in particular another choice has become very popular in recent literature, where the extra dimension y is compactified in a orbifold, $S^1/\mathbb{Z}_2$.

This kind of compactification, whose advantages will become clear soon, is shown in Fig. A.1. It correspond to a circle S^1 with the extra identification of y with $-y$, that gives a manifold which is an interval: $y \in [0, L]$, $L \equiv \pi R$. Therefore the manifold has boundaries at $y = 0$ and $y = L$, delimiting its "bulk". Although this is not a smooth manifold, it seems to be a consistent compactification in string theory.

As a consequence of the presence of boundaries, the action alone does not completely define the theory: the boundary conditions (BCs) at $y = 0$ and $y = L$ have also to be specified. These must be chosen so that the variation of the action vanishes, upon evaluation of the equation of motion, both in the bulk and on the boundaries.
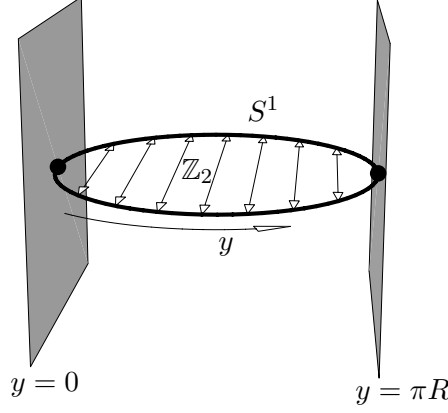
Figure A.1: The $S^1/\mathbb{Z}_2$ orbifold.

As an example, we take again the action (A.43), this time with orbifold fifth dimension, and we work out its variation:

$$\frac{\delta S_5}{\delta \Phi}\delta\Phi = -\int \mathrm{d}^4x \int_0^L \mathrm{d}y \left[(\partial_\mu\partial^\mu + \partial_y\partial^y)\Phi^* + 2g_5^2|\Phi|^2\Phi^*\right]\delta\Phi - \int \mathrm{d}^4x\left[\partial_y\Phi^*\delta\Phi\right]_0^L ,$$

(A.46)

The first term of the r.h.s. of the previous formula vanishes upon evaluation on the bulk equation of motion. The second term, instead,

$$\int \mathrm{d}^4x\left[\partial_y\Phi^*\delta\Phi\right]_0^L ,$$

must vanish when the BCs at $y_i = 0, L$ are imposed. It is easy to see that there can be two different choices of BC:

$$\text{Neumann BC } (+): \qquad \partial_y\Phi(y_i) = 0 , \qquad\qquad\qquad (A.47)$$

$$\text{Dirichlet BC } (-): \qquad \Phi(y_i) = 0 . \qquad\qquad\qquad (A.48)$$

Specifying whether of these two BCs are chosen at the two boundaries $y = 0, L$ completes the description of the theory. In the following, we will use the short notation (s_0, s_L) to indicate the selected choice: $s_i = \pm$ indicate the chosen BC at the boundary $i = 0, L$. Thus, for example, $(-, +)$ means that we are using Dirichlet conditions at $y = 0$ and Neumann conditions at $y = L$.

We have now made explicit calculations in the case of a scalar field, without a bulk mass term. To extend these considerations also to fermion and gauge bosons fields, some additional subtleties have to be taken into account. We will not discuss them in detail, just stating the results of a careful dissertation, that can be found e.g. in [9]. We anticipate that, once paid attention to those subtleties, basically what can be found is that, again, only Neumann $(+)$ or Dirichlet $(-)$ BCs are allowed.

In the case of fermions one has to consider that their equations of motion entangle together the two chiralities. It can be shown that, once decided the BCs of one chiral component, the other should have opposite ones. In formulas, the two allowed

configurations for the BCs of a 5D fermion field (i.e. a Dirac fermion[2]) Ψ are:

$$
\begin{cases} \Psi_L(y_i) = 0 & (-) \\ \partial_y \Psi_R(y_i) = 0 & (+) \end{cases} \quad \text{or} \quad \begin{cases} \partial_y \Psi_L(y_i) = 0 & (+) \\ \Psi_R(y_i) = 0 & (-) \end{cases} . \tag{A.49}
$$

Very interesting considerations can be made when applying the KK reduction in this framework. In this case, the Fourier modes along the fifth dimension are different according to the BCs of the field under analysis. In particular, it is easy to see that only $(+, +)$ BCs give a non-vanishing massless zero-mode. But we have just argued that, if the choice $(+, +)$ is made for e.g. Ψ_L, then we automatically have to associate $(-, -)$ with Ψ_R; thus only one chiral component can have a zero-mode. Then, in these theories, a spectrum of chiral fermions at low energy naturally arises as a result of the KK reduction. This is one of the main reasons that motivate the compactification in a orbifold.

Even more fascinating conclusions can be drawn concerning the BCs to be imposed to the gauge bosons. Let us consider a general 5D gauge symmetry $\mathcal{G}$, whose associated gauge bosons[3] are A_M^A (with $M = \{\mu, y\}$), with generators T^A. Now one has to be careful when defining the BCs, in order to formulate them in a gauge invariant manner. Using consistency arguments (and neglecting possible mass terms localized at the boundaries), it can be shown that the BCs should satisfy the following restrictions:

(i) The components A_μ^A of a gauge field should have BCs equal to each other and opposite to A_y^A;

(ii) The set of generators T^a, associated with the fields A_M^a satisfying $(+)$ conditions at one boundary, should belong to a definite subgroup of $\mathcal{G}$.

Using the above constraints, the most general set of BCs that can be consistently applied to the gauge fields A_M^A are:

$$
\begin{aligned}
A_\mu^a(+,+), & \quad A_y^a(-,-) & T^a \in \text{Alg}\,\{\mathcal{H} = \mathcal{H}_1 \cap \mathcal{H}_0\} \ , \\
A_\mu^{\bar{a}}(+,-), & \quad A_y^{\bar{a}}(-,+) & T^{\bar{a}} \in \text{Alg}\,\{\mathcal{H}_0/\mathcal{H}\} \ , \\
A_\mu^{\dot{a}}(-,+), & \quad A_y^{\dot{a}}(+,-) & T^{\dot{a}} \in \text{Alg}\,\{\mathcal{H}_1/\mathcal{H}\} \ , \\
A_\mu^{\hat{a}}(-,-), & \quad A_y^{\hat{a}}(+,+) & T^{\hat{a}} \in \text{Alg}\,\{\mathcal{G}/\mathcal{H}_0\} \cap \text{Alg}\,\{\mathcal{G}/\mathcal{H}_1\} \ ,
\end{aligned} \tag{A.50}
$$

where $\mathcal{H}_{0,1}$ are subgroups of $\mathcal{G}$. These subgroups represent the unbroken gauge symmetry on the boundaries, since only the fields associated with $\mathcal{H}_0$ ($\mathcal{H}_1$) do not vanish at $y = 0$ ($y = L$). This situation is sketched in Fig. A.2.

We now apply the KK reduction to the gauge fields using the set of conditions (A.50). This procedure results in the following considerations:

---

[2]Indeed the smallest irreducible representation of the 5-dimensional Lorentz group $SO(1, 4)$ is a Dirac fermion.

[3]Clearly the gauge bosons, since they lies in the fundamental representation of the 5D Lorentz group $SO(1, 4)$, have five components. When considering a brane $y = k$ (with k a constant), under the residual $SO(1, 3)$ invariance (the customary 4D Lorentz group) the first four components A_μ^A form a vector representation, while the fifth component A_y^A is a scalar.

$$\mathcal{H}_0 \qquad\qquad \mathcal{G} \qquad\qquad \mathcal{H}_1$$

$$\vdash\!\!\!-\!\!\!-\!\!\!-\!\!\!-\!\!\!-\!\!\!-\!\!\!-\!\!\!-\!\!\!-\!\!\!\dashv$$

$$y = 0 \qquad\qquad\qquad\qquad y = L$$
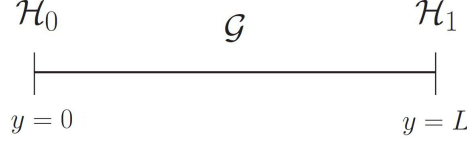
Figure A.2: Representation of the boundary conditions on the gauge fields: the bulk gauge symmetry $\mathcal{G}$ is reduced to the subgroup $\mathcal{H}_0$ at the boundary $y = 0$, and to $\mathcal{H}_1$ at $y = L$.

- As already observed, only fields with $(+, +)$ conditions admits a non-vanishing massless zero-mode. Thus, the low energy spectrum of gauge bosons is $A_\mu^a T^a \in$ Alg $\{\mathcal{H}\}$. According to this spectrum, the low energy gauge invariance is $\mathcal{H} = \mathcal{H}_1 \cap \mathcal{H}_0$. This can be thought of as a spontaneous symmetry breakdown process;

- Together with the above vector bosons, the low energy spectrum presents also a set of 4D scalars $A_y^{\hat{a}}$ living in Alg $\{\mathcal{G}/\mathcal{H}_0\} \cap$ Alg $\{\mathcal{G}/\mathcal{H}_1\}$. They are naturally light since a potential (and then a mass) for such particles can arise only at one-loop level from non local operators[4];

- Among the various KK (i.e. massive) modes, only the $A_\mu^{(n)}$ are physical fields. The heavy resonances $A_y^{(n)}$ are eaten order by order in a Higgs mechanism to give mass to the $A_\mu^{(n)}$ fields. In fact, it can be shown that there is always a gauge transformation that eliminates the y dependence of A_y from the very beginning, leaving only its zero-mode (if not vanishing).

We have then seen that in these class of theories, using the freedom in setting the BCs, one is able to design the desired pattern of gauge symmetries and to obtain a set of naturally light scalars. All of this suggests an analogy between these models and CH models described in section 3.2.

This parallel becomes more striking when using an "holographic" approach [9, 83]. Let us adopt the point of view of a 4-dimensional observer located on one of the two boundaries, for example at $y = 0$. We then have to reduce the 5D action S_5 to an effective 4D action S_{eff}, describing the physics on the $y = 0$ brane. This can be done using the holographic method reviewed in [83].

At the conceptual level, this procedure can be illustrated using the functional integral approach. We initially have a set of bulk fields $\Phi(x_\mu, y)$ defining the bulk action $S_5[\Phi]$ and possible action terms $S_0[\Phi_0 \equiv \Phi(x_\mu, 0)]$ localized at $y = 0$. The generating functional of the 5D theory is then:

$$Z = \int \mathrm{d}\Phi \, e^{iS_5[\Phi] + iS_0[\Phi_0]} \,. \tag{A.51}$$

We perform the above integral in two steps. First, we integrate over the bulk fields

---

[4]It is easy to see that in 5D gauge theories there is no way of building gauge invariant terms with only A_y and no four-dimensional derivative.
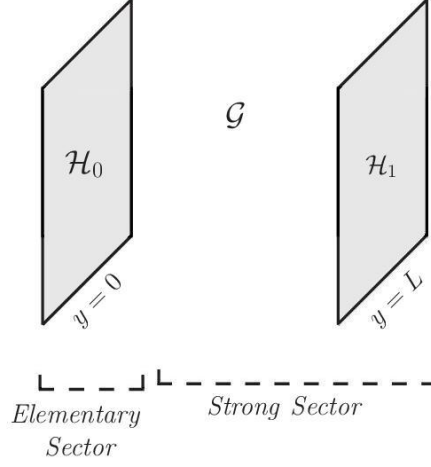
Figure A.3: Holographic interpretation of the 5D theory. The fields at $y = 0$ constitute a weak interacting sector, while the holographic projection of the value of the fields in the bulk and at the $y = L$ brane form a strong interacting sector.

Φ while keeping their value at $y = 0$ fixed:

$$Z = \int \mathrm{d}\Phi_0 \, e^{iS_0[\Phi_0]} \int_{\Phi_0} \mathrm{d}\Phi \, e^{iS_5[\Phi]} = \int \mathrm{d}\Phi_0 \, e^{iS_0[\Phi_0] + iS_{eff}[\Phi_0]} \, , \qquad (A.52)$$

$$iS_{eff} \equiv \log \int_{\Phi_0} \mathrm{d}\Phi \, e^{iS_5[\Phi]} \, , \qquad (A.53)$$

obtaining an effective 4D description of the same theory, in terms of the holographic fields Φ_0. As a second step, one integrates over all values of Φ_0.

The action S_{eff} of Eq. (A.53) encodes all the dynamics described above, in terms of a 4D field theory. From this perspective, the values of the bulk fields at the $y = 0$ boundary (as well as possible localized fields) act like a 4D sector with local invariance $\mathcal{H}_0$. On the other hand, the dynamics associated with the degrees of freedom living in the bulk and at the $y = L$ boundary, once "projected" on the $y = 0$ brane, can be interpreted as a 4D strongly interacting sector, with a global invariance $\mathcal{G}$ broken down to $\mathcal{H}_1$. Further, it can be shown that the symmetry breaking in the strong sector $\mathcal{G} \to \mathcal{H}_1$ is spontaneous rather than explicit, and the associated NG bosons are exactly the zero-modes of A_y.

In summary, our effective 4D theory has a weakly interacting sector (we will call it the elementary sector) with gauge invariance $\mathcal{H}_0$, and a strong interacting sector with a pattern of global symmetry breaking $\mathcal{G} \to \mathcal{H}_1$, as illustrated in Fig. A.3. We have then exactly reproduced, within the new language of extra dimensions theories, the symmetry structure of general CH theories, Fig. 3.1.

All these arguments, and in particular the holographic procedure in Eqs. (A.51)–(A.53), thus define a correspondence between CH theories and 5D theories. Within this equivalence, the KK modes of the 5D theory must be interpreted as the mass eigenstates resulting from the admixture of the massive resonances of the strong sector with the fields of the elementary sector. This is in fact in complete analogy with the

discussion of partial compositeness of section 3.2: the SM and heavy fields of the CH theories are, respectively, the zero mode and the KK modes of the bulk fields in the language of 5D theories.

This strict parallelism between this two models is extremely useful to shed light to both of them. On the one hand, 5D theories furnish a method to define the strong dynamics, which in the discussion of section 3.2 was just assumed to behave in a certain manner. Further, they provide a different framework to perform calculations, and this is desirable since in strong interacting theories computations are typically too difficult to be handled. On the other hand, 4D theories gives a clearer qualitative understanding of the physics, since QFT in four dimension are far more understood than QFT in higher dimensions.

To conclude, it is important to stress one point that has been left loose from the above discussion. The distinction between an elementary sector (living at $y = 0$) and a strong sector (associated with the dynamics in the bulk and at $y = L$) truly makes sense only if the former is weakly coupled, to itself and to the strong sector. This assumption was made without further justifications. In the context of one flat extra dimension theories, this requests can be fulfilled by introducing large kinetic terms for the elementary fields, localized at the $y = 0$ brane (that is using the S_0 action term in Eq. (A.51)). Remarkably, models with one warped extra dimension automatically satisfy the above condition, provided the elementary sector to live in the so-called UV brane [38].

A.3 Feynman rules for the two-site model

Here are listed the Feynman rules involving leptons for the two-site model discussed in section 4.1 in the mass insertion approximation, namely using the Lagrangian (4.14). We express them in a straightforward generalization of the Feynman–'t Hooft gauge ($\xi = 1$).

A.3.1 Propagators

$$\mu \overset{W, Z}{\underset{k}{\sim\!\sim\!\sim\!\sim\!\sim}} \nu \qquad \frac{-i}{k^2 - M_{W,Z}^2}\eta_{\mu\nu} \qquad\qquad (A.54)$$

$$\mu \overset{\rho}{\underset{k}{\approx\!\approx\!\approx}} \nu \qquad \frac{-i}{k^2 - M_{\rho}^2}\eta_{\mu\nu} \qquad\qquad (A.55)$$

$$\xrightarrow[p]{} \qquad \frac{i\not{p}}{p^2} \qquad\qquad (A.56)$$

$$\xLongrightarrow[p]{} \qquad \frac{i(\not{p} + m_f)}{p^2 - m_f^2} \qquad\qquad (A.57)$$

$$\overset{h}{\underset{p}{-\!-\!-\!-\!-\!-\!-}} \qquad \frac{i}{p^2 - M_h^2} \qquad\qquad (A.58)$$

$$\overset{\varphi_Z}{\underset{p}{-\!-\!-\!-\!-\!-\!-}} \qquad \frac{i}{p^2 - M_Z^2} \qquad\qquad (A.59)$$

$$\overset{\varphi^{\pm}}{\underset{p}{-\!-\!-\!-\!-\!-\!-}} \qquad \frac{i}{p^2 - M_W^2} \qquad\qquad (A.60)$$

A.3.2 Triple fermion-boson interactions

The fermion-boson interactions, in the basis we are using, are all flavor diagonal. Both elementary and composite leptons interact with SM and heavy gauge bosons.

Together with the SM coupling definitions (4.13), the following notations are used:

$$\tan\theta_W \;\equiv\; \frac{g_2^{SM}}{g_1^{SM}}\;, \tag{A.61}$$
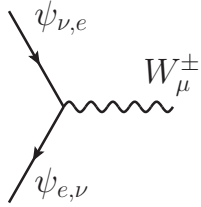
$$\tan\omega_{\mathrm{el}} \;\equiv\; \frac{g_2^{SM}\tan\theta_2}{g_1^{SM}\tan\theta_1}\;, \tag{A.62}$$

$$\tan\omega_{\mathrm{comp}} \;\equiv\; \frac{g_2^{SM}\cot\theta_2}{g_1^{SM}\cot\theta_1}\;, \tag{A.63}$$
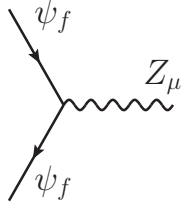
$$v_f^{SM} \;=\; \frac{1}{2}T_3^f - Q_f\sin^2\theta_W; \qquad a_f \;=\; \frac{1}{2}T_3^f\;, \tag{A.64}$$

$$v_f^{\mathrm{el}} \;=\; \frac{1}{2}T_3^f - Q_f\sin^2\omega_{\mathrm{el}}\;, \tag{A.65}$$

$$v_f^{\mathrm{comp}} \;=\; \frac{1}{2}T_3^f - Q_f\sin^2\omega_{\mathrm{comp}}\;. \tag{A.66}$$
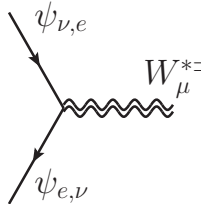
$$i\frac{g_1^{SM}}{\sqrt{2}}\gamma^\mu P_L \tag{A.67}$$
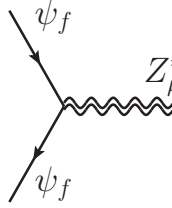
$$i\frac{g_1^{SM}}{\cos\theta_W}\gamma^\mu(v_f^{SM}-a_f\gamma^5) \tag{A.68}$$
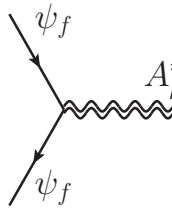
$$ieQ_f\gamma^\mu \tag{A.69}$$
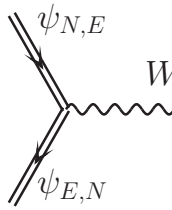
$$-i\left(\frac{g_1^{SM}}{\sqrt{2}}\tan\theta_1\right)\gamma^\mu P_L \tag{A.70}$$
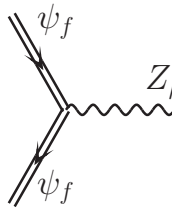
$$i\frac{g_1^{SM}\tan\theta_1}{\sqrt{2}\cos\omega_{\mathrm{el}}}\gamma^\mu(v_f^{\mathrm{el}}-a_f\gamma^5) \tag{A.71}$$

$$ig_1^{SM}\tan\theta_1\sin\omega_{\mathrm{el}}\,Q_f\,\gamma^\mu \tag{A.72}$$
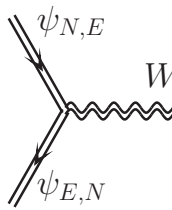
$$i\frac{g_1^{SM}}{\sqrt{2}}\gamma^\mu P_L \tag{A.73}$$

$$i\frac{g_1^{SM}}{\cos\theta_W}\gamma^\mu(v_f^{SM}-a_f\gamma^5) \tag{A.74}$$

$$ieQ_f\gamma^\mu \tag{A.75}$$

$$i(\frac{g_1^{SM}}{\sqrt{2}}\cot\theta_1)\gamma^\mu P_L \tag{A.76}$$
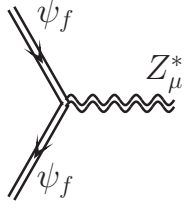
$$i\frac{g_1^{SM}\cot\theta_1}{\sqrt{2}\cos\omega_{\mathrm{comp}}}\gamma^\mu(v_f^{\mathrm{comp}}-a_f\gamma^5) \qquad (A.77)$$
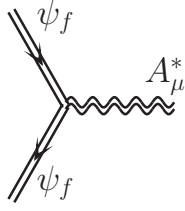
$$ig_1^{SM}\cot\theta_1\sin\omega_{\mathrm{comp}}\,Q_f\,\gamma^\mu \qquad (A.78)$$
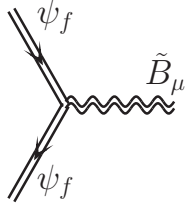
$$i\frac{g_2^{SM}}{\sin\theta_2}\,Q_f\,\gamma^\mu \qquad (A.79)$$

A.3.3   Mass insertion interactions

$$-i(\tilde{\Delta}^\dagger)_{ji}P_R \qquad (A.80)$$
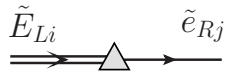
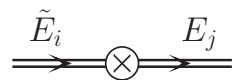$$-i(\tilde{\Delta})_{ji}P_L \qquad (A.81)$$
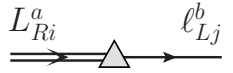
$$-i\delta^{ab}(\Delta)_{ji}P_R \qquad (A.82)$$
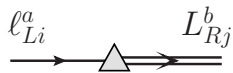
$$-i\delta^{ab}(\Delta^\dagger)_{ji}P_L \qquad (A.83)$$

$$-i\frac{v}{\sqrt{2}}[(Y_R^*)_{ji}P_R+(Y_L^*)_{ji}P_L] \qquad (A.84)$$

$$\overrightarrow{E_i \quad \otimes \quad \tilde{E}_j} \qquad -i\frac{v}{\sqrt{2}}[(Y_L^{*\dagger})_{ji}P_R + (Y_R^{*\dagger})_{ji}P_L] \qquad (A.85)$$

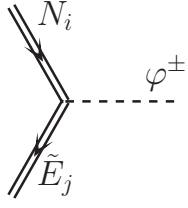## A.3.4 Trilinear fermion-Higgs and fermion-Goldstone interactions

$$\frac{-i}{\sqrt{2}}[(Y_R^*)_{ji}P_R + (Y_L^*)_{ji}P_L] \qquad (A.86)$$

$$\frac{-i}{\sqrt{2}}[(Y_L^{*\dagger})_{ji}P_R + (Y_R^{*\dagger})_{ji}P_L] \qquad (A.87)$$

$$\frac{1}{\sqrt{2}}[(Y_R^*)_{ji}P_R + (Y_L^*)_{ji}P_L] \qquad (A.88)$$

$$-\frac{1}{\sqrt{2}}[(Y_L^{*\dagger})_{ji}P_R + (Y_R^{*\dagger})_{ji}P_L] \qquad (A.89)$$

$$-i[(Y_R^*)_{ji}P_R + (Y_L^*)_{ji}P_L] \qquad (A.90)$$

$$-i[(Y_L^{*\dagger})_{ji}P_R + (Y_R^{*\dagger})_{ji}P_L] \qquad\qquad (A.91)$$

A.4 Detailed computations for the dipole operator

Here we report the detailed computations for the amplitudes A_2, B_1 and B_2 of Fig. 4.2, in section 4.2.

A.4.1 The A_2 amplitude.

The steps of the calculations are the same as for the amplitude A_1, so we will use the same techniques and trick without recalling them. In Fig. A.4 are represented the conventions adopted for the loop momenta, while for the flavor indices we use the same convention as in Fig. 4.2. Again a sum over all flavor indices a, b, c, d is understood.

$$
A_2 = \bar{e}_{Lj}(p')\,(-i(\Delta)_{jd}P_R)\,\frac{i(\not{p}' + m_d)}{p'^2 - m_d^2}\left[\frac{-i}{\sqrt{2}}\left((Y_L^*)_{dc}P_L + (Y_R^*)_{dc}P_R\right)\right] \times
$$

$$
\times \left\{\int \frac{\mathrm{d}^4 k}{(2\pi)^4}\frac{i(\not{k} - \not{q} + \tilde{m}_c)}{(k-q)^2 - \tilde{m}_c^2}\,(-ie\gamma^\alpha \varepsilon_\alpha(q))\,\frac{i(\not{k} + \tilde{m}_c)}{k^2 - \tilde{m}_c^2} \times \right.
$$

$$
\times \left[\frac{-iv}{\sqrt{2}}\left((Y_L^{*\dagger})_{cb}P_R + (Y_R^{*\dagger})_{cb}P_L\right)\right]\frac{i(\not{k} + m_b)}{k^2 - m_b^2}\frac{i}{(k-p)^2 - M_h^2}\right\} \times
$$

$$
\times \left[\frac{-i}{\sqrt{2}}\left((Y_L^*)_{ba}P_L + (Y_R^*)_{ba}P_R\right)\right]\frac{i(\not{p} + \tilde{m}_a)}{p^2 - \tilde{m}_a^2}\left(-i(\tilde{\Delta}^\dagger)_{ai}P_R\right)\tilde{e}_{Ri}(p)
$$

$$
= \frac{ev}{2\sqrt{2}}\frac{1}{\tilde{m}_a m_d}(\Delta)_{jd}(Y_R^*)_{dc}(Y_R^*)_{ba}(\tilde{\Delta}^\dagger)_{ai}\,\varepsilon_\alpha \times
$$

$$
\times \bar{e}_{Lj}\left\{\int \frac{\mathrm{d}^4 k}{(2\pi)^4}\frac{1}{[k^2 - \tilde{m}_c^2][k^2 - m_b^2][(k-q)^2 - \tilde{m}_c^2][(k-p)^2 - M_h^2]} \times \right.
$$

$$
\times (\not{k} - \not{q} + \tilde{m}_c)\gamma^\alpha(\not{k} + \tilde{m}_c)\left((Y_L^{*\dagger})_{cb}P_R + (Y_R^{*\dagger})_{cb}P_L\right)(\not{k} + m_b)\right\}\tilde{e}_{Ri}
$$

$$
= \frac{ev}{2\sqrt{2}}\frac{1}{\tilde{m}_a m_d}(\Delta)_{jd}(Y_R^*)_{dc}(Y_R^*)_{ba}(\tilde{\Delta}^\dagger)_{ai}\,\varepsilon_\alpha \times
$$

$$
\times \bar{e}_{Lj}\left\{\int \frac{\mathrm{d}^4 k}{(2\pi)^4}\frac{1}{[k^2 - \tilde{m}_c^2][k^2 - m_b^2][(k-q)^2 - \tilde{m}_c^2][(k-p)^2 - M_h^2]} \times \right.
$$

$$
\times m_b\tilde{m}_c(Y_L^{*\dagger})_{cb}(2k^\alpha - \not{q}\gamma^\alpha) + (Y_R^{*\dagger})_{cb}(k^2(\not{k} - \not{q})\gamma^\alpha + \tilde{m}_c^2\gamma^\alpha\not{k})\right\}\tilde{e}_{Ri}\,. \quad \text{(A.92)}
$$

To deal with the denominator of (A.92), we use the same technique as for the A_1 calculation. Actually, we can fully restore those calculations once performed the substitutions $m_b \leftrightarrow \tilde{m}_c$, $q \to -q$ and $p' \to p$. We then get automatically:

$$
\frac{1}{[k^2 - \tilde{m}_c^2][k^2 - m_b^2][(k-q)^2 - \tilde{m}_c^2][(k-p)^2 - M_h^2]}
$$

$$
= \frac{2}{m_b^2 - \tilde{m}_c^2}\int_0^1 \mathrm{d}x \int_0^{1-x} \mathrm{d}y \frac{1}{\{[k+Q']^2 - \Omega_1'\}^3} - \frac{1}{\{[k+Q']^2 - \Omega_2'\}^3}\,, \quad \text{(A.93)}
$$
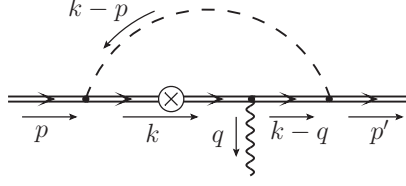
Figure A.4: Convention for the loop momenta in the calculation of the amplitude A_2.

where

$$\begin{cases} Q' & \equiv & -yq - (1-x-y)p \\ \Omega_1' & \equiv & xm_b^2 + y\tilde{m}_c^2 + (1-x-y)M_h^2 \\ \Omega_2' & \equiv & (x+y)\tilde{m}_c^2 + (1-x-y)M_h^2 \end{cases} . \qquad (A.94)$$

We now perform in the expression (A.92) the change of variable

$$k \to k - Q' , \qquad (A.95)$$

starting from the numerator inside the integral. We get:

$$\varepsilon_\alpha \bar{e}_{Lj} \left[m_b \tilde{m}_c (Y_L^{*\dagger})_{cb} (2k^\alpha - \slashed{q}\gamma^\alpha) + (Y_R^{*\dagger})_{cb} (\tilde{m}_c^2 \gamma^\alpha \slashed{k} + k^2 (\slashed{k} - \slashed{q})\gamma^\alpha) \right] \tilde{e}_{Ri}$$

$$\to \varepsilon_\alpha \bar{e}_{Lj} \Big\{ m_b \tilde{m}_c (Y_L^{*\dagger})_{cb} \left[2k^\alpha + 2yq^\alpha + 2(1-x-y)p^\alpha - \slashed{q}\gamma^\alpha \right]$$

$$+ (Y_R^{*\dagger})_{cb} \left[\tilde{m}_c^2 \gamma^\alpha \slashed{k} + \tilde{m}_c^2 \gamma^\alpha y\slashed{q} + \tilde{m}_c^2 \gamma^\alpha (1-x-y)\slashed{p} \right.$$

$$+ (k^2 + 2yk\cdot q + 2(1-x-y)k\cdot p)(\slashed{k} - (1-y)\slashed{q} + (1-x-y)\slashed{p}) \gamma^\alpha \Big] \Big\} \tilde{e}_{Ri}$$

$$= \varepsilon_\alpha \bar{e}_{Lj} \Big\{ m_b \tilde{m}_c (Y_L^{*\dagger})_{cb} \left[2(1-x-y)p^\alpha - \slashed{q}\gamma^\alpha \right] + (Y_R^{*\dagger})_{cb} \left[\tilde{m}_c^2 \gamma^\alpha y\slashed{q} + \right.$$

$$+ k^2(-(1-y)\slashed{q} + (1-x-y)\slashed{p})\gamma^\alpha + 2k\cdot(yq + (1-x-y)p)\slashed{k}\gamma^\alpha \Big] \Big\} \tilde{e}_{Ri}$$

$$= - \left[m_b \tilde{m}_c (Y_L^{*\dagger})_{cb} (x+y) + (Y_R^{*\dagger})_{cb} \tilde{m}_c^2 y - (Y_R^{*\dagger})_{cb} \frac{1}{2} k^2 (1-3x) \right] Q_{\gamma L} . \qquad (A.96)$$

Plugging Eqs. (A.93) and (A.96) into Eq. (A.92) we obtain:

$$A_2 = - \frac{ev}{2\sqrt{2}} \frac{1}{\tilde{m}_a m_d} (\Delta)_{jd} (Y_R^*)_{dc} (Y_R^*)_{ba} (\tilde{\Delta}^\dagger)_{ai} \frac{2}{m_b^2 - \tilde{m}_c^2} \times$$

$$\times \left\{ \int_0^1 dx \int_0^{1-x} dy \left[m_b \tilde{m}_c (Y_L^{*\dagger})_{cb} (x+y) + (Y_R^{*\dagger})_{cb} \tilde{m}_c^2 y \right] F_1(\Omega_1', \Omega_2') \right.$$

$$- \left[(Y_R^{*\dagger})_{cb} \frac{1}{2} (1-3x) \right] F_2(\Omega_1', \Omega_2') \Big\} Q_{\gamma L} , \qquad (A.97)$$

where the integrals over loop momentum F_1 and F_2 are the one defined and solved
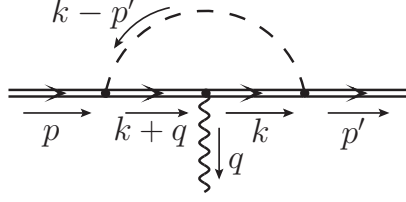
Figure A.5: Convention for the loop momenta in the calculation of the amplitudes B_1 and B_2.

in (4.81) and (4.82) respectively. Then:

$$A_2 = \frac{iev}{32\sqrt{2}\pi^2} \frac{1}{\tilde{m}_a m_d} (\Delta)_{jd} (Y_R^*)_{dc} (Y_R^*)_{ba} (\tilde{\Delta}^\dagger)_{ai} \frac{1}{m_b^2 - \tilde{m}_c^2} \times$$

$$\times \left\{ \int dx \int dy \left[\frac{1}{\Omega_1'} - \frac{1}{\Omega_2'} \right] \left[m_b \tilde{m}_c (Y_L^{*\dagger})_{cb} (x+y) + \tilde{m}_c^2 (Y_R^{*\dagger})_{cb} y \right] \right.$$

$$\left. - \log \frac{\Omega_1'}{\Omega_2'} \left[(Y_R^{*\dagger})_{cb} (1-3x) \right] \right\} Q_{\gamma L} . \tag{A.98}$$

We can straightforwardly exploit the integrals (4.84) by simply performing the substitution $m_b \leftrightarrow \tilde{m}_c$ in order to calculate the integrals over the Feynman variables.

The final result for the A_2 amplitude is then:

$$A_2 = \frac{iev}{32\sqrt{2}\pi^2} \frac{1}{\tilde{m}_a m_d} (\Delta)_{jd} (Y_R^*)_{dc} (Y_R^*)_{ba} (\tilde{\Delta}^\dagger)_{ai} \frac{1}{m_b^2 - \tilde{m}_c^2} \times$$

$$\times \frac{1}{2} \left[(Y_L^{*\dagger})_{cb} \left(-\frac{m_b}{\tilde{m}_c} + \frac{m_b \tilde{m}_c}{m_b^2 - \tilde{m}_c^2} \log \frac{m_b^2}{\tilde{m}_c^2} \right) \right] Q_{\gamma L}$$

$$= \frac{iev}{64\sqrt{2}\pi^2} \frac{1}{\tilde{m}_a m_d} (\Delta)_{jd} (Y_R^*)_{dc} (Y_L^{*\dagger})_{cb} (Y_R^*)_{ba} (\tilde{\Delta}^\dagger)_{ai} \frac{1}{m_b^2 - \tilde{m}_c^2} \times$$

$$\times \left[\left(-\frac{m_b}{\tilde{m}_c} + \frac{m_b \tilde{m}_c}{m_b^2 - \tilde{m}_c^2} \log \frac{m_b^2}{\tilde{m}_c^2} \right) \right] Q_{\gamma L} . \tag{A.99}$$

A.4.2 The B_1 and B_2 amplitudes.

We now switch to the B_1 and B_2 diagrams of Fig. 4.2. We use the same convention as above for the flavor indices, whereas the loop momenta conventions are represented in Fig. A.5.

Starting from B_1:

$$B_1 = \bar{e}_{Lj}(p') \left(-i(\Delta)_{jd} P_R \right) \frac{i(\not{p}' + m_d)}{p'^2 - m_d^2} \left[\frac{-iv}{\sqrt{2}} \left((Y_L^*)_{dc} P_L + (Y_R^*)_{dc} P_R \right) \right] \times$$

$$\times \frac{i(\not{p}' + \tilde{m}_c)}{p'^2 - \tilde{m}_c^2} \left[\frac{-i}{\sqrt{2}} \left((Y_L^{*\dagger})_{cb} P_R + (Y_R^{*\dagger})_{cb} P_L \right) \right] \times$$

$$\times \left\{ \int \frac{\mathrm{d}^4 k}{(2\pi)^4} \frac{i(\slashed{k} + m_b)}{k^2 - m_b^2} (-ie\gamma^\alpha \varepsilon_\alpha(q)) \frac{i(\slashed{k} + \slashed{q} + m_b)}{(k+q)^2 - m_b^2} \frac{i}{(k-p')^2 - M_h^2} \right\} \times$$

$$\times \left[\frac{-i}{\sqrt{2}} ((Y_L^*)_{ba} P_L + (Y_R^*)_{ba} P_R) \right] \frac{i(\slashed{p} + \tilde{m}_a)}{p^2 - \tilde{m}_a^2} \left(-i(\tilde{\Delta}^\dagger)_{ai} P_R \right) \tilde{e}_{Ri}(p)$$

$$= -\frac{ev}{2\sqrt{2}} \frac{1}{\tilde{m}_a \tilde{m}_c m_d} (\Delta)_{jd} (Y_R^*)_{dc} (Y_L^{*\dagger})_{cb} (Y_R^*)_{ba} (\tilde{\Delta}^\dagger)_{ai} \varepsilon_\alpha \times$$

$$\times \bar{e}_{Lj} \left\{ \int \frac{\mathrm{d}^4 k}{(2\pi)^4} \frac{(\slashed{k} + m_b)\gamma^\alpha(\slashed{k} + \slashed{q} + m_b)}{[k^2 - m_b^2][(k+q)^2 - m_b^2][(k-p)^2 - M_h^2]} \right\} \tilde{e}_{Ri}$$

$$= -\frac{ev}{2\sqrt{2}} \frac{1}{\tilde{m}_a \tilde{m}_c m_d} (\Delta)_{jd} (Y_R^*)_{dc} (Y_L^{*\dagger})_{cb} (Y_R^*)_{ba} (\tilde{\Delta}^\dagger)_{ai} \varepsilon_\alpha \times$$

$$\times \bar{e}_{Lj} \left\{ \int \frac{\mathrm{d}^4 k}{(2\pi)^4} \frac{m_b(2k^\alpha + \gamma^\alpha \slashed{q})}{[k^2 - m_b^2][(k+q)^2 - m_b^2][(k-p)^2 - M_h^2]} \right\} \tilde{e}_{Ri} . \quad \text{(A.100)}$$

The recasting of the denominator using the Feynman parametrization is completely analogous to the computations carried out for the A_1 amplitude, namely Eqs. (4.73) to (4.76). We can then immediately write:

$$\frac{1}{[k^2 - m_b^2][(k+q)^2 - m_b^2][(k-p)^2 - M_h^2]} = 2 \int_0^1 \mathrm{d}x \int_0^{1-x} \mathrm{d}y \frac{1}{\{[k+Q]^2 - \Omega_2\}^3} , \quad \text{(A.101)}$$

with Q and Ω_2 given in (4.76), once having substituted p' with p.

Performing in the numerator inside the loop integral of (A.100) the change of variable $k \to k - Q$, we get:

$$\varepsilon_\alpha \bar{e}_{Lj} \left[m_b(2k^\alpha + \gamma^\alpha \slashed{q}) \right] \tilde{e}_{Ri}$$
$$\to m_b \varepsilon_\alpha \bar{e}_{Lj} \left[2k^\alpha - 2yq^\alpha + 2(1 - x - y)p'^\alpha + \gamma^\alpha \slashed{q} \right] \tilde{e}_{Ri}$$
$$= -m_b(x+y)Q_{\gamma L} . \quad \text{(A.102)}$$

Then we have:

$$B_1 = \frac{ev}{2\sqrt{2}} \frac{1}{\tilde{m}_a \tilde{m}_c m_d} (\Delta)_{jd} (Y_R^*)_{dc} (Y_L^{*\dagger})_{cb} (Y_R^*)_{ba} (\tilde{\Delta}^\dagger)_{ai} \times$$

$$\times 2m_b \left\{ \int_0^1 \mathrm{d}x \int_0^{1-x} \mathrm{d}y (x+y) \int \frac{\mathrm{d}^4 k}{(2\pi)^4} \frac{1}{[k^2 - \Omega_2]^3} \right\} Q_{\gamma L}$$

$$= -\frac{iev}{32\sqrt{2}\pi^2} \frac{1}{\tilde{m}_a \tilde{m}_c m_d} (\Delta)_{jd} (Y_R^*)_{dc} (Y_L^{*\dagger})_{cb} (Y_R^*)_{ba} (\tilde{\Delta}^\dagger)_{ai} \times$$

$$\times m_b \left\{ \int_0^1 \mathrm{d}x \int_0^{1-x} \mathrm{d}y (x+y) \frac{1}{\Omega_2} \right\} Q_{\gamma L}$$

$$= -\frac{iev}{64\sqrt{2}\pi^2} \frac{1}{\tilde{m}_a m_b \tilde{m}_c m_d} (\Delta)_{jd} (Y_R^*)_{dc} (Y_L^{*\dagger})_{cb} (Y_R^*)_{ba} (\tilde{\Delta}^\dagger)_{ai} Q_{\gamma L} . \quad \text{(A.103)}$$

The calculations for B_2 are rather identical. They involve essentially the same loop integral, once provided the substitution $m_b \to \tilde{m}_c$ (and then $\Omega_2 \to \Omega_2'$ according

to (A.94)):

$$B_2 = \bar{e}_{Lj}(p')\,(-i(\Delta)_{jd}P_R)\,\frac{i(\slashed{p}' + m_d)}{p'^2 - m_d^2}\left[\frac{-i}{\sqrt{2}}\left((Y_L^*)_{dc}P_L + (Y_R^*)_{dc}P_R\right)\right]\times$$

$$\times\left\{\int\frac{\mathrm{d}^4k}{(2\pi)^4}\frac{i(\slashed{k} + \tilde{m}_c)}{k^2 - \tilde{m}_c^2}\left(-ie\gamma^\alpha\varepsilon_\alpha(q)\right)\frac{i(\slashed{k} + \slashed{q} + \tilde{m}_c)}{(k+q)^2 - \tilde{m}_c^2}\frac{i}{(k-p')^2 - M_h^2}\right\}\times$$

$$\times\left[\frac{-i}{\sqrt{2}}\left((Y_L^{*\dagger})_{cb}P_R + (Y_R^{*\dagger})_{cb}P_L\right)\right]\frac{i(\slashed{p} + m_b)}{p^2 - m_b^2}\times$$

$$\times\left[\frac{-iv}{\sqrt{2}}\left((Y_L^*)_{ba}P_L + (Y_R^*)_{ba}P_R\right)\right]\frac{i(\slashed{p} + \tilde{m}_a)}{p^2 - \tilde{m}_a^2}\left(-i(\tilde{\Delta}^\dagger)_{ai}P_R\right)\tilde{e}_{Ri}(p)$$

$$= -\frac{ev}{2\sqrt{2}}\frac{1}{\tilde{m}_a m_b m_d}(\Delta)_{jd}(Y_R^*)_{dc}(Y_L^{*\dagger})_{cb}(Y_R^*)_{ba}(\tilde{\Delta}^\dagger)_{ai}\varepsilon_\alpha\times$$

$$\times\bar{e}_{Lj}\left\{\int\frac{\mathrm{d}^4k}{(2\pi)^4}\frac{(\slashed{k} + \tilde{m}_c)\gamma^\alpha(\slashed{k} + \slashed{q} + \tilde{m}_c)}{[k^2 - \tilde{m}_c^2][(k+q)^2 - \tilde{m}_c^2](k-p')^2}\right\}\tilde{e}_{Ri}$$

$$= \frac{ev}{2\sqrt{2}}\frac{1}{\tilde{m}_a m_b m_d}(\Delta)_{jd}(Y_R^*)_{dc}(Y_L^{*\dagger})_{cb}(Y_R^*)_{ba}(\tilde{\Delta}^\dagger)_{ai}\times$$

$$\times 2\tilde{m}_c\left\{\int_0^1\mathrm{d}x\int_0^{1-x}\mathrm{d}y(x+y)\int\frac{\mathrm{d}^4k}{(2\pi)^4}\frac{1}{[k^2 - \Omega_2']^3}\right\}Q_{\gamma L}$$

$$= -\frac{iev}{32\sqrt{2}\pi^2}\frac{1}{\tilde{m}_a m_b m_d}(\Delta)_{jd}(Y_R^*)_{dc}(Y_L^{*\dagger})_{cb}(Y_R^*)_{ba}(\tilde{\Delta}^\dagger)_{ai}\times$$

$$\times\tilde{m}_c\left\{\int_0^1\mathrm{d}x\int_0^{1-x}\mathrm{d}y(x+y)\frac{1}{\Omega_2'}\right\}Q_{\gamma L}$$

$$= -\frac{iev}{64\sqrt{2}\pi^2}\frac{1}{\tilde{m}_a m_b \tilde{m}_c m_d}(\Delta)_{jd}(Y_R^*)_{dc}(Y_L^{*\dagger})_{cb}(Y_R^*)_{ba}(\tilde{\Delta}^\dagger)_{ai}Q_{\gamma L}\,. \tag{A.104}$$

Bibliography

[1] G. Aad *et al.* [ATLAS Collaboration], Phys. Lett. B **716** (2012) 1 [arXiv:1207.7214 [hep-ex]].

[2] S. Chatrchyan *et al.* [CMS Collaboration], Phys. Lett. B **716** (2012) 30 [arXiv:1207.7235 [hep-ex]].

[3] G. Buchalla, A. J. Buras and M. E. Lautenbacher, Rev. Mod. Phys. **68** (1996) 1125 [hep-ph/9512380].

[4] M. Neubert, hep-ph/0512222.

[5] A. J. Buras, P. Gambino, M. Gorbahn, S. Jager and L. Silvestrini, Phys. Lett. B **500** (2001) 161 [hep-ph/0007085].

[6] G. D'Ambrosio, G. F. Giudice, G. Isidori and A. Strumia, Nucl. Phys. B **645** (2002) 155 [hep-ph/0207036].

[7] D. B. Kaplan, Nucl. Phys. B **365** (1991) 259.

[8] M. J. Dugan, H. Georgi and D. B. Kaplan, Nucl. Phys. B **254** (1985) 299.

[9] R. Contino, arXiv:1005.4269 [hep-ph].

[10] R. Contino, T. Kramer, M. Son and R. Sundrum, JHEP **0705** (2007) 074 [hep-ph/0612180].

[11] P. A. R. Ade *et al.* [Planck Collaboration], arXiv:1303.5076 [astro-ph.CO].

[12] G. Jungman, M. Kamionkowski and K. Griest, Phys. Rept. **267** (1996) 195 [hep-ph/9506380].

[13] M. S. Turner, Phys. Rept. **197** (1990) 67.

[14] A. D. Sakharov, Pisma Zh. Eksp. Teor. Fiz. **5** (1967) 32 [JETP Lett. **5** (1967) 24] [Sov. Phys. Usp. **34** (1991) 392] [Usp. Fiz. Nauk **161** (1991) 61].

[15] P. A. R. Ade *et al.* [BICEP2 Collaboration], arXiv:1403.3985 [astro-ph.CO].

[16] M. C. Gonzalez-Garcia and M. Maltoni, "Phenomenology with Massive neutrino", Phys. Rept. **460** (2008) 1; A. Strumia and F. Vissani, hep-ph/0606054; M. C. Gonzalez-Garcia and Y. Nir, Rev. Mod. Phys. **75** (2003) 345 [hep-ph/0202058]; T. Schwetz, M. A. Tortola and J. W. F. Valle, New J. Phys. **10** (2008) 113011 [arXiv:0808.2016 [hep-ph]].

[17] M. B. Green, J. H. Schwarz and E. Witten, "Superstring Theory", (Cambridge Univ. Press, 1987).

[18] P. Langacker and N. Polonsky, Phys. Rev. D **47** (1993) 4028 [hep-ph/9210235].

[19] P. Langacker, Phys. Rept. **72** (1981) 185; S. Raby, hep-ph/0608183.

[20] W. Buchmuller and D. Wyler, Nucl. Phys. B **268** (1986) 621.

[21] A. Goobar, S. Hannestad, E. Mortsell and H. Tu, JCAP **0606** (2006) 019 [astro-ph/0602155].

[22] J. Beringer *et al.* [Particle Data Group], Phys. Rev. D **86**, 010001 (2012).

[23] G. 't Hooft, C. Itzykson, A. Jaffe, H. Lehmann, P. K. Mitter, I. M. Singer and R. Stora, NATO Adv. Study Inst. Ser. B Phys. **59** (1980) pp.1.

[24] P. Binetruy, in "Supersymmetry", Ch. I, (Oxford, 2006) (ISBN 0198509545).

[25] L. L. Chau and W. Y. Keung, Phys. Rev. Lett. **53** (1984) 1802.

[26] L. Wolfenstein, Phys. Rev. Lett. **51** (1983) 1945.

[27] J. Charles *et al.* [CKMfitter Collaboration], Eur. Phys. J. **C41**, 1 (2005) [hep-ph/0406184], *online update at* http://ckmfitter.in2p3.fr/www/html/ckm_results.html

[28] B. Grzadkowski, M. Iskrzynski, M. Misiak and J. Rosiek, JHEP **1010** (2010) 085 [arXiv:1008.4884 [hep-ph]].

[29] G. Isidori, arXiv:1302.0661 [hep-ph].

[30] V. Cirigliano, B. Grinstein, G. Isidori and M. B. Wise, Nucl. Phys. B **728** (2005) 121 [hep-ph/0507001].

[31] T. Hurth, G. Isidori, J. F. Kamenik and F. Mescia, Nucl. Phys. B **808** (2009) 326 [arXiv:0807.5039 [hep-ph]].

[32] M. Bona *et al.* [UTfit Collaboration], JHEP **0803** (2008) 049 [arXiv:0707.0636 [hep-ph]].

[33] T. Feldmann and T. Mannel, JHEP **0702** (2007) 067 [hep-ph/0611095].

[34] A. L. Kagan, G. Perez, T. Volansky and J. Zupan, Phys. Rev. D **80**, 076002 (2009) [arXiv:0903.1794 [hep-ph]].

[35] A. J. Buras, Acta Phys. Polon. B **34** (2003) 5615 [arXiv:hep-ph/0310208].

[36] L. Mercolli and C. Smith, Nucl. Phys. B **817** (2009) 1 [arXiv:0902.1949 [hep-ph]].

[37] P. Binetruy, "Supersymmetry", (Oxford, 2006) (ISBN 0198509545).

[38] L. Randall and R. Sundrum, Phys. Rev. Lett. **83** (1999) 3370 [hep-ph/9905221].

[39] F. Wilczek, Class. Quant. Grav. **30** (2013) 193001 [arXiv:1307.7376 [hep-ph]].

[40] M. R. Douglas, hep-th/0602266; arXiv:1204.6626 [hep-th].

[41] S. Weinberg, Phys. Rev. Lett. **59** (1987) 2607.

[42] G. Degrassi, S. Di Vita, J. Elias-Miro, J. R. Espinosa, G. F. Giudice, G. Isidori and A. Strumia, JHEP **1208** (2012) 098 [arXiv:1205.6497 [hep-ph]].

[43] M. E. Peskin and T. Takeuchi, Phys. Rev. D **46** (1992) 381.

[44] S. Kaptanoglu and N. K. Pak, Fortsch. Phys. **30** (1982) 451.

[45] K. Agashe, R. Contino and A. Pomarol, Nucl. Phys. B **719** (2005) 165 [hep-ph/0412089].

[46] B. Gripaios, A. Pomarol, F. Riva and J. Serra, JHEP **0904** (2009) 070 [arXiv:0902.1483 [hep-ph]].

[47] B. Keren-Zur, P. Lodone, M. Nardecchia, D. Pappadopulo, R. Rattazzi and L. Vecchi, Nucl. Phys. B **867** (2013) 394 [arXiv:1205.5803 [hep-ph]].

[48] M. De Gerone [MEG Collaboration], EPJ Web Conf. **73** (2014) 07002.

[49] A. M. Baldini, F. Cei, C. Cerri, S. Dussoni, L. Galli, M. Grassi, D. Nicolo and F. Raffaelli *et al.*, arXiv:1301.7225 [physics.ins-det].

[50] Project X and the Science of Intensity Frontier: A White Paper, 2009, see http://projectx.fnal.gov/.

[51] U. Bellgardt *et al.* [SINDRUM Collaboration], Nucl. Phys. B **299** (1988) 1.

[52] A. Blondel, A. Bravar, M. Pohl, S. Bachmann, N. Berger, M. Kiehn, A. Schoning and D. Wiedner *et al.*, arXiv:1301.6113 [physics.ins-det].

[53] C. Dohmen *et al.* [SINDRUM II. Collaboration], Phys. Lett. B **317** (1993) 631;
W. H. Bertl *et al.* [SINDRUM II Collaboration], Eur. Phys. J. C **47** (2006) 337.

[54] Y. Kuno, *Muon to electron conversion experiment, Nucl.Phys.Proc.Suppl.* **217** (2011) 337–340.

[55] "The Mu2e Conceptual Design Report 2012." http://mu2e-docdb.fnal.gov/cgi-bin/ShowDocument?docid=1169, 2012.

[56] B. Aubert *et al.* [BaBar Collaboration], Phys. Rev. Lett. **104** (2010) 021802 [arXiv:0908.2381 [hep-ex]].

[57] K. Hayasaka [Belle and Belle II Collaboration], J. Phys. Conf. Ser. **408** (2013) 012069.

[58] K. Hayasaka, K. Inami, Y. Miyazaki, K. Arinstein, V. Aulchenko, T. Aushev, A. M. Bakich and A. Bay *et al.*, Phys. Lett. B **687** (2010) 139 [arXiv:1001.3221 [hep-ex]].

[59] G. F. Giudice, P. Paradisi and M. Passera, JHEP **1211** (2012) 113 [arXiv:1208.6583 [hep-ph]].

[60] F. Jegerlehner and A. Nyffeler, Phys. Rept. **477** (2009) 1 [arXiv:0902.3360 [hep-ph]].

[61] J. Baron *et al.* [ACME Collaboration], Science **343** (2014) 6168, 269 [arXiv:1310.7534 [physics.atom-ph]].

[62] C. E. Vayonakis, Lett. Nuovo Cim. **17** (1976) 383.

[63] B. Keren-Zur, P. Lodone, M. Nardecchia, D. Pappadopulo, R. Rattazzi and L. Vecchi, Nucl. Phys. B **867** (2013) 394 [arXiv:1205.5803 [hep-ph]].

[64] C. Delaunay, C. Grojean and G. Perez, JHEP **1309** (2013) 090 [arXiv:1303.5701 [hep-ph]].

[65] V. Lubicz and C. Tarantino, Nuovo Cim. B **123** (2008) 674 [arXiv:0807.4605 [hep-lat]].

[66] A. J. Schwartz, arXiv:0911.1464 [hep-ex].

[67] A. L. Kagan and M. D. Sokoloff, Phys. Rev. D **80** (2009) 076008 [arXiv:0907.3917 [hep-ph]].

[68] Y. Amhis *et al.* [Heavy Flavor Averaging Group Collaboration], arXiv:1207.1158 [hep-ex].

[69] A. J. Buras, D. Guadagnoli and G. Isidori, Phys. Lett. B **688** (2010) 309 [arXiv:1002.3612 [hep-ph]].

[70] A. J. Buras, M. Jamin and P. H. Weisz, Nucl. Phys. B **347** (1990) 491;
S. Herrlich and U. Nierste, Nucl. Phys. B **419** (1994) 292 [hep-ph/9310311];
S. Herrlich and U. Nierste, Phys. Rev. D **52** (1995) 6505 [hep-ph/9507262];
S. Herrlich and U. Nierste, Nucl. Phys. B **476** (1996) 27 [hep-ph/9604330].

[71] K. G. Chetyrkin, M. Misiak and M. Munz, Phys. Lett. B **400** (1997) 206 [Erratum-ibid. B **425** (1998) 414] [hep-ph/9612313].

[72] E. Lunghi and J. Matias, JHEP **0704** (2007) 058 [hep-ph/0612166].

[73] U. Haisch, arXiv:0805.2141 [hep-ph].

[74] A. Ali, E. Lunghi, C. Greub and G. Hiller, Phys. Rev. D **66** (2002) 034002 [hep-ph/0112300].

[75] W. Altmannshofer, P. Ball, A. Bharucha, A. J. Buras, D. M. Straub and M. Wick, JHEP **0901** (2009) 019 [arXiv:0811.1214 [hep-ph]].

[76] S. Hall [LHCb Collaboration], EPJ Web Conf. **71** (2014) 00053.

[77] A. J. Buras, F. Schwab and S. Uhlig, Rev. Mod. Phys. **80** (2008) 965 [hep-ph/0405132].

[78] D. Bryman, A. J. Buras, G. Isidori and L. Littenberg, Int. J. Mod. Phys. A **21** (2006) 487 [hep-ph/0505171].

[79] T. Kaluza, Sitzungsber. Preuss. Akad. Wiss. Berlin (Math. Phys.) **1921** (1921) 966.

[80] A. Pomarol, CERN Yellow Report CERN-2012-001, 115-151 [arXiv:1202.1391 [hep-ph]].

[81] O. Klein, Z. Phys. **37** (1926) 895 [Surveys High Energ. Phys. **5** (1986) 241].

[82] N. Arkani-Hamed, S. Dimopoulos and G. R. Dvali, Phys. Lett. B **429** (1998) 263 [hep-ph/9803315]; Phys. Rev. D **59** (1999) 086004 [hep-ph/9807344].

[83] M. Serone, New J. Phys. **12** (2010) 075013 [arXiv:0909.5619 [hep-ph]].